ASPECTS OF TECHNETIUM CHEMISTRY

BY

© KENNETH JAMES FRANKLIN, B.Sc., M.Sc.

A Thesis

Submitted to the Faculty of Graduate Studies

in Partial Fulfilment of the requirements

for the degree

Doctor of Philosophy

McMaster University

November, 1982

ASPECTS OF TECHNETIUM CHEMISTRY

TO MY WIFE

DOCTOR OF PHILOSOPHY (1982) McMASTER UNIVERSITY
(Chemistry) Hamilton, Ontario

TITLE: Aspects of Technetium Chemistry

AUTHOR: Kenneth James Franklin, B.Sc. (Brock University, St. Catharines, Ont.)

M.Sc. (Brock University)

SUPERVISOR: Professor C. J. L. Lock

NUMBER OF PAGES: xiv, 137

ABSTRACT

Interest in technetium chemistry is derived from the fact that it is a recently-discovered element and from the use of technetium-99m as a radioactive label in diagnostic medicine. Compounds related to both sources of interest have been characterized by X-ray crystallography, vibrational spectroscopy and multinuclear nuclear magnetic resonance spectroscopy.

The crystal structure of a penicillamine complex of technetium consists of an oxotechnetium(V) core bonded to the S, N, and O atoms of one penicillamine moiety and the S and N atoms of a second. Further characterization, including tracer studies with ^{99m}Tc, indicate that this complex is identical to an hepatobiliary agent erroneously formulated as a technetium(IV) species. The crystal structure of an anionic catechol complex of technetium also contains the oxotechnetium(V) core and suggests that the technetium(IV) formulation for a number of other radiopharmaceuticals is incorrect. The crystal structure determination of a complex containing the ethylenebis(2-mercaptoacetamide) ligand forms part of a larger program to design, systematically, new scanning agents.

Technetium complexes involving cyanide ligands are shown to be similar to their rhenium analogs.

Several new technetium(VII) species were synthesized and used to establish ranges for parameters in the nuclear magnetic resonance spectroscopy of ^{99}Tc.

NOMENCLATURE

d	deuteron
n	neutron
g	gram
MW	megawatt
n.m.r.	nuclear magnetic resonance
h	hour, Planck's constant
y	year
keV	kiloelectron volt
MeV	megaelectron volt
I.T.	isomeric transition
DTPA	diethylenetriaminepentaacetic acid
EDTA	ethylenediaminetetraacetic acid
MIDA	methyliminodiacetic acid
HEDP	(hydroxyethylidene)diphosphonate
I	nuclear spin quantum number
μ	magnetic moment
γ	magnetogyric ratio
σ	shielding factor, standard deviation
ppm	parts per million
Ξ	absolute frequency
TMS	tetramethylsilane

Nomenclature (continued)

MHz	megahertz
J	coupling constant
T_1	spin-lattice relaxation time
T_2	spin-spin relaxation time
Å	Angstrom
deg	degree
min	minute
mm	millimeter
μs	microsecond
cm	centimeter
R_f	retention time
mL	milliliter
pH	$-\log_{10}[H^+]$
nm	nanometer
ε	molar extinction coefficient
δ	chemical shift
av	average
mCi	millicurie
HIDA	N(2,6-dimethylcarbamoylmethyl)iminodiacetic acid
Hz	Hertz
X	gram susceptibility
μ_{eff}	effective magnetic moment
f	internal force constant
F	symmetry force constant

Nomenclature (continued)

mdyne	millidyne
en	ethylenediamine
FEP	fluoroethylene polymer
$\Delta\nu$	line width

ACKNOWLEDGEMENTS

I would like to thank Professor Colin Lock for his relentless drive which kept me working, his flexibility which allowed me to explore some of my own interests and his encouragement and friendship which made the whole thing possible.

I am grateful to the members of my committee, Drs. Grundy and Tomlinson, for their guidance as to the direction of my work.

I would like to thank Dr. Gary Schrobilgen for his assistance with n.m.r. spectroscopy and high-oxidation-state compounds of technetium, Dr. Helen Howard-Lock for her help with vibrational spectroscopy and Dr. Barry Bowen for his assistance in the tracer study.

I wish to acknowledge the stimulation and cooperation of other members of our research group, Jim Britten, Debbie Harvey, Pierre Pilon, and others too numerous to mention.

Thanks are also due to Romolo Faggiani, Brian Sayer, Ian Thompson and Lee Gowers for invaluable technical assistance and to Marilyn Foster for typing this thesis.

Financial assistance in the form of scholarships from the National Research Council Canada and the Ontario Graduate Fellowship Program, as well as Scholarships and Teaching Assistantships from the Department of Chemistry, is gratefully acknowledged.

Above all, I would like to thank my wife for the years of financial and moral support and my parents for trying to understand.

TABLE OF CONTENTS

Table of Contents (continued)

Table of Contents (continued)

LIST OF TABLES

List of Tables (continued)

LIST OF FIGURES

List of Figures (continued)

CHAPTER 1

GENERAL INTRODUCTION

1.1 Historical Background

The periodic classification of the elements was discovered independently by L. Meyer and D. I Mendeleev in 1869 (1). In addition to providing a convenient classification of the known elements, the periodic table enabled scientists to predict the existence and properties of new elements. Such predictions were widely tested and many of the blank spaces in the table were quickly filled. However, element 43, a second row transition metal, was one of a select few which could not be isolated from natural sources, despite several claims to the contrary (2).

The discovery of element 43 was only made possible by the development of new techniques in nuclear physics and radiochemistry. In 1937, Perrier and Segré reported some chemical properties of element 43 based on an analysis of a molybdenum plate which had been subjected to deuteron irradiation from a cyclotron (3). They later suggested that this element be called technetium (chemical symbol, Tc) from the Greek word technetos, meaning artificial, since it was the first previously-unknown element to be made by man (4).

The nuclear reactions relating to the discovery of technetium are:

$$^{94}Mo(d,n)^{95m}Tc$$

and

$$^{96}Mo(d,n)^{97m}Tc$$

where ^{95m}Tc denotes the metastable isomer of ^{95}Tc (5). At present, a total of twenty isotopes and six isomers of technetium are known with half-lives that range from one second to several million years (5). Of these, only ^{99}Tc ($t_{\frac{1}{2}} = 2.12 \times 10^5$ years) has been obtained on a macro scale. The ready availability of this isotope is a byproduct of the nuclear age since ^{99}Tc is a major component in spent reactor fuels. This is illustrated by the fission yield curves (Figure 1) where ^{99}Tc represents approximately six per cent of the fission products from ^{233}U, ^{235}U and ^{239}Pu (6). With estimates of 2.5 g of ^{99}Tc produced each day by a single 100 MW nuclear reactor, it is very probable that the world supply of this man-made element exceeds that of its third row congener, rhenium, which occurs naturally (5).

By 1955, gram amounts of technetium were available to chemists and the number of studies on technetium grew rapidly (7). In 1965, two monographs were published in which the chemistry of technetium and rhenium was reviewed (8,9). At that time, technetium was considered to be a true anomaly in the periodic table since its chemistry was apparently so different from that of rhenium. Two examples will serve to illustrate the confusion that existed and how the differences were eventually resolved.

The preparation of cyclopentadiene complexes of transition metals typically involves a reaction between the metal halide and sodium cyclopentadienide in tetrahydrofuran or a similar solvent (10). Huggins and Kaesz used this method to prepare the technetium complex from $TcCl_4$ (11). In contrast to observations by Wilkinson and co-workers on the previously prepared rhenium complex, $(C_5H_5)_2ReH$ (12),

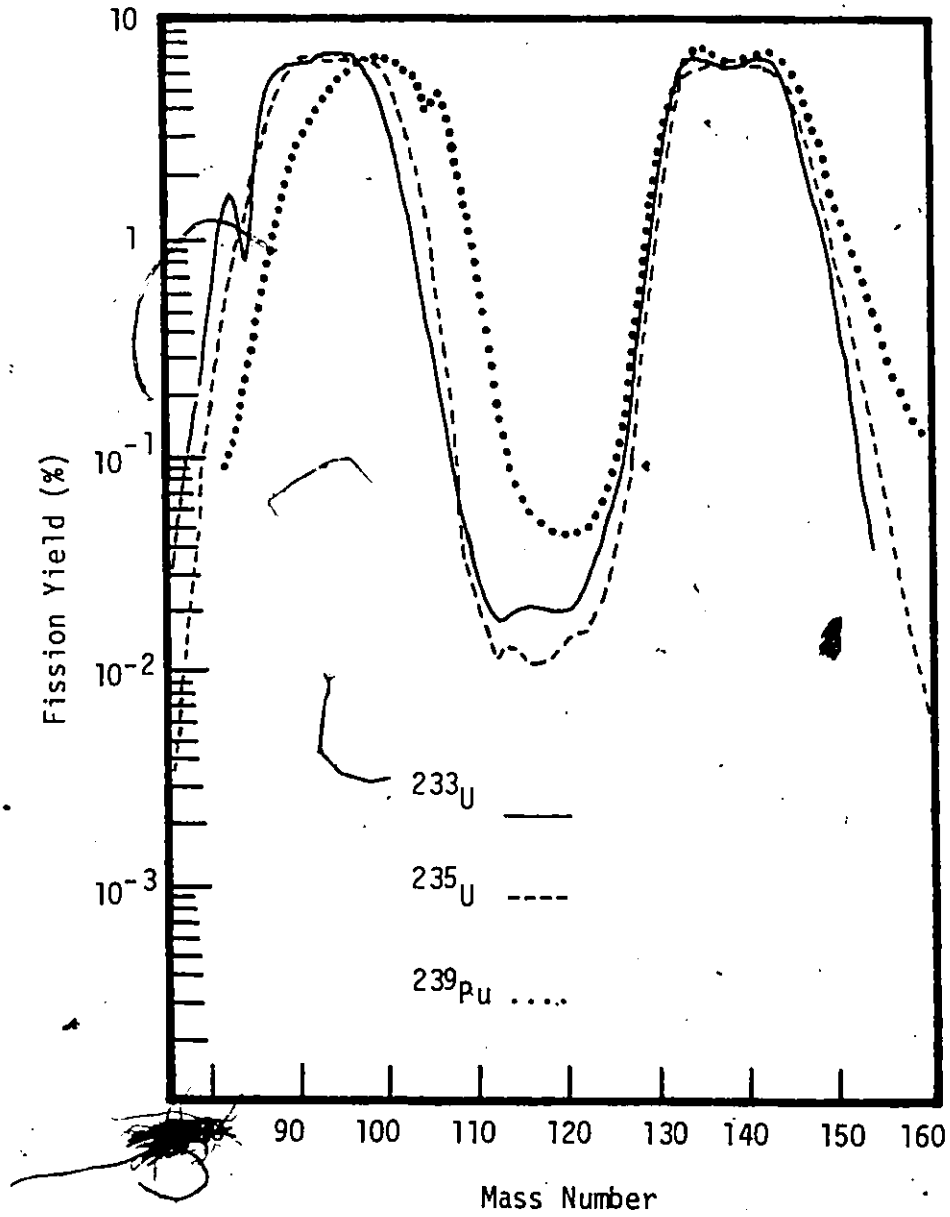

FIGURE 1. Fission Yield Curves for ^{233}U, ^{235}U and ^{239}Pu (from ref. 6)

they did not observe a metal hydride band in the infrared spectrum nor was there a signal in the low frequency region of the ^1H n.m.r. spectrum characteristic of hydridic protons. This information along with the diamagnetism of the complex and a determination of the molecular weight, led them to suggest that the product was a dimer with the formula $[(C_5H_5)_2Tc]_2$ (11). However, later work by Fischer and Schmidt demonstrated that the standard preparation resulted in the formation of a technetium complex directly analogous to that of rhenium (13). A force constant calculation showed that the Tc-H bond was somewhat weaker than the ReH bond (13). This trend parallels that found for $Mo(C_6H_5)_2H_2$ and its tungsten analog, as might be expected.

The second example involves the hexachlorides of these two metals. In 1962, Colton reported the synthesis of $TcCl_6$ from the action of chlorine gas on technetium metal (14). Since second row elements are not expected to form higher chlorides than their third row counterparts, Colton predicted that $ReCl_6$ should be stable although previous attempts to synthesize the compound had been unsuccessful (14). Shortly thereafter, Colton fulfilled this prediction by reporting the synthesis of $ReCl_6$ (15). However, in an effort to study the anomalous magnetic properties of $ReCl_6$, Guest and Lock discovered that the published synthesis produced only $ReOCl_4$ and $ReCl_5$ (16). A subsequent study of the technetium system by the same workers showed that the products actually obtained were TcO_3Cl and $TcOCl_4$ (17). An alternate synthesis of $ReCl_6$ involving halogen exchange between ReF_6 and BCl_3 or PCl_3 has likewise been shown to be incorrect (18,19). Thus, the highest known

chlorides of these metals are $TcCl_4$ and $ReCl_5$ respectively, in agreement with the observed trends both across and down the remainder of the periodic table.

Other inconsistencies listed in 1965 have also not withstood careful examination (20) and it is generally accepted that the chemistry of technetium is analogous to that of rhenium (10). A brief outline of this chemistry is presented in the following section. More extensive reviews have been published (2,5,7,21,22,23,24).

1.2 Outline of Technetium Chemistry

The outer shell electron configuration for technetium is $4d^6 5s^1$ and each of the expected oxidation states from VII to -I have been observed (10). Characteristic examples of technetium in the various oxidation states are described below.

The technetium (VII) compound, Tc_2O_7, is the only product obtained when the metal is burned in excess oxygen at 400°C (2). It is readily purified by sublimation and dissolves in water to give pertechnetic acid, $HTcO_4$ (21). The pertechnetate anion is a much weaker oxidizing agent than the permanganate ion but can be reduced by HCl, HBr or HI (10). Numerous pertechnetate salts have been fully characterized with ammonium pertechnetate being the form most commonly used for synthetic purposes (24). The insoluble heptasulfide, Tc_2S_7, is important in the isolation of technetium from various sources, especially spent reactor fuels (21). Other technetium (VII) compounds include TcO_3F and TcO_3Cl which are liquids at room temperature, and TcH_9^{2-} which is one of few examples of coordination number nine (10).

Several technetium (VII) species are discussed in Chapter 6.

The hexavalent oxidation state is represented by compounds such as TcO_4^{2-}, TcO_3, TcF_6 and $TcOF_4$ (24). There are relatively few examples since technetium (VI) compounds tend to disproportionate according to the reaction (2):

$$3Tc(VI) \rightarrow 2Tc(VII) + Tc(IV)$$

Although simple anionic halide and pseudohalide complexes of technetium (V) exist, the chemistry of the pentavalent state is dominated by three types of oxotechnetium (V) cores: TcO^{3+}, trans-TcO_2^+ and linear $Tc_2O_3^{4+}$ (24). The first of these may exhibit a coordination number of five ($TcOCl_4^-$) (25), six (pyrazolyl-$TcOCl_2$) (26) or seven ($TcO(EDTA)^{2-}$) (27). The five coordinate complexes have geometries based on a square pyramidal arrangement with the oxo group at the apex and the base formed by the remaining four ligands (7). The trans-TcO_2^+ core is found in technetium (V) complexes with the most common nitrogen ligands (e.g. en), leading to the suggestion that the π-donor ability of the equatorial ligands is the determining factor between mono and dioxo species (28). The complex μ-$O[O(Et_2NCS_2)_2Tc]_2$ is the only example of the linear $Tc_2O_3^{4+}$ unit reported thus far (29). Oxotechnetium (V) chemistry is the basis for much of the research presented in this work.

The most common technetium (IV) compounds are technetium dioxide and the hexahalo-dianions, TcX_6^{2-}. The former is very stable and a common, usually undesirable, product in the reduction of pertechnetates (10). The latter are easily hydrolyzed and serve as starting materials for a variety of reactions (30).

Polarizable ("soft") ligands such as triphenylphosphine and/or the formation of metal-metal bonds seem to be necessary for the stabilization of technetium in the lower oxidation states. Although such compounds are normally prepared under anhydrous conditions, Davison and co-workers have recently shown that isonitrile complexes of technetium(I) can be prepared by direct reduction of pertechnetate in aqueous solution (31).

1.3 Technetium and Nuclear Medicine

The field of nuclear medicine has developed from the tracer principle first described by Hevesy who used radioactive isotopes of lead to trace the assimilation and distribution of that element in plants (32). In nuclear medicine, this concept has been extended to include a wide variety of radioactive compounds administered to patients as diagnostic aids (the most common application), therapeutic agents (e.g., ^{131}I in the treatment of hyperthyroidism), or simply as metabolic tracers (e.g. drug distribution studies) (33). The importance of radiopharmaceuticals in diagnostic medicine is derived from the fact that the physiological function of an organ, as well as its structure, can be visualized (24). The availability of this additional information has resulted in a better understanding of disease and thereby improved the practice of medicine (34).

In 1960, Richards suggested that ^{99m}Tc possessed radiophysical properties that were ideally suited for use in diagnostic imaging (35). These properties, summarized schematically in Figure 2, include: a short half-life (6 hours) which gives ^{99m}Tc a high specific activity;

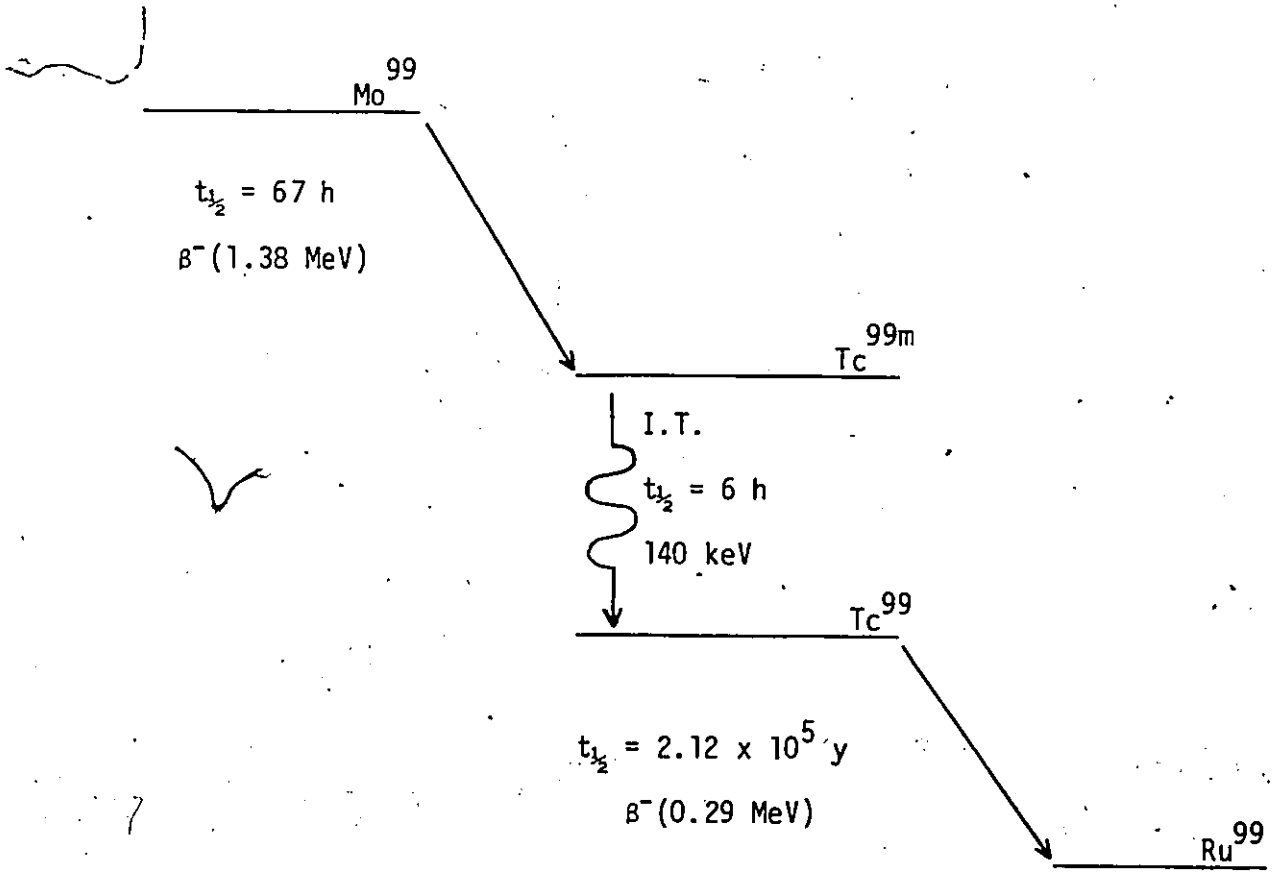

Figure 2. Decay Scheme for Technetium

a γ-ray energy (140 keV) which is in the optimal range for detection by scintillation cameras and which is poorly absorbed by body tissues; a relatively stable daughter nuclide which minimizes any long-term hazard from particulate radiation and a relatively stable parent nuclide, ^{99}Mo (35). The last characteristic led to the development of a generator which made ^{99m}Tc available on demand at any hospital (36). The generator consisted of ^{99}Mo absorbed on an alumina column from which ^{99m}Tc, in the form of pertechnetate, could be periodically eluted with a saline solution (36). Other generators, based on sublimation of Tc_2O_7 or on solvent extraction with methyl ethyl ketone have since been developed (37,38). The advantages, disadvantages and future prospects for a number of generator types form the subject of a recent review article (39).

Although pertechnetate can be used directly as an imaging agent, the majority of ^{99m}Tc radiopharmaceuticals involve coordination complexes of technetium in lower oxidation states. These complexes can be divided into two broad classes, namely, technetium-tagged and technetium-essential radiopharmaceuticals (40). In the class of tagged compounds, ^{99m}Tc is bound to large substances such as colloids, cells or proteins. The presence of the metal ion creates only a small perturbation and the biodistribution is unchanged from that of the untagged material. Technetium-essential radiopharmaceuticals consist of smaller molecules such as drugs or low-molecular-weight peptides labelled with ^{99m}Tc. In this class, the biodistribution of the complex is often very different from that of the parent substance. The ideal properties of ^{99m}Tc and the ease of formation of a variety of scanning agents have made ^{99m}Tc the most

widely-used radionuclide in nuclear medicine (41). A summary of ^{99m}Tc-radiopharmaceuticals currently in use is presented in Table 1 (40).

The typical labelling procedure consists of mixing $^{99m}TcO_4^-$ from a ^{99}Mo generator with a reducing agent in the presence of the desired ligand. Various reducing agents, including stannous ion, ferric chloride plus ascorbic acid, ferrous ion, sodium borohydride and concentrated hydrochloric acid, have been used (42). The concentration of the labelled product is usually at the nanomolar level which is sufficient to produce the image required for diagnosis but which is too low to allow examination by most of the standard chemical methods. Analysis of radiopharmaceuticals has largely been based on chromatographic techniques and the detailed structures of the complexes and even the oxidation state of the metal ion often remain unknown. This lack of chemical knowledge has meant that serendipity has been the major factor in radiopharmaceutical developments thus far (43).

Some of the difficulties can be overcome by using an alternate method of preparation. The aqueous reduction of pertechnetate in the presence of a ligand is subject to several limitations: only one type of ligand can be introduced; the final oxidation state, coordination number and coordination geometry in the product are not controlled; the reductant is often incorporated into the final product; excess reductant is injected into the patient; and a mixture of technetium complexes, rather than a single product, is usually obtained (44). However, reactions which involve the substitution of ligands onto a pre-reduced and isolated technetium centre allow control over the oxidation state

Table 1. ^{99m}Tc-Radiopharmaceuticals Currently in Use

Technetium-Tagged Radiopharmaceuticals

1. Particles and colloids

   Tc-albumin microspheres, Tc-ferric hydroxide aggregates, Tc-sulfur colloid, Tc-phytate.

2. Proteins

   Albumin, streptokinase, urokinase, fibrinogen

3. Cells

   Erythrocytes, leukocytes, platelets, lymphocytes

4. Small molecules

   Bone agents, e.g., polyphosphates, pyrophosphate, diphosphonates.

Technetium-Essential Radiopharmaceuticals

1. Kidney function agents

   Tc-DTPA, Tc-EDTA, Tc-MIDA(methyliminodiacetic acid), Tc-citrate

2. Kidney structure agents

   Tc-gluconate, Tc-glucoheptonate, Tc-Fe-ascorbate, Tc-inulin, Tc-mannitol, Tc-dimercaptosuccinic acid

3. Infarct avid agents

   Tc-pyrophosphate, Tc-glucoheptonate, Tc-tetracycline and Tc-HEDP (HEDP=(hydroxyethylidene)diphosphonate)

4. Hepatobiliary agents

   Tc-dihydrothioctic acid, Tc-HIDA, Tc-pyridoxylideneglutamate

and ligand environment of the technetium product (44). Davison and co-workers have shown that the anion, $TcOX_4^-$ (X = Cl,Br) is a useful substrate for such substitution reactions (25,29,45). The hexahalodianions, TcX_6^{2-} (X = Cl,Br) have also been used as starting materials in the synthesis of radiopharmaceuticals (44). Simple substitution reactions hold considerable promise as preparative routes since the clinical usefulness of a labelled compound is partially determined by its ease of preparation by unskilled personnel.

In order to allow the completely rational design of new scanning agents, the structural features and chemical behaviour of a number of complexes need to be correlated with their respective biodistributions. This may be accomplished by studying the chemistry of the complex based on the more stable ^{99}Tc nucleus and then using ^{99m}Tc and the tracer principle to determine the biodistribution of that complex. The characterizations of several compounds relating to this process are presented in the following chapters.

1.4 Nuclear Magnetic Resonance Spectroscopy

The history, theory and instrumentation of nuclear magnetic resonance (n.m.r.)spectroscopy have been described in a number of general texts (46,47,48). The following outline has been derived from such sources to provide a background for the discussions in Chapter 6.

Each isotope of an element can be assigned a ground state nuclear spin quantum number, I, which is also known as simply the spin of that isotope. The value of I may be zero, half-integral or integral,

corresponding to the number of protons and the number of neutrons being both even, of opposite parity or both odd, respectively. When $I \neq 0$, the nucleus has a magnetic moment, μ, given by:

$$\mu = \frac{\gamma h[I(I+1)]^{\frac{1}{2}}}{2\pi}$$

where γ, the magnetogyric ratio, is a characteristic of the particular nucleus. The receptivity of the nucleus is defined as:

$$\gamma^3 N(I)(I+1)$$

where N is the natural abundance of the isotope of interest. The receptivity is usually expressed as a value relative to that of ^1H or of ^{13}C and is an indication of the ease with which an observable signal can be obtained from an n.m.r. active nucleus.

When a nucleus with a non-zero spin is placed in a strong magnetic field, B_o, the orientation of the spin axis becomes quantized. Each orientation corresponds to a different energy, E, given by:

$$E = \frac{-\gamma h}{2\pi} \; m \; B_o, \; m = -I, -I+1, \ldots, I-1, I$$

At equilibrium, the populations of these energy levels are described by a Boltzmann distribution. The n.m.r. experiment consists of detecting transitions between the energy levels that are induced by the application of suitable radiofrequency radiation. The three main types of parameters of chemical interest that can be obtained by n.m.r. spectroscopy are chemical shifts, coupling constants and relaxation times.

Chemical shifts in the resonance frequency result from the

shielding of the nucleus by the surrounding electronic environment. This can be expressed mathematically by:

$$B_N = B_0(1-\sigma)$$

where B_N is the actual local magnetic field experienced by the nucleus and σ is a shielding factor. Several phenomena contribute to the observed σ including local diamagnetic and paramagnetic currents, effects from neighbouring atoms and external electric fields. Since the shielding parameter is dependent on the field strength, chemical shifts are generally reported in parts per million (ppm) relative to the resonance of some suitable reference compound. An alternate system is based on absolute frequencies, Ξ, which are scaled to a standard magnetic field in which the protons in tetramethylsilane (TMS) resonate at exactly 100 MHz. By definition (49):

$$\Xi_X = \frac{100\ \gamma_X\ (1-\sigma_X)}{\gamma(^1H)[1-\sigma^{TMS}(^1H)]}$$

Spin-spin coupling occurs between two nuclei (both with $I \neq 0$) when the spin states of one nucleus act to split the energy levels of the other. Coupling is not affected by the tumbling of the molecule and is independent of B_0, at least to a first approximation. The interaction, which is reciprocal in nature, can be decomposed into three contributions; spin-dipolar, spin-orbital and spin-contact mechanisms. The latter, also known as the Fermi contact mechanism, is the dominant mode in high resolution n.m.r. spectroscopy. This mechanism involves the polarization of the spins of the electrons in the intervening

chemical bonds and varies as the fraction of "s" character in those bonds. The nature and relative importance of various coupling mechanisms have recently been reviewed (50).

Experimentally, a nucleus coupled to a set of n nuclei with spin I will have its resonance split into 2nI + 1 lines. For a nucleus coupled to nuclei with I = ½, the relative intensities of these lines are given by the coefficients of the binomial expansion. The frequency separation between the lines is known as the coupling constant, J. Spin-spin coupling provides useful information about the structure of the compound while the magnitude of the coupling constant can be related to the electron density about the nucleus.

Two relaxation times (T_1 and T_2) are used to characterize the first order rate processes by which the Boltzmann distribution of populations into the available energy levels is re-established. Spin-lattice relaxation (T_1) is achieved through interactions between the nuclei and the surrounding molecules which are collectively known as the lattice. The motions of molecules in solution, the unpaired electrons in paramagnetic substances and the quadrupole moments present in nuclei with I > ½, all contribute to this process. Spin-spin relaxation (T_2) involves the direct exchange of energy between nuclei. Under conditions permitting rapid molecular motions, $T_2 \simeq T_1$.

The chemical shifts, coupling constants and relaxation times for a number of technetium species, particularly as they relate to the development of ^{99}Tc n.m.r. spectroscopy, are discussed in Chapter 6.

1.5 Summary

The study of technetium chemistry is of interest from a number of perspectives. As a major component of spent reactor fuels, technetium, especially in the form of stable, water soluble pertechnetate, is a factor in the safe disposal of nuclear wastes. Secondly, since relatively few technetium compounds have been fully characterized, it is interesting to test the trends predicted by the Periodic Law. Furthermore, a much better understanding of technetium chemistry is necessary for the rational design of new radiopharmaceuticals based on ^{99m}Tc. Finally, the development of ^{99}Tc n.m.r. spectroscopy requires the study of a number of compounds in order to establish the range of n.m.r. parameters, chemical shifts, line widths and coupling constants, that may be observed. These parameters constitute a sensitive probe of the structures of technetium complexes in solution.

In Chapters 3 and 4, the crystal structures of complexes containing the oxotechnetium(V) core bonded to penicillaminato, catecholato or ethylenebis(2-mercaptoacetamido) ligands are described. These results demonstrate that the formulation of certain classes of ^{99m}Tc-radiopharmaceuticals as technetium(IV) species is incorrect. In Chapter 5, two cyano complexes of technetium, $TcO_2(CN)_4^{3-}$ and $Tc(CN)_7^{4-}$, are characterized and shown to be similar to their rhenium analogs by X-ray crystallography and vibrational spectroscopy. In Chapter 6, several new technetium(VII) species are synthesized, and used, together with other complexes, to demonstrate the utility of ^{99}Tc n.m.r. spectroscopy.

CHAPTER 2

EXPERIMENTS

2.1 Handling of Radioactive Materials

All work involving $^{99}_{43}Tc$ was performed according to the regulations and recommendations of the Canadian Atomic Energy Control Board. All transfers of radioactive material as well as most syntheses were carried out in fume hoods with very high flow rates. In order to minimize the risk from accidental spills, the floors of the fume hoods were lined with plastic sheeting and then absorbent paper. Both components were replaced on a regular basis. Radioactive samples required for syntheses on the vacuum line, for analysis by various spectroscopic methods or for single crystal structure determinations were transported from the fume hoods in closed containers. All laboratory areas in which technetium was used were monitored routinely by the McMaster Health Physics Group for radioactive contamination.

2.2 Preparation and Analysis

Details of the preparation of compounds studied in this thesis are given in the appropriate chapters.

Elemental analysis for 1-oxo-2,3,6-(D-penicillaminato-S,N,O)-4,5-(D-penicillaminato-N,S)technetium(V) was performed by:

Canadian Microanalytical Service Ltd.
5704 University Blvd.
Vancouver, B.C. V6T 1K6

Crystals which are discussed in Chapters 4 and 5 as well as some of the n.m.r. samples in Chapter 6 were obtained from:

Professor Alan Davison

Massachusetts Institute of Technology

Cambridge, Massachusetts

Professor Davison was also responsible for obtaining elemental analyses for these compounds.

Densities of all crystals were determined by flotation in the solvent mixtures given in the appropriate chapters.

2.3 X-ray Crystallography

2.3.1 Single crystals

Small crystals with well-developed faces were examined under a polarizing microscope for homogeneity and the best of these were chosen for data collection. The crystals were then mounted on thin glass fibres or inside glass capillaries and aligned on precession cameras. Space groups were determined from the symmetry and systematic absences observed on zero and first layer precession photographs. The crystals were then transferred to either a Syntex $P2_1$ or a Nicolet P3 automatic diffractometer. An orientation matrix was determined from a rotation photograph taken with Polaroid film. Unit cell parameters were then obtained from a least-squares refinement from fifteen well-centered, medium angle reflections.

Intensity data were measured using graphite monochromated MoKα radiation (λ0.71069Å) to a maxium $2\theta = 55^{o}$. Data were collected using a coupled θ(crystal)-2θ(counter) scan with scan rates that ranged from 5.0 deg min^{-1} for weak reflections to 29.3 deg min^{-1} for

strong reflections. Scan rates were determined by the program supplied with the instrument on the basis of the counting rate at the centre of the reflection (51).

The stability of each system was monitored by measuring two standard reflections after every forty-eight reflections. This information was used to normalize all data to the initial intensity of the standard reflections. Stationary counts at the limits of each scan were made for half the scan time to establish the background. The net intensity, I, of a reflection was taken as $I = N_T - N_{B_1} - N_{B_2}$, where N_T is the total peak count and N_{B_1} and N_{B_2} are the background counts. The standard deviations, $\sigma(I)$, of the net intensities were taken as $\sigma(I) = (N_T + N_{B_1} + N_{B_2})^{\frac{1}{2}}$.

2.3.2 Data Processing (52)

Unscaled structure amplitudes, F_o, and their standard deviations, $\sigma(F)$, were calculated from the expressions:

$$F_o = \left(\frac{I}{Lp}\right)^{\frac{1}{2}}$$

$$\sigma(F) = \frac{1}{2}\,\frac{1}{(Lp)^{\frac{1}{2}}}\left(\frac{\sigma(I)^2}{I}\right)^{\frac{1}{2}}$$

where Lp is the combined form of the Lorentz and polarization factors given by $(1 + \cos^2 2\theta)/(2 \sin 2\theta)$. Where necessary, corrections for secondary extinction were made using the method of Larson (53).

Unscaled structure amplitudes, Fc, were calculated using the equation

$$F_c(hk\ell) = \sum_{j=1}^{n} T_j f_j \exp[2\pi i(hx_j+ky_j+\ell z_j)]$$

where f_j is the scattering factor of the jth atom in the unit cell and x_j, y_j and z_j are the fractional coordinates of the jth atom along the three crystallographic axes, a, b and c, respectively. The temperature factor, T_j, describes the magnitude of vibration of the atoms about their mean positions as:

$$T_j = \exp[-2\pi^2 U_j (d_{hk\ell})^{-2}]$$

where U_j is the isotropic thermal parameter expressed in terms of mean square amplitudes in $\AA^2$ for the jth atom in the unit cell and $d_{hk\ell}$ is the interplanar spacing for the set of planes defined by the Miller indices, h, k, ℓ. The general temperature factor expression is

$$T = \exp[-2\pi^2(U_{11}h^2a^{*2}+U_{22}k^2b^{*2}+U_{33}\ell^2c^{*2} +$$

$$2U_{12}hka^*b^*+2U_{13}h\ell a^*c^*+2U_{23}k\ell b^*c^*)]$$

where U_{ij} are the anisotropic temperature factors expressed in terms of mean square amplitudes of vibration in $\AA^2$ and a*, b* and c* are the reciprocal cell axes.

The computer programs used for initial data treatment, DATCOS and DATRDN, were taken from the XRAY 76 package (54). Structure solution and refinement used SHELX 76 (55). Least-square planes, dihedral angles and torsional angles were calculated by the program NRC-22 (56). Diagrams were prepared using the program ORTEP II (57).

All calculations were carried out on a Cyber 170-730 computer. Scattering curves and anomalous dispersion corrections for all atoms were taken from the "International Tables for X-ray Crystallography" (58,59).

2.3.3 Structure Solution and Refinement

All structures were solved by the heavy atom method in which the coordinates of the heaviest atoms (technetium or technetium and arsenic) were found from three-dimensional Patterson syntheses. Least squares refinement of the heavy atom positions followed by three-dimensional electron difference maps revealed the nonhydrogen atoms. Initially, isotropic temperature factors were used for all atoms. Starting with the heavier atoms, temperature factors were then made sequentially anisotropic. Tests were made at each stage to show that the use of the increased parameters was justified (60). The positions of hydrogen atoms were generally found on subsequent difference maps and were either fixed in calculated positions or refined. Temperature factors for hydrogen atoms were fixed at values 20% greater than the isotropic temperature factors of the atom to which they were attached.

Further refinement using full-matrix least-squares, minimizing $\Sigma w(|F_o| - |F_c|)^2$, where w is the weighting term, was terminated when the maximum shift/error was less than 0.2 for nonhydrogen atoms. The residuals used in SHELX 76 are:

$$R_1 = \frac{\Sigma||F_o| - |F_c||}{\Sigma|F_o|}$$

$$R_2 = \left(\frac{\Sigma w(|F_o| - |F_c|)^2}{\Sigma w F_o^2}\right)^{\frac{1}{2}}$$

Reflections with $I \leq 0$ were classified as unobserved and not used in the refinement process. The moduli of F_o and F_c for all reflections for the structures reported in Chapters 3, 4 and 5 are listed in reference 61.

2.4 Infrared Spectroscopy

Infrared spectra were recorded on a Perkin-Elmer Model 283 Spectrophotometer. The samples were ground with dry KBr and pressed into disks using a (manual) Wilks Mini-Press. The barrel of the Mini-Press also acted as a holder for the KBr disk, thereby minimizing the risk of contaminating the infrared spectrophotometer. Spectra were calibrated with polyethylene or indene.

2.5 Raman Spectroscopy

Raman spectra were recorded on a SPEX 14018 double monochromator using the green (λ 5145Å) exciting line from a Spectra-Physics Model 164 argon ion laser. The spectra were obtained at either room temperature or liquid-nitrogen temperature (or both). Powder samples were contained in glass melting point tubes and liquid samples in n.m.r. tubes.

2.6 Nuclear Magnetic Resonance Spectroscopy

Nuclear magnetic resonance spectra were variously obtained on 250 MHz Bruker WM-250 (^{99}Tc and ^{13}C), 90 MHz Bruker WH-90 (^{99}Tc, ^{19}F and ^{17}O) and 80 MHz Bruker WP-80 (^{13}C and ^{1}H) Fourier transform spectrometers.

Spectra were ^{2}H-locked by using either a deuterated solvent or an external D_2O lock sample located in the probe head, or in the annular cavity formed by placing the sample tube inside a larger precision glass tube. The ^{1}H spectra of TcH_9^{2-} were run in a 5 mm precision glass tube containing an acetone-d_6 capillary for locking. A few spectra, notably for those samples containing HF as a solvent, were obtained without a ^{2}H-lock. ^{99}Tc n.m.r. spectra were recorded with use of a 20μs pulse width. Spectra involving other nuclei were obtained by standard operating procedures.

Spin-lattice relaxation times, T_1, were measured in degassed, vacuum sealed samples by the standard $(\pi-\tau-\pi/2)$ sequence with accumulation of the free induction decay after the $\pi/2$ pulse. The results reported in Chapter 6 were obtained from a least-squares linear regression analysis of the data.

Variable temperature studies were carried out with use of Bruker temperature controllers. Temperatures were measured with a thermocouple inserted directly into the sample region of the probe and were accurate to $\pm$ 1°C.

Magnetic susceptibility measurements by the n.m.r. method were performed on the 60 MHz Varian T60 continuous wave spectrometer.

2.7 Electronic Absorption Spectroscopy

Electronic spectra were recorded on a Cary 14 recording spectrophotometer. The samples were contained in spectrophotometer cells from Hellma. The pathlength in these cells was the normal 1.00 cm but the lateral dimension of the window was 0.40 cm. This feature permitted

the use of small volumes of solution and reduced the risk of radioactive contamination.

2.8 Experiments with Technetium-99m

In the study of penicillamine complexes of technetium (Chapter 3), Whatman Chromatography Paper #1 was used to obtain descending paper chromatograms. Thin layer chromatograms were obtained on silica gel strips from Gelman Instrument Company. In both cases, the solvent was n-butanol-acetic acid-water (4:1:1) and R_f values for species containing ^{99m}Tc were determined with the use of a Packard Model 7201 Radiochromatogram scanner. D-(-)-penicillamine was identified on the chromatograms using a solution of ninhydrin (0.1% in butanol). The paper chromatogram of 1-oxo-2,3,6-(D-penicillaminato-N,S,O)-4,5-(D-penicillaminato-N,S) technetium(V) was cut into twelve strips of equal width and each strip was analyzed for ^{99}Tc with a Chicago Nuclear proportional counter in the Health Physics Department.

Radioscans of the rabbits used in this study were obtained on an Ohio Nuclear Inc. Sigma 410 Radioisotope camera at various time intervals following intravenous injection of the ^{99m}Tc preparations. The data were accumulated on a Digital PDP 11/45 computer and optimized images were displayed on a video screen. These images were then photographed using Polaroid film.

Several 5 to 8 mL aliquots of $^{99m}TcO_4^-$ were eluted from a ^{99}Mo generator. The ^{99m}Tc in these samples was allowed to decay for several weeks in sealed vials. The samples were then used to test the sensitivity of ^{99}Tc n.m.r. spectroscopy (Chapter 6).

CHAPTER 3

TECHNETIUM AND D-PENICILLAMINE

3.1 Introduction

In the early years of radiopharmaceutical development, amino acids and their derivatives were widely used to complex various radionuclides. In particular, technetium-99m complexed by penicillamine was used as such, as well as a means of obtaining other labelled compounds (62). It was soon discovered that a variety of complexes, each with different chemical, chromatographic and physiological behaviour, could be formed with relatively small changes in pH, temperature or reactant concentrations (62). Kits for the routine preparation of ^{99m}Tc-penicillamine complexes as liver, gallbladder and kidney scanning agents took advantage of this sensitivity to labelling conditions (63,64,65,66). Yokoyama and coworkers have reported chromatographic and spectrophotometric characteristics for several penicillamine complexes of technetium (67,68,69,70,71). However, the detailed structures of these complexes remain unknown.

Results from studies of the chemistry of penicillamine complexes of technetium are presented in this chapter. A stable compound was synthesized by ligand substitution of $TcOCl_4^-$, following a procedure outlined by Davison and coworkers (25,26). The crystal structure of this material was determined by X-ray crystallography (72). Nuclear magnetic resonance, vibrational and electronic absorption spectra of

this compound were analyzed (72). A brief tracer study was performed in an effort to relate this work to published reports. Preliminary results involving reduced technetium centres are also reported.

3.2 Preparation of $C_{10}H_{19}N_2O_5S_2Tc$

A solution of $NH_4(TcOCl_4)$ was prepared by dissolving 0.36 g (0.002 mol) of NH_4TcO_4 (Amersham) in 15 mL of concentrated hydrochloric acid. After 10 minutes at room temperature, 3 mL of the dark green solution was added to 0.12 g (0.0008 mol) of D(-)-Penicillamine (Aldrich) dissolved in 5 mL of distilled water. On mixing, the solution became dark reddish brown. It was allowed to evaporate to dryness in air, and crystals suitable for X-ray examination were obtained by recrystallizing the residue from water. Analysis: Calculated for $C_{10}H_{19}N_2O_5S_2Tc$: C, 29.3; H, 4.4; N, 6.8. Found: C, 28.5; H, 4.1; N, 6.3. The density was obtained by flotation in a carbon tetrachloride-bromoform mixture.

3.3 X-ray Studies

Precession photographs showed the crystal was orthorhombic with systematic absences that are consistent with the space group $P2_12_12_1$. An acentric space group was expected since only one enantiomer of a chiral ligand was used in preparing the compound. Crystal data and other numbers related to data collection and structure refinement are summarized in Table 2. The atom parameters from the final refinement are listed in Table 3 and interatomic distances

Table 2

Compound	$C_{10}H_{19}N_2O_5S_2Tc$
Formula weight	410.30
Crystal size (mm)	cylinder, r = 0.05; ℓ = 0.25
Systematic absences	h00; h = 2n+1
	0k0; k = 2n+1
	00ℓ; ℓ = 2n+1
Space group	$P2_12_12_1$
Unit cell parameters (Å)	a = 21.878(5)
	b = 11.711(2)
	c = 5.924(1)
Cell determination	15 reflections, $17.3^o < 2\theta < 25.2^o$
Volume ($Å^3$)	1517.9(5)
Z	4
ρ_{calc}, ρ_{obs} (g cm^{-3})	1.80, 1.78
Linear abs. coefficient (cm^{-1})	11.82
Maximum error on F_o (%)	< 1.5

Table 2 (continued)

Maximum 2θ; reflections measured	55^{o}; h, k, $\pm$ ℓ
Standard reflections (e.s.d. %)	341 (1.30), 032 (1.37)
Temperature (^{o}C)	22
Number of independent reflections	3401
Number with I > 0	3223*
Number with I < 0	178
Final R_1, R_2	0.0592, 0.0439
Final shift/error maximum (average)	
Non hydrogen atoms	0.130 (0.020)
All parameters	0.261 (0.035)
Number of variables	188
Final difference map	
Highest peak (e $\AA^{-3}$); location	1.1; 0.40, 0.58; 0.01 and 0.36, 0.04, 0.14
Lowest valley (e $\AA^{-3}$); location	-1.1; -0.06, 0.22, 0.08 and 0.42, 0.35, 0.52
Weighting scheme	$w = [\ \sigma^2 + (0.0160\ F_o)^2\ ]^{-1}$
Error in an observation of unit weight	0.8453

Table 2 (continued)

F	(0,0,0)	886.8

* 200 reflection was suppressed because of an uneven background (probably beam stop at low 2θ); thus only 3222 reflections were used in the refinement.

Table 3 . Atomic coordinates ($\times 10^4$) and isotropic temperature factors ($Å^2$)($\times 10^3$) for nonhydrogen atoms in $C_{10}H_{18}N_2O_5S_sTc$

Atom	x	y	z	U_{iso}/U_{eq} **
Tc	4018(0)	3051(0)	971(1)	22.4(3)**
O(3)	4564(2)	3168(4)	2894(7)	36(2)**
S	4247(1)	1452(1)	-1107(3)	32.5(7)**
C(1)	3747(3)	371(5)	294(10)	28(1)
C(2)	4120(4)	-334(7)	1915(13)	38(2)
C(3)	3484(4)	-407(7)	-1572(13)	41(2)
C(4)	3230(3)	1019(5)	1510(10)	26(1)
N	3505(2)	1850(5)	3138(9)	27(3)**
C(5)	2872(3)	1782(5)	-95(10)	27(1)
O(1)	3092(2)	2766(3)	-431(6)	26(2)**
O(2)	2397(2)	1412(3)	-1003(9)	38(2)**
S(a)	4287(1)	4193(1)	-1988(3)	32.2(9)**
C(1a)	3990(3)	5595(4)	-1047(10)	24(1)
C(2a)	3902(4)	6348(7)	-3114(13)	43(2)
C(3a)	4441(3)	6146(6)	561(11)	33(2)
C(4a)	3356(3)	5301(5)	14(11)	24(1)
N(a)	3460(3)	4519(4)	1935(9)	24(3)**
C(5a)	2982(3)	6353(5)	622(10)	26(1)
O(1a)	3185(2)	6901(4)	2354(8)	36(2)**
O(2a)	2543(2)	6631(4)	-523(8)	43(3)**

Anisotropic temperature factors U_{ij} ($Å^2$)($\times 10^3$)

Atom	U_{11}	U_{22}	U_{33}	U_{23}	U_{13}	U_{12}
Tc	18.7(2)	17.8(2)	30.6(2)	-1.5(2)	1.9(2)	0.9(2)
03	29(2)	34(3)	44(2)	-6(2)	-8(2)	2(2)
S	30.0(8)	21.1(7)	46.4(9)	-5.5(8)	12.2(9)	-1.0(6)
N	24(3)	30(3)	27(2)	4(3)	-3(2)	8(3)

Table 3 . (continued)

Atom	U_{11}	U_{22}	U_{33}	U_{23}	U_{13}	U_{12}
O(1)	29(2)	15(2)	33(3)	2(2)	-3(2)	-1(2)
O(2)	30(2)	22(2)	62(3)	6(3)	-18(3)	-4(2)
S(a)	37.0(9)	23.8(8)	35.7(9)	-3.4(7)	14.8(7)	-2(7)
N(a)	27(3)	15(3)	31(3)	1(2)	4(2)	-1(2)
O(1a)	36(3)	32(2)	40(2)	-12(2)	-8(2)	17(2)
O(2a)	39(3)	40(3)	50(3)	-7(2)	-22(2)	12(2)

Atomic coordinates and isotropic temperature factors ($\mathring{A}^2$) for hydrogen atoms ($\times 10^3$)

Atom	x	y	z	U
H(21)	442(3)	-78(5)	123(12)	43
H(22)	394(3)	-87(6)	290(11)	43
H(23)	433(3)	11(6)	292(12)	43
H(31)	384(3)	-79(6)	-237(11)	45
H(32)	326(3)	7(6)	-280(13)	45
H(33)	324(3)	-82(6)	-78(13)	45
H(4)	296(3)	64(5)	229(10)	30
H(N1)	319(3)	225(5)	396(11)	31
H(N2)	372(3)	156(5)	402(11)	31
H(21a)	384(3)	706(7)	-262(12)	51
H(22a)	354(3)	609(6)	-411(12)	51
H(23a)	432(3)	641(6)	-375(12)	51
H(31a)	431(3)	683(6)	108(11)	37
H(32a)	481(3)	626(5)	-38(10)	37
H(33a)	452(3)	564(6)	173(11)	37

Table 3. (continued)

Atom	x	y	z	U*
H(4a)	311(3)	489(5)	-106(12)	29
H(N1a)	361(3)	497(6)	290(13)	30
H(N2a)	316(3)	427(6)	241(11)	30
H(O1a)	298(3)	741(6)	281(12)	43

* Temperature factors were fixed at values 20% greater than the isotropic temperature factors of the atoms to which they were attached.

** $U_{eq} = \frac{1}{3}(U_{11} + U_{22} + U_{33})$

and angles are listed in Table 4. The structure reported is consistent with the known chirality of the ligand. Nevertheless, the opposite chirality was tested by changing the signs of all positional parameters and refining until the maximum shift/error was less than the value in Table 2. The residual indices $R_1 = 0.0617$ and $R_2 = 0.0539$ indicate the reported structure is correct at the 99.5% confidence level (60).

The molecule is shown in Figure 3. The structure comprises a distorted octahedron of ligand atoms about the technetium atom. There is a short Tc-O(oxo) bond (1.657(4)Å), which is a characteristic feature of metal-oxo centres in many Tc(V) and Re(V) complexes (73,74). The S and N atoms of the two ligating D-penicillamine groups form a cis arrangement in the equatorial plane and are bent away from the oxo group in the usual manner. The reason the O(3)-Tc-N angle is smaller than O(3)-Tc-N(a) (91.1(2) vs. 99.1(2)°) appears to be because of the steric effects of the sixth coordinated oxygen atom, O(1), of the ionized carboxylate group. Coordination angles involving this atom and other ligand atoms in the same D-penicillamine molecule are all smaller than between O(1) and corresponding atoms in the other D-penicillamine group (O(1)-Tc-S, 82.9(1) vs. 92.1(1)°; O(1)-Tc-N, 70.0(2) vs. 72.9(2)°). The Tc-O(1) distance (2.214(4)Å) is much longer than the Tc-O(3) distance but is comparable to the Tc-N distances and appears to indicate a relatively strong bond, in contrast to many bonds trans to a M - O group (74,75). The reason for this argument is that the nonbonded O(1)...N , N(a), and O(1)...S distances (2.537(7), 2.613(6), 2.986(4)Å) are generally considerably shorter than the sum

Table 4. Interatomic distances (Å) and angles (deg) for $C_{10}H_{19}N_2O_5S_2Tc$*

Tc-O(1)	2.214(4)	Tc-N	2.209(6)	Tc-S	2.296(2)
Tc-O(3)	1.657(4)	Tc-N(a)	2.185(5)	Tc-S(a)	2.283(2)
N-C(4)	1.497(8)	C(4)-C(1)	1.541(9)	C(1)-S	1.868(7)
N(a)-C(4a)	1.478(8)	C(4a)-C(1a)	1.563(9)	C(1a)-S(a)	1.852(5)
C(1)-C(2)	1.507(10)	C(1)-C(3)	1.544(10)	C(4)-C(5)	1.521(9)
C(1a)-C(2a)	1.522(10)	C(1a)-C(3a)	1.515(9)	C(4a)-C(5a)	1.523(9)
C(5)-O(1)	1.265(7)	C(5)-O(2)	1.248(7)		
C(5a)-O(1a)	1.289(7)	C(5a)-O(2a)	1.220(7)		
O(3)-Tc-S	106.2(2)	O(3)-Tc-N	91.1(2)	O(1)-Tc-S	82.9(1)
O(3)-Tc-S(a)	107.0(2)	O(3)-Tc-N(a)	99.1(2)	O(1)-Tc-S(a)	92.1(1)
O(1)-Tc-N	70.0(2)	S-Tc-N	84.5(2)	S-Tc-N(a)	154.7(2)
O(1)-Tc-N(a)	72.9(2)	S(a)-Tc-N(a)	83.3(2)	S(a)-Tc-N	161.8(2)
O(1)-Tc-O(3)	158.5(2)	S-Tc-S(a)	90.55(6)	N-Tc-N(a)	93.7(2)
Tc-S-C(1)	100.8(2)	S-C(1)-C(2)	109.7(5)	S-C(1)-C(3)	107.5(4)
Tc-S(a)-C(1a)	101.4(2)	S(a)-C(1a)-C(2a)	108.5(4)	S(a)-C(1a)-C(3a)	109.8(4)
S-C(1)-C(4)	107.7(4)	C(2)-C(1)-C(3)	109.6(6)	C(2)-C(1)-C(4)	111.7(5)
S(a)-C(1a)-C(4a)	103.7(4)	C(2a)-C(1a)-C(3a)	110.0(5)	C(2a)-C(1a)-C(4a)	109.7(5)
C(3)-C(1)-C(4)	110.6(6)	C(1)-C(4)-C(5)	112.0(5)	C(1)-C(4)-N	109.1(5)
C(3a)-C(1a)-C(4a)	114.8(5)	C(1a)-C(4a)-C(5a)	113.2(5)	C(1a)-C(4a)-N(a)	108.0(5)
N-C(4)-C(5)	103.2(5)	C(4)-N-Tc	104.1(4)	C(4)-C(5)-O(2)	119.7(5)
N(a)-C(4a)-C(5a)	113.7(5)	C(4a)-N(a)-Tc	111.8(4)	C(4a)-C(5a)-O(2a)	120.5(5)
C(4)-C(5)-O(1)	115.9(5)	O(2)-C(5)-O(1)	124.4(6)	C(5)-O(1)-Tc	115.2(4)
C(4a)-C(5a)-O(1a)	113.9(5)	O(2a)-C(5a)-O(1a)	125.6(6)		

* Possible hydrogen bonds (Å): O(2)-O(1a), 2.544(6); O(2a)-N, 3.008(7); O(2a)-N(a), 2.982(7).

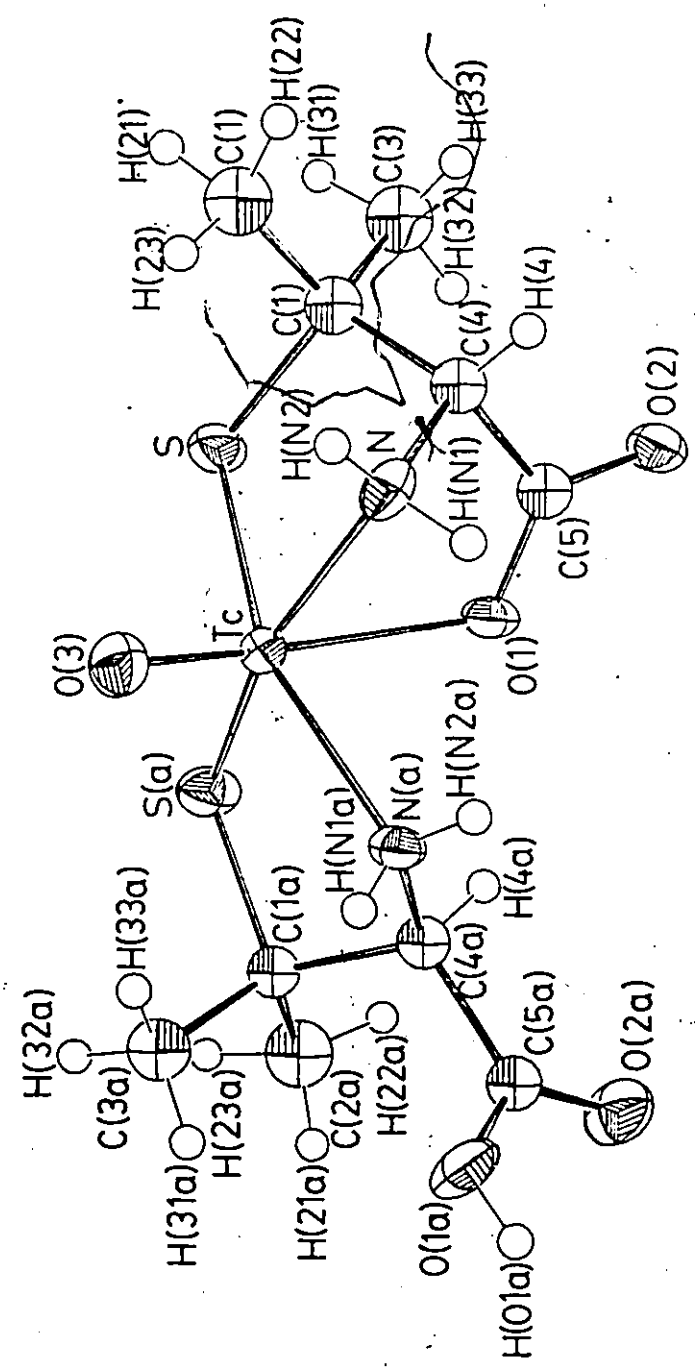

Figure 3. The molecule $C_{10}H_{19}N_2O_5S_2Tc$.

of the van der Waals radii (2.90, 3.25Å), (76) implying strong repulsion which must be countered by strong bonding; and even O(1)...S(a) (3.238(4)Å) is comparable to the O(3)-S distances and to the sum of the radii. This effect has also been observed in a rhenium complex where a coordinated oxygen atom was found to be trans to a M=O group (77).

The Tc-S distances are normal (73) as are most of the bond lengths and angles within the D-penicillamine molecule (78,79). Angles in the bound ligands involving the coordinated atoms differ slightly from those in the free ligand (78,79) and M-S-C(1), M-S(a)-C(1a), M-N-C(4), M-N(a)-C(4a) and M-O(1)-C(5) are all 2-3° larger than corresponding angles in a cobalt complex (M = Tc or Co) (80,81). The Tc-N bonds (2.185(5), 2.209(6)Å) are longer than normal (range 2.07-2.16Å)(26,82,83) and close to the value obtained for Tc-N trans to Tc=O (2.259(4)Å)(26) where a structural trans effect is known to occur (74). There is no such structural effect present here, and yet, as noted above, the Tc-N bonds are as long as Tc-O(1), which is trans to Tc=O. The lengthening of Tc-N must be caused by the steric interactions mentioned above.

It is interesting to compare this structure to structures that have been postulated for Tc-penicillamine complexes (71,84). Firnau has suggested that an oxotechnetium(IV) core is chelated by the S and N atoms of two penicillamine molecules (84). The structure reported here is quite different but it still satisfies the requirements that Firnau identified as necessary for substances that are excreted by the liver and is more consistent with the known chemistry of technetium

and rhenium. Yokoyama has suggested that a compound labelled Complex I has a structure involving tridentate (S,N,O) and bidentate (S,N) penicillamine moieties but also has assigned an oxidation state of (IV) to technetium in a Tc=O core (71). Evidence supporting the reformulation of both these postulated structures to that of the complex reported here is presented in later sections of this chapter.

The packing of the molecule within the unit cell is shown in Figure 4. The most important feature of the packing is a very strong hydrogen bond between O(2) of one molecule and O(1a) of a molecule related by the 2_1 axis at ¼, ½, 0. The molecules thus form a spiral up the c direction. There are further, weaker hydrogen bonds between pairs of molecules in this spiral (O(2a)...N(a) , 2.982(7)Å; O(2a)... N, 3.008(7)Å). Between spirals, the interactions are solely van der Waals, and as a result, the spirals pack in an hexagonal net, as shown in Figure 5.

3.4 Spectroscopic Studies

The electronic spectrum is shown in Figure 6 for reference purposes since Kramer (85) has suggested that the colour of technetium complexes is very dependent on whether the pairs of N and S atoms in the equatorial planes are mutually cis or mutually trans. An absorption maximum of 420 nm has been reported as characteristic of Yokoyama's Complex I (67).

The ^{1}H and ^{13}C n.m.r. spectra of the complex are presented in Table 5. The resonances occur in the regions expected for each of the functional groups (86,87). Because each region contains pairs of peaks, the solid state structure appears to persist in solution. The doubling

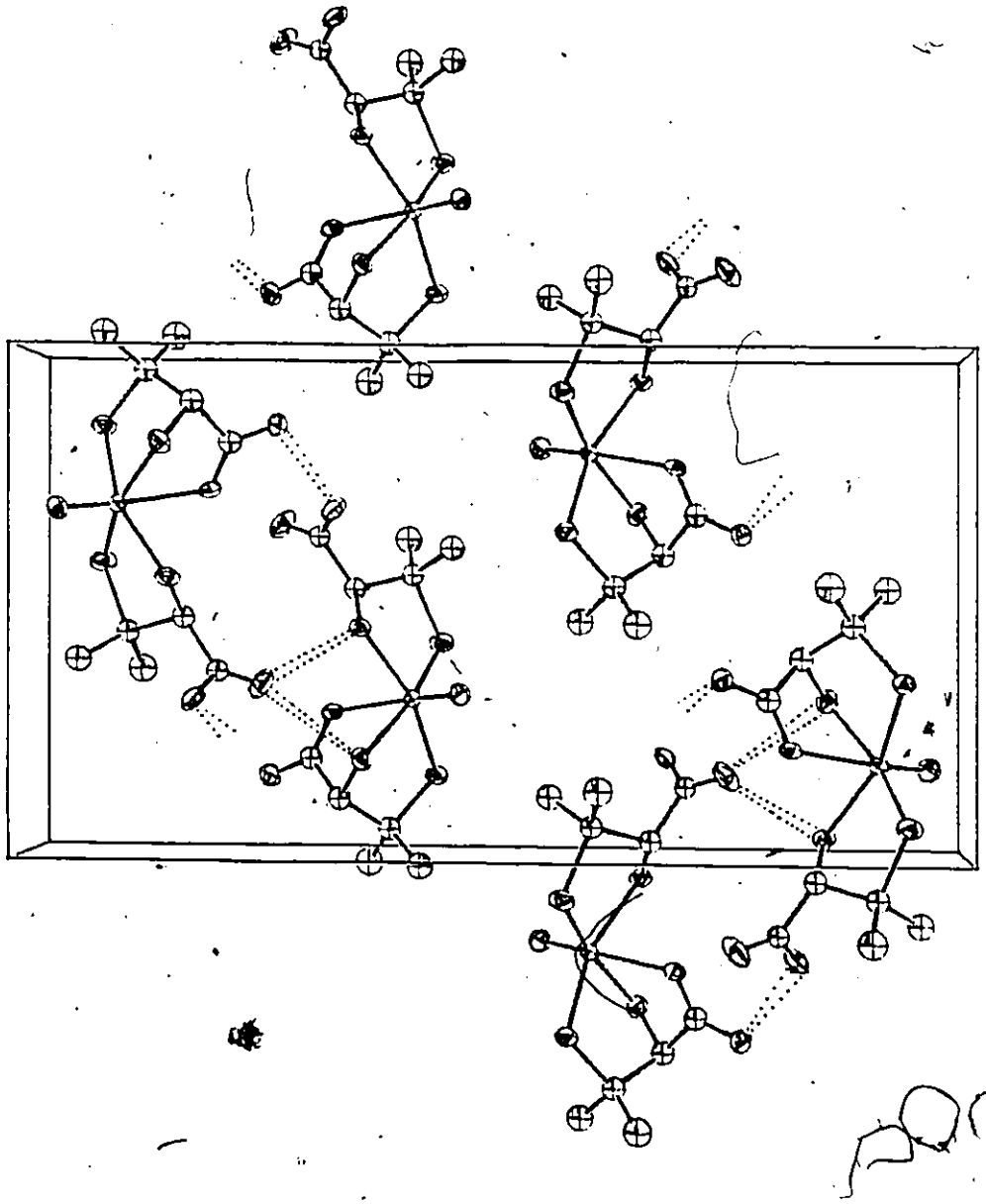

Figure 4. The unit cell contents of $C_{10}H_{19}N_2O_5S_2Tc$. The $\underset{\sim}{a}$ and $\underset{\sim}{b}$ axes are parallel to the bottom and side of the page, respectively, and the view is along $\underset{\sim}{c}$.

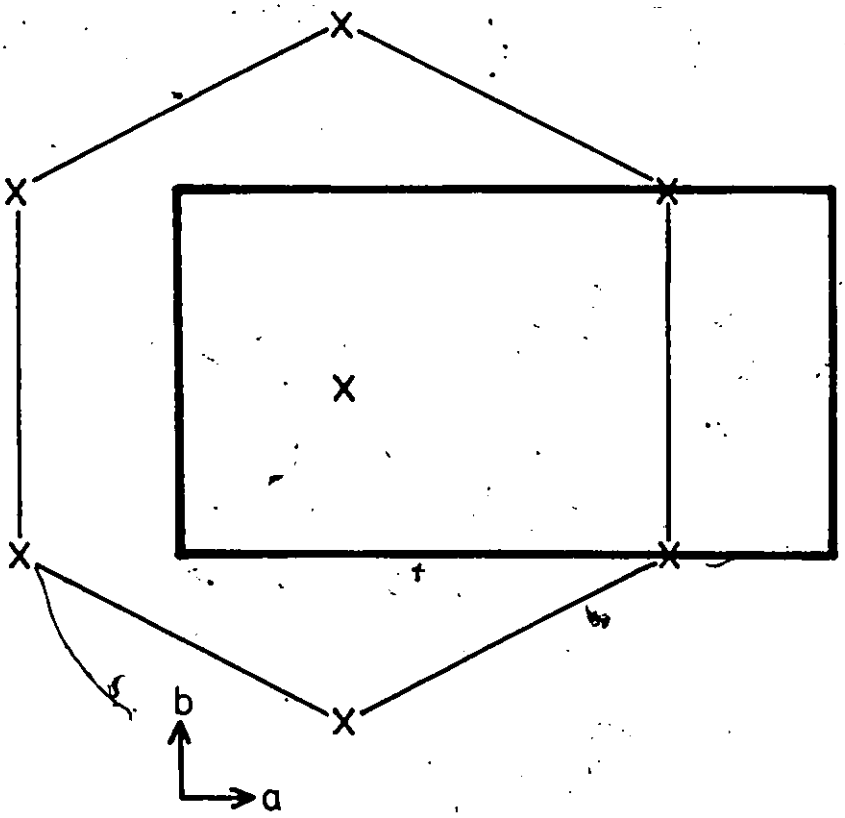

Figure 5. Arrangement of the spiral chains in the unit cell, showing the hexagonal net. X marks the spiral axis. The projection is the same as in Figure 4.

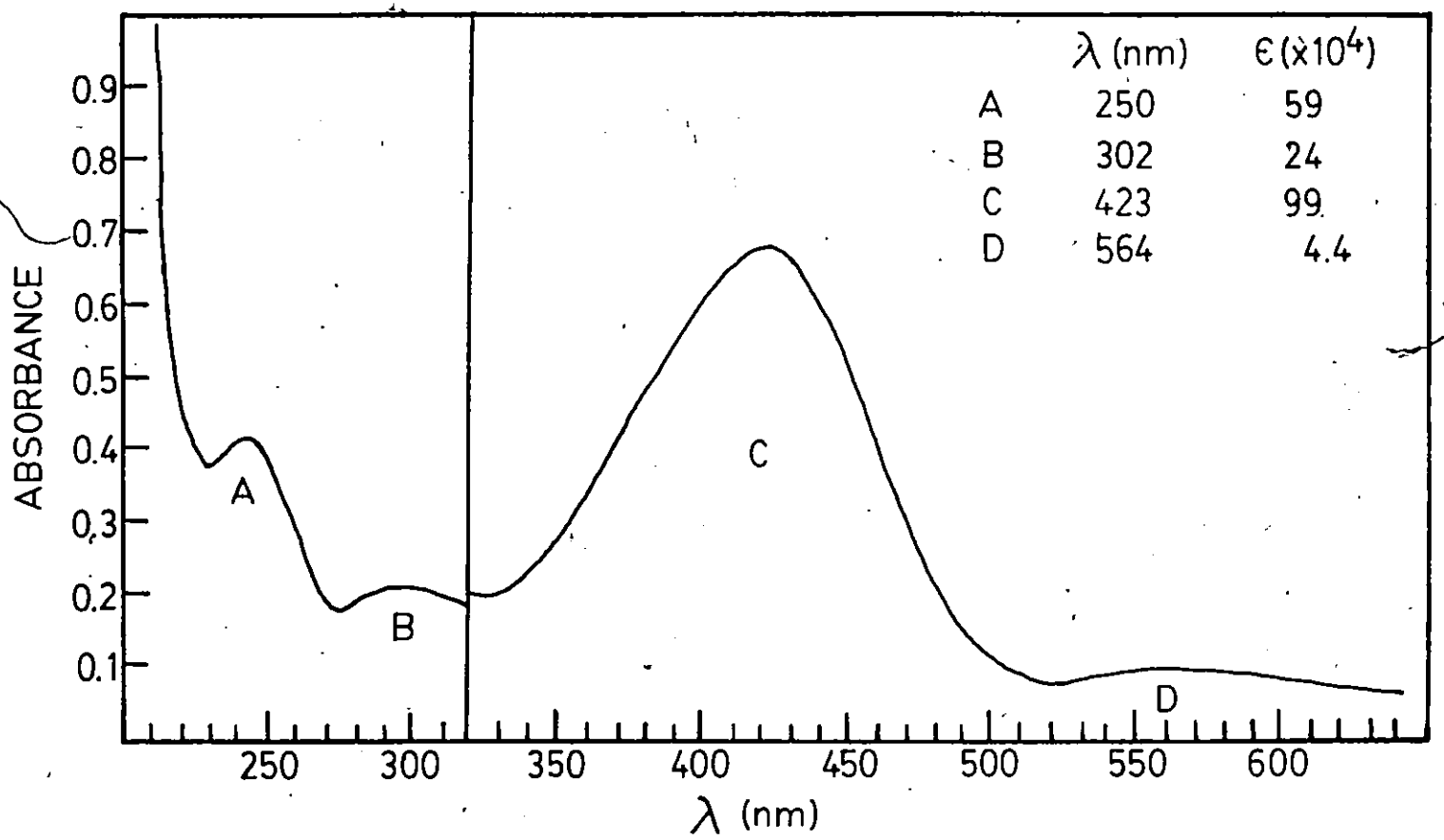

Figure 6. Electronic absorption spectrum of $C_{10}H_{19}N_2O_5S_2Tc$

Table 5. ^{1}H and ^{13}C n.m.r. spectra of $C_{10}H_{19}N_2O_5S_2Tc$ *

Functional Group	$\delta_{^1H}$, ppm	$\delta_{^{13}C}$, ppm
— CH_3	1.44 1.48 1.71 1.84	24.32 28.92 30.10+
— C —		52.98** 56.05**
— C — H	3.19 3.55	66.94** 71.77**
— NH_2	5.68# 6.52#	
— COO^-		171.87 173.11

---

* Samples (0.09M) were dissolved in DMSO-d_6. Chemical shifts are with respect to internal TMS.

\+ This resonance was approximately twice as intense as other peaks in the spectrum.

** Assignments are based on an off-resonance spectrum.

\# Broad lines (no special precautions were taken to dry the solvent).

of the signals is shown schematically in Figure 7 for the ^{13}C n.m.r. spectrum of $C_{10}H_{19}N_2O_5S_2Tc$. The ^{13}C n.m.r. spectrum of a cobalt(III) complex in which penicillamine is N,S bonded to the metal is included for comparison (88). There is no clear-cut correlation between these two spectra, so assignment of individual peaks to the tri- or bidentate D-penicillamine moieties was not attempted. It is interesting to note that signals from the two carboxylate carbon atoms in the technetium complex are so close to each other.

The vibrational spectra of the technetium complex and D-penicillamine are given in Table 6. Some assignments of the bands have been attempted based on previous work (89,90,91) and the arguments contained herein.

The D-penicillamine ligand exhibits a typical Zwitterion spectrum in the infrared; that is, it has the vibrations of both an ionized carboxyl group (CO_2^-) and an amine salt (NH_3^+). The NH_3^+ asymmetric and symmetric stretching vibrations give rise to a broad, strong band over the range 3200-2400 cm^{-1}. There are several peaks on the low-frequency wing, which continues to 2200 cm^{-1}, and a prominent, isolated band at 2027 cm^{-1} (a combination band produced by NH_3^+ motions).

The NH_3^+ deformations are assigned as 1588 (asymmetric) and 1518 cm^{-1} (symmetric)(typical ranges 1665-1585 and 1530-1490 cm^{-1}). The CO_2 stretches are assigned as 1612 (asymmetric) and 1397 cm^{-1} (symmetric)(typical ranges 1605-1555 cm^{-1} and 1425-1393 cm^{-1}). The C-H and CH_3 vibrations occur virtually unshifted for both ligand and complex and fall in characteristic regions: the C-H deformation occurs at

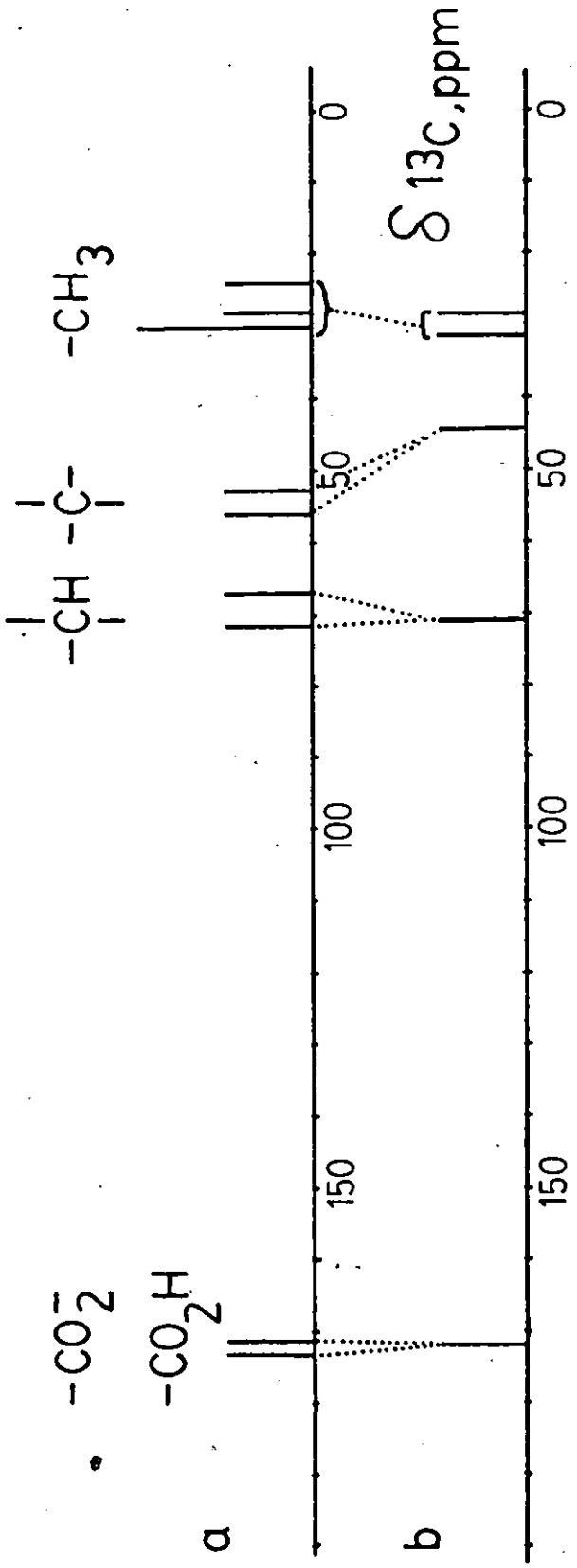

Figure 7. ^{13}C n.m.r. spectra of (a) $C_{10}H_{19}NO_5S_2Tc$ and (b) $C_9H_{18}N_5O_2SCo$

Table 6. Vibrational spectra(cm^{-1})(Relative intensities in parentheses)

D-penicillamine		$C_{10}H_{19}N_2O_5S_2Tc$		
IR	Raman	IR	Raman (av of 3 spectra)	Assignment
		3314(44)		
		3244(64)		$\nu(NH_2)$asym
		3224sh		$\nu(NH_2)$asym
3162(75)				$\nu(NH_3^+)$asym
		3157(21)		
		3135sh		$\nu(NH_2)$sym
3145sh				$\nu(NH_3^+)$sym
	3015(19)			
	2980(56)			$\nu(CH_3)$asym, several components
		2862(25)		
2958(91)	2961(27			double
2923(90)	2929(77)	2941(17)		
2903sh	2902(14)	2907(5)		$\nu(CH)+2x1457$
2864(33)	2862(7)	2862(11)		$\nu(CH_3)$sym
2853(32)				$\nu(CH_3)$sym
2781sh	2777(4)			2x1397
2741(24)				2x1373
2721(22)				
2601(11)br				
	2590(10)			
2504(8)	2511(50)br			ν(S-H)

Table 6 (continued)

D-penicillamine		$C_{10}H_{19}N_2O_5S_2Tc$		
IR	Raman	IR	Raman (av of 3 spectra)	Assignment
2261(5)				
2027(3)				NH_3^+ comb band
		1677(73)br		ν(C=O)
1612(38)	1626(5)br			$\nu(CO_2^-)$asym
1588(98)	1596(4)br	1589(62)		$\delta(NH_3^+)$asym(ligand), $\delta(NH_2)$complex
1556(38)				
1518(100)	1515(7)			$\delta(NH_3^+)$sym
1472(11)	1471(4)			
1457(7)	1454(21)	1457(47)		$\delta(CH_3)$asym
1437(13)	1439(21)	1437(5)		
		1413(72)br		ν(C-O)
1397(34)	1394(19)			$\nu(CO_2^-)$sym
1387(15)	1386(14)	1387(22)		$\delta(CH_3)$sym, in-phase and out-of-phase
1373(12)		1372(44)		
1336(25)	1336(30)			δ(C-H)
		1314(14)		δ(C-H)+$\nu(CO_2^-)$sym
		1303(10)		
1278(27)	1279(6)			NH_3^+ rock
		1249(20)		NH_2 twist
1208(6)		1208(16)		ν(C-N)
1195(28)	1192(12)	1193(10)		

Table 6 (continued)

D-penicillamine		$C_{10}H_{19}N_2O_5S_2Tc$		
IR	Raman	IR	Raman (av of 3 spectra)	Assignment
1163(33)	1159(15)	1156(18)br		CH_3 twists
1138(8)				
	1119(12)sh	1113sh	1119(10)	ν(C-C-N)
1092(38)	1090(15)	1097(34)		
1054(43)	1052(10)	1047(33)		CH_3 wag
1012(37)	1008(9)	1002(22)		ν(C-C)
961(33)	959(24)	958(100)	952(100)	ν(Tc=O) complex
				NH_2 wag
918(24)	918(24)	914(32)		CH_3 rock
		896(22)		NH_2 wag
885(33)	883(12)	883(12)		ν(N-C-C)
869(54)	869(23)			δ(SH)
		824(49)		NH_2 rock
754(72)	754(24)	763(67)		CH_3 rock
		735		NH_2 rock
		724(8)		
		709(37)		δ(C=O)
		698(7)		π(C=O)
674(37)	673(26)			CO_2 scissor
		609(71)		CO_2^- rock
570(67)	575(33)			

Table 6 (continued)

D-penicillamine		$C_{10}H_{19}N_2O_5S_2Tc$		
IR	Raman	IR	Raman (av of 3 spectra)	Assignment
540(63)	546(100)	555(39)		ν(C-S)
		489(25)	491(6)	ν(Tc-O)
464(54)	466(6)			$\tau(NH_3^+)$
		458(42)		ν(Tc-N)
		443(29)	440(11)	
405(42)	402(10)	412(51)	406(18)	δ(O-C-C-N)
		384(56)	386(25)	δ(O-Tc-O)
355(25)	355(24)	360(33)		δ(C-C-S)
321(28)br	329(11)	330(5)		δ(C-C-S), CH_3 torsion
		293(33		ν(Tc-S)
	281(13)	286(5)		
		272(14)		δ(O-Tc-O)
246(6)	252(12)	249(6)		
	208(14)		208w	δ(Tc-N)
	150(37)			
	135(13)		140w	δ(S-Tc-S)
	114(40)		114(9)	
	100(8)			

1336 cm^{-1} (typical range 1340-1315cm^{-1}). The bands at 1387 and 1373 cm^{-1} result from the in-phase and out-of-phase interaction of the symmetric deformations of the CH_3 group; the bands at 1457 and 1437 cm^{-1} result from the asymmetric deformations. CH_3 group twists, wags, and rocks are assigned to bands that follow the usual order of frequency and for which wags show greater intensity than twists. The NH_3^+ group (ligand) and NH_2 group (complex) twists, wags, and rocks fall in similar order.

The ligand can coordinate to a metal via the N, S, and O sites, and the Tc complex contains one ligand coordinated at all three sites and one ligand coordinated through N and S only. Neither retains the Zwitterion form.

The spectra of the Tc complex are therefore expected to show several major differences from those of the ligand: (1) presence of pairs of Tc-S, Tc-N, and single Tc=O, Tc-O stretching and deformation vibrations, (2) presence of two types of CO_2 group vibrations -- carboxylic acid in one ligand and coordinated CO_2 groups in the other, (3) absence of S-H vibrations, and (4) absence of Zwitterion spectra and presence of NH_2 group vibrations.

In addition, we may expect a general doubling of the other vibrations in the complex because of the presence of two ligands and some frequency shifting of vibrations in the complex.

(1) The region 760-300 cm^{-1} of both spectra contain several bands: some unique to the ligand, others unique to the complex. The C-S, Tc-S, Tc-O, and Tc-N stretches and the CO_2 deformations are all

expected to fall in this region, and obviously there will be ambiguities; thus, although we can make reasonable tentative assignments for these bands, positive assignments are not possible. The Tc=O stretch is assigned as the very intense 958-cm^{-1} band and happens to fall near the NH_2 wag (and NH_3^+ wag of the ligand). The Tc-N stretches are tentatively assigned as 458 and 443 cm^{-1}. The Tc-S stretch is assigned as the 293-286 cm^{-1} doublet.

(2) Two CO stretches are assigned for the complex. Only the C-O bond lengths of the carboxylic acid ligand are significantly different and hence the C-O band may appear broadened rather than split. Bands between 502 and 555 cm^{-1} which show shifts of +40 cm^{-1} on formation of a metal complex have been designated as CO_2^- rock modes in the Zwitterions of several amino acids (89). For D-penicillamine, such behaviour is found in the Tc complex where the band at 570 cm^{-1} (ir, ligand) disappears in the complex and a new band of similar intensity appears at 609 cm^{-1} (+ 39 cm^{-1}). This can be assigned as the CO_2^- rock. By comparison with alanine, the D-penicillamine bands at 754, 674 and 570 cm^{-1} probably all have a substantial CO_2^- contribution (89). Other CO_2 deformations are assigned at 709 and 698 cm^{-1} (complex) and 674 and 464 cm^{-1} (ligand).

(3) The S-H stretching vibration occurs at 2511 cm^{-1} and the deformation at 869 cm^{-1} (for the ligand only); these bands are absent for the complex, as expected.

(4) The complex shows the presence of NH_2 vibrations, and the Zwitterion spectrum is absent, as expected.

Groups containing S tend to have bands that are more intense in the Raman than in the infrared region. Comparison with other thiols

suggests that ν(C-S) should occur close to 585 cm^{-1} (similar to 2-methyl-2-propane-thiol and tert-butyl sulfides). Further studies of the penicillamine molecule have shown that the band at 548 cm^{-1} exhibits the characteristics of C-S modes: it does not shift on deuteration; it is the most intense Raman band; and it is highly polarized (92). The band at 555 cm^{-1} (ir, complex) is the most likely candidate for ν(C-S) in the complex because the C-S bond lengths are similar and we do not expect a large ligand-complex frequency shift.

Metal-sulfur complexes exhibit bands in the range 250-360 cm^{-1} (ν(M-S)) and also one or two bands in the range 586-654 cm^{-1}. The origin of the latter is uncertain although they have the magnitude of ν(M-S) overtones and could result from Fermi resonance between such overtones and ν(C-S) modes. Also, the ligand may show two ν(C-S) bands because of rotational isomerism. Deformations of the S-M-S unit occur at 145-155 cm^{-1}.

3.5 Tracer Studies

Solutions for tracer studies were prepared as follows. Approximately 40 mCi of $^{99m}TcO_4^-$ in saline solution (0.2-0.8 mL) was added to a small vial containing 60 mg of D-penicillamine. For "carrier-added" experiments, the vial also contained 2-6 mg of $NH_4{}^{99}TcO_4$. The resulting solutions were made acidic by addition of two or three drops of concentrated hydrochloric acid and allowed to stand for fifteen to twenty minutes. The solutions were then titrated to pH 7 with 1N NaOH and diluted to a total volume of 6-10 mL.

Descending paper chromatograms showed that the bulk of the

radioactivity was located at an R_f value of 0.7. This value corresponds to that for the coloured spot present in the carrier-added solutions. It is also identical to that of the complex whose structure is reported above. Some chromatograms presented a small fraction (less than 20%) of the total radioactivity at R_f = 0.25 which can be assigned to $^{99m}TcO_4^-$. D-penicillamine itself had an R_f value of 0.6. With thin layer chromatography, R_f values for the complex were 0.85. D-penicillamine was not well resolved and $^{99m}TcO_4$ was not observed by this technique.

Radioscans of the rabbit injected with a "carrier-free" solution are shown in Figure 8. Within two minutes, much of the radioactivity had localized in the kidneys (shown in black because of the setting of the upper threshold limit) with some activity in the heart. At ten minutes, the liver was poorly defined but visible and considerable radioactivity had appeared in the bladder. The image of the liver was somewhat improved at twenty minutes when the experiment was halted.

A second rabbit was injected with a solution to which carrier $NH_4\ ^{99}TcO_4$ had been added. At three minutes, (Figure 9), much of the activity was located in the kidneys as before but here, the crescent shape of the liver is much more visible. At ten minutes, the bladder was well defined. At thirty minutes, the kidneys were no longer visible and and some radioactivity was observed in the gut. The latter is consistent with the technetium complex passing through the gallbladder. This process was virtually complete after forty-five minutes.

Although the second rabbit was larger than the first, it received proportionately a much larger dose of ^{99m}Tc (900μCi vs 500μCi). This fact, together with the differences in the size and age of the rabbits

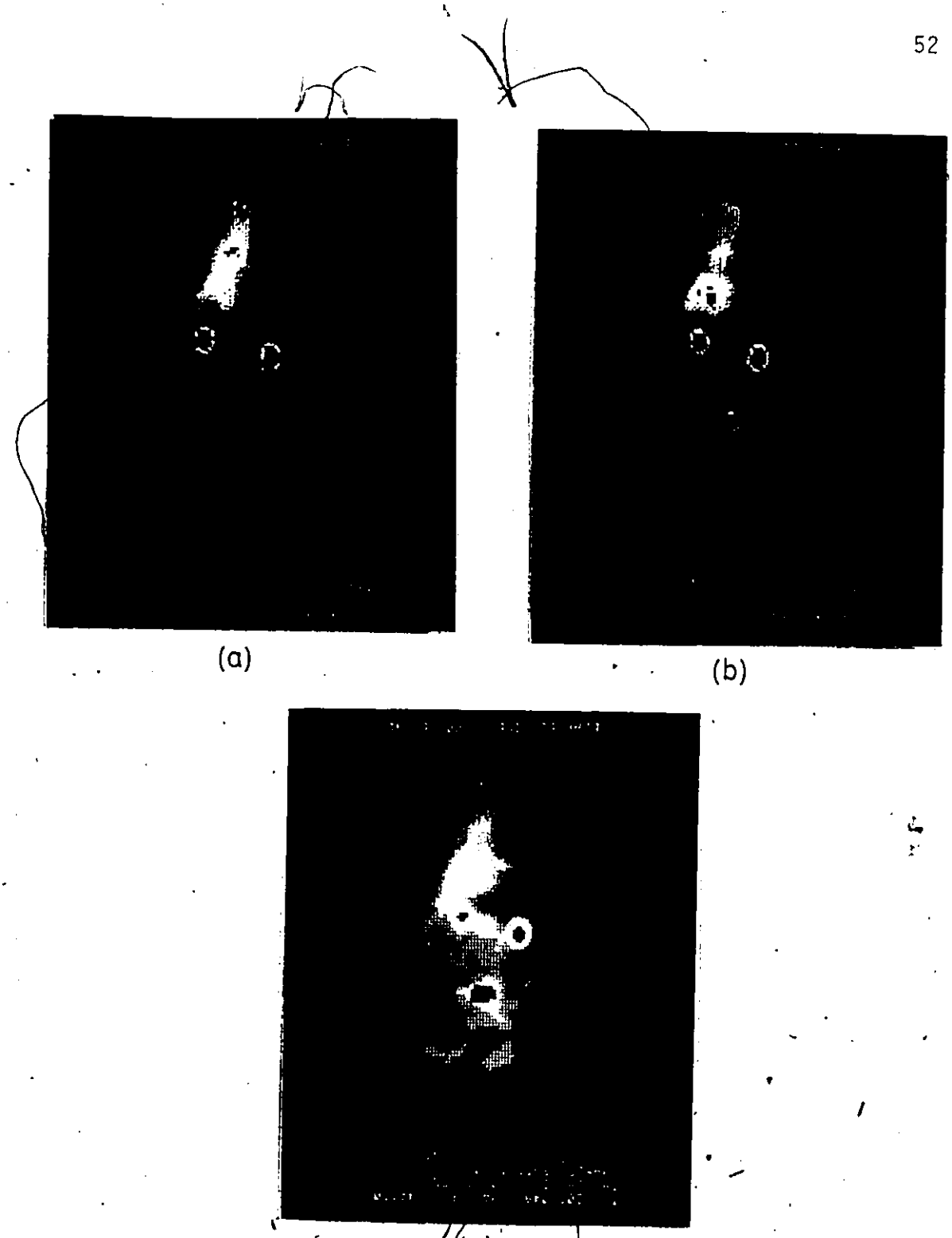

Figure 8. Radioscans of [illegible] injected with a "carrier-free" Tc-penicillamine preparation: [illegible] minutes; (b) 10 minutes; (c) 20 minutes.

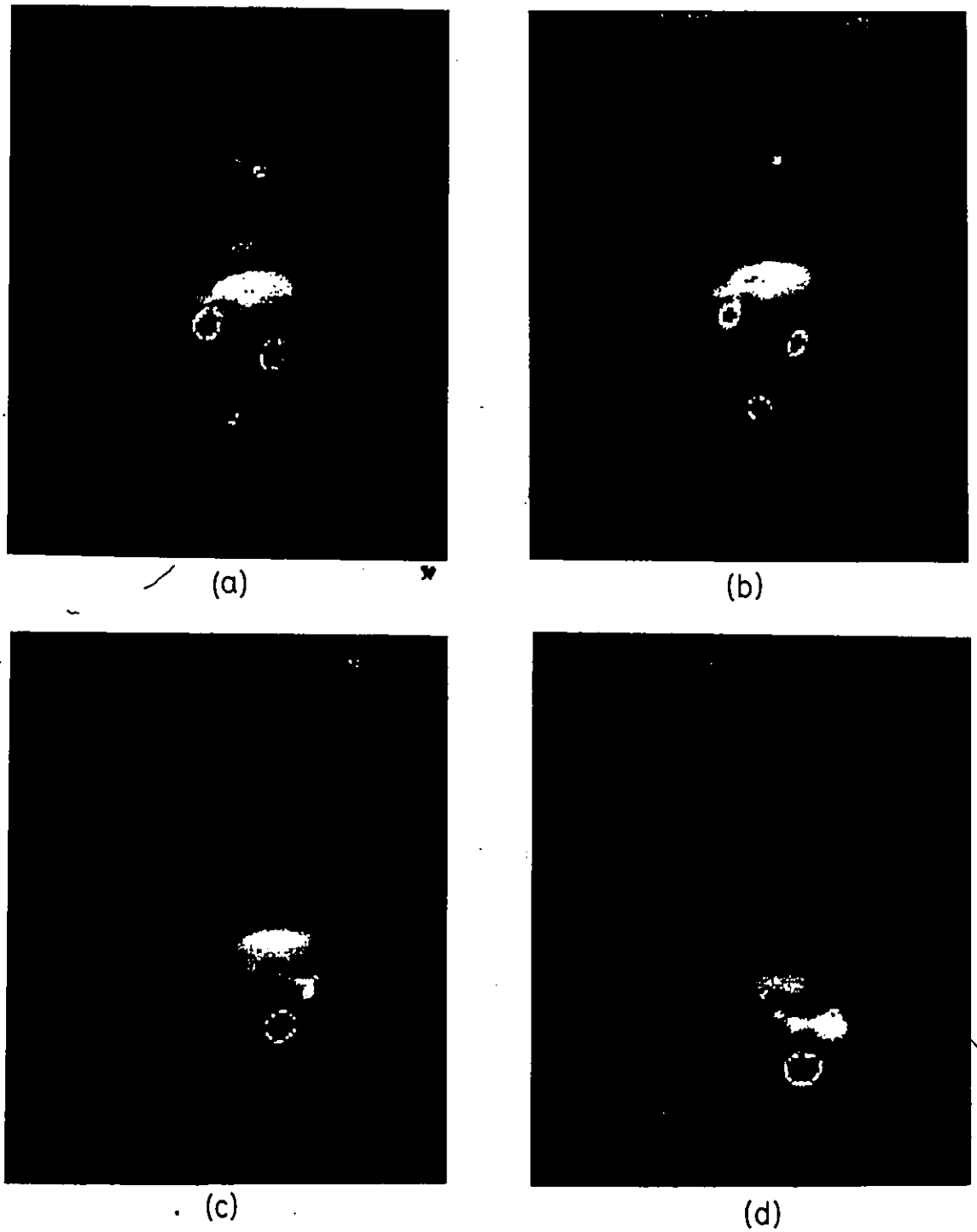

Figure 9. Radioscans of a rabbit injected with a "carrier-added" Tc-penicillamine preparation: (a) 3 minutes; (b) 10 minutes; (c) 30 minutes; (d) 45 minutes.

may account for the differences between the two series of images. All experiments are consistent, however, with results quoted by Krishnamurthy and coworkers who used a similar procedure to prepare an hepatobiliary scanning agent (63,64). The R_f values obtained here are identical to those found by Krishnamurthy who likewise observed radioactivity in the kidneys and bladder (63,64). Our results show that less than 5% of the administered dose appears in the liver or gallbladder. Krishnamurthy does not quote results in these terms but estimates based on the data reported are in good agreement with this low fraction. Direct comparisons are not possible since the earlier images were obtained with a pinhole collimator (64) as opposed to the parallel-hole collimator used here.

This brief tracer study serves to establish that the complex used by Krishnamurthy (63,64) has the molecular structure described in section 3.3 and that the structure suggested by Firnau (84) is incorrect with respect to the oxidation state of technetium, the coordination of a carboxylate group and the cis arrangement of sulfur atoms.

It should be noted that the low specificity of this preparation makes it undesirable for routine use as an hepatobiliary scanning agent -- a role which is currently filled by complexes of ^{99m}Tc involving substituted iminodiacetic acids (e.g. ^{99m}Tc-HIDA where HIDA = N(2,6-dimethylphenylcarbamoylmethyl)iminodiacetic acid) or pyridoxylidene glutamate as ligands (93).

3.6 Reduced Species

Various reducing agents, including sodium dithionite, triphenylphosphine and sodium borohydride were added to solutions of the Tc-

penicillamine complex described above in an effort to obtain a complex in which both penicillamine molecules were bound to the metal ion in a tridentate manner. The fact that these experiments were not successful indicates that the above complex is very stable.

An alternate synthetic route to a reduced complex involved substitution of chloride ligands in salts of $TcCl_6^{2-}$ by D-penicillamine. This method produced unstable orange-coloured solutions (λ_{max} 470 nm) in both aqueous and alcoholic media. The colour changed to reddish brown in the space of a few hours (aqueous) or days (methanol or ethanol). The stability was only slightly improved by degassing the solvents or by working under a vacuum.

Solutions with identical absorption spectra could be obtained with K_2TcBr_6 as a reactant, indicating that the orange complex probably does not incorporate halide ions. Similar results were obtained when a thiourea complex of technetium(III), $Tc(SC(NH_2)_2)_6Cl_3$, was used as a starting material. This result, together with the known reducing power of penicillamine itself, suggested that the orange complex contained technetium in the oxidation state III. A measurement of the magnetic susceptibility of a freshly-prepared sample using the n.m.r. method of Evans (94) gave an effective magnetic moment of 2.53 Bohr magnetons (Table 7). This value is in good agreement with that found by the same method for the thiourea complex (Table 7). This effective magnetic moment corresponds to two unpaired electrons which would be expected for a low-spin complex of technetium(III) and is reduced from the spin-only value by spin-orbit coupling.

Table 7. Magnetic Susceptibility Measurements

	Orange Complex	$Tc(SC(NH_2)_2)_6Cl_3$
$\Delta\nu$(Hz)*	37.5	38.0
C(g mL^{-1})**	4.26×10^{-2}	6.05×10^{-2}
χ***	6.28×10^{-6}	4.28×10^{-6}
Molecular Weight(M)	397.42+	662.08
χ_M^{corr}++	2.69×10^{-3}	2.93×10^{-3}
μ_{eff}(Bohr magnetons)#	2.53	2.65

---

* $\Delta\nu$ is the frequency separation between two ^1H n.m.r. signals from the methyl protons of t-butanol in two different environments -- one signal is from t-butanol in a 5 mm tube containing D_2O and the other is from t-butanol in an insert containing the metal complex dissolved in D_2O.

** C is the concentration of the metal complex in the insert.

*** $\chi = \frac{3\Delta\nu}{2\pi\nu C} + \chi_o$, where ν = 60 MHz and $\chi_o = -0.72\times10^{-6}$.

\+ Based on the formulation, $Tc(penicillamine)_2$.

++ $\chi_M^{corr} = M\chi - \chi_{DIA}$, ($\chi_{DIA}$ is a diamagnetic correction).

\# $\mu_{eff} = 2.83(\chi_M^{corr}T)^{\frac{1}{2}}$, (T=298 K)

The orange complex is insoluble in nonpolar solvents such as benzene, which suggests the possibility of an ionic species. Addition of $(C_4H_9)_4NCl$ or $NaPF_6$, however, failed to precipitate a salt. Small amounts of an orange solid could be precipitated, presumably as a potassium salt, from original solutions in ethanol by volume reduction and subsequent addition of diethyl ether. The vibrational spectra of this solid are presented in Table 8. There is no band in the 950 cm^{-1} region which indicates that the complex does not include a Tc=O group. Bands arising from CO_2^- rocking and deformation modes are also absent. At the same time, strong bands at 1650 and 1385 cm^{-1} are observed in the infrared spectrum. These values are characteristic of coordinated carboxylate groups and the large frequency separation of 265 cm^{-1} indicates considerable covalent character in the M-O bond (95). The most intense bands in the Raman were observed in the region of metal ligand stretches (350-500 cm^{-1}).

Based on the available evidence, the orange complex is tentatively identified as an anionic complex of technetium (III) which is chelated by all three binding sites of each of two penicillamine molecules. The instability of such a complex would be expected since the oxygen and nitrogen ligands are not very polarizable and therefore would not help stabilize this lower oxidation state. A similar instability has been observed in the complex $Tc(HIDA)_2^{2-}$ in which oxygen and nitrogen ligands are coordinated to a technetium(III) centre (96). The HIDA complex is known to reduce water to produce hydrogen gas (96). The reducing ability of technetium(III) in this complex may explain why the orange complex is fairly stable in ethanol but is unstable in aqueous solutions even when

Table 8. Vibrational spectra (cm^{-1}) for the orange complex

Infrared	
3450 s,br	1335 m,br
3110 s,vbr	1275 m
2985 s,br	1215 w
2965 s,br s,br	1130 w
1720 w,br	1025 w
1650 s,br	905 w
1590 sh	780 m
1505 m,br	540 w
1460 sh	465 w
1395 s,br	402 w
1385 s	320 w

Raman	
492 vw	332w
464 m	305 w
440 vw	292 w
397 s	252 w
358 w	

the water has been thoroughly degassed and the solution is kept under a vacuum.

The orange complex is readily oxidized to form the complex described in section 3.3. This was established by the electronic absorption spectra of aging solutions of the orange complex which were identical to that shown in Figure 6. Furthermore, precession photographs showed that the only crystalline material isolated from these preparations was the same as the above complex (section 3.3). These results demonstrate the stability of the technetium(V) complex and relate to Yokoyama's Complex I which was also obtained from the reaction of $TcCl_6^{2-}$ with penicillamine (70). Complex I likewise had an absorption maximum at 420 nm, was very stable in a variety of environments and behaved similarly to Krishnamurthy's complex (63,64) when injected into rats. Therefore, the hepatobiliary agent of Krishnamurthy and the Complex I of Yokoyama can both be identified with the technetium(V) complex characterized in this chapter.

Yokoyama has reported the formation of a large number of complexes involving penicillamine and technetium (67). During the study of the orange complex described here, solutions of several different colours and various degrees of instability were observed. None of these solutions could be identified with any of the absorption maxima reported by Yokoyama. This serves to emphasize the complexity of the chemistry of penicillamine, with its three binding sites of differing polarizability, when in the presence of a metal which can exist in a variety of oxidation states.

CHAPTER 4

TOWARD RADIOPHARMACEUTICAL DESIGN

4.1 Introduction

In the previous chapter, the synthesis and characterization of a complex containing the stable oxotechnetium(V) core was described. The stability of such a complex, particularly in aqueous solution, makes it suitable for use as a scanning agent. Davison and others have studied a series of bis(dithiolato) (45,73,97) and bis(2-mercapto-ethanolato) (8) complexes of oxotechnetium(V). Both classes of complexes can be readily synthesized by the reduction of pertechnetate in the presence of the dithiol or 2-mercaptoethanol ligand or by metathesis from $TcOCl_4^-$. X-ray crystallographic studies (73,98) have established the core structures of these complexes to be square pyramids with the oxo-oxygen occupying the apical position and either four sulfur atoms or two oxygen atoms and two sulfur atoms constituting the basal plane.

The catechol complex of technetium, whose crystal structure is described in the following section, forms a logical extension of this series to include a $Tc(V)OO_4$ core structure. There are a number of ^{99m}Tc-containing radiopharmaceuticals with ligands that are purely oxygen donors, including citrate ion, glucoheptonate, gluconate and mannitol (40). The oxidation state of technetium in these polyol complexes was assumed to be IV (99). The characterization of the catechol and ethyleneglycolate (100) complexes is a strong indication that the

correct oxidation state of technetium in such radiopharmaceuticals is V.

On the basis of this work, the concept arose of a ligand that would be capable of sequestering the oxotechnetium(V) core after reduction of TcO_4^- in aqueous solution, and that could be functionalized with a variety of groups and molecules to generate, conceivably, a family of radiopharmaceuticals. The ligand was designed to be tetradentate so that it would exploit the geometrical preferences of the oxotechnetium(V) core by spanning the basal plane of a square pyramid; avoid the geometrical isomerism possible with unsymmetric bidentate ligands; maximize the kinetic inertness of the final complex by taking advantage of the chelate effect; and provide a backbone amenable to chemical modification (100). The complex whose structure is described in section 4.3 forms part of a study into ligands which satisfy these criteria.

4.2 The Crystal Structure of Tetrabutylammonium Bis(catecholato) oxotechnetate(V)

Crystals of the title compound were obtained from A. Davison. The synthesis, method of crystallization and elemental analysis of the salt have been reported elsewhere (100). The density was obtained by flotation in an aqueous zinc bromide solution. Precession photographs showed the crystals were monoclinic with systematic absences that were consistent with the space group C2/c or Cc. The centric space group was chosen and justified by the successful solution of the structure. The structure was initially solved using data collected at room temperature.

The temperature factors of two carbon atoms (C(13),C(14)), suggested they were disordered so each was replaced by two carbon atoms and parameters, including the occupancy, were allowed to vary. In an effort to avoid the disorder problem, a second data set was collected at -55°C. Although the disorder persisted, the temperature factors of all atoms in the structure were reduced, thus improving the overall accuracy of the structure. This low temperature data set was used to provide the structural information reported here. Geometric calculation showed that two sets of atoms involved in the disorder had to be correlated and so the occupancy of each disordered atom was fixed at 0.5.

Crystal data and other numbers related to data collection and structure refinement are summarized in Table 9. The atom parameters from the final refinement are listed in Table 10, and interatomic distances and angles are listed in Table 11. Least squares planes and dihedral angles are listed in Table 12.

The anion is shown in Figure 10. The coordination geometry is square pyramidal, just like the $TcOS_4$ and $TcOS_2O_2$ complexes studied (43,73,98) previously, with the Tc atom 0.701(1)Å above the plane of the four oxygen atoms. Because each pair of catechol oxygen atoms is nearly coplanar with their benzene ring, the rings are bent away from the oxo-group, making a dihedral angle of 162° with the base of the square pyramid and 144° with each other. The Tc-O distances (Tc-O(1) 1.648(5), Tc-O(2) 1.956(3), Tc-O(3) 1.958(3)Å) are consistent with values found previously for Tc=O (range 1.610(4)-1.679(5)Å) (25,26,45, 72,73,98,101,102,103) and Tc-O bonds (1.950(6)Å) (73). C(1)-C(2)

Table 9.

Compound	$C_{28}H_{44}NO_5Tc$
Formula weight	573.66
Crystal size (mm)	approx. cylinder, r = 0.11, ℓ = 0.25
Systematic absences	hkℓ; h + k = 2n + 1
	hoℓ; ℓ = 2n + 1
	oko; k = 2n + 1
Space group	C2/c
Unit cell parameters	a = 10.392(3), β = 101.74(3)
(Å and deg)	b = 13.835(3)
	c = 20.643(5)
Cell determination	15 reflections; $23.6^{\circ} < 2\theta < 31.9^{\circ}$
Volume ($Å^3$)	2906(1)
Z	4
ρ calc, ρobs (g cm^{-3})	1.28, 1.27(1)*
Linear abs. coefficient (cm^{-1})	5.29
Maximum error on F_o (%)	< 1.0

Table 9 (continued)

Maximum 2θ, reflections measured	55^{o}, ±h, k, ± ℓ
Standard reflections (e.s.d. %)	311(3.74);-1-15(2.34)
Temperature (^{o}C)	-55
Number of independent reflections	2887
Number with I > 0	2755
Number with I < 0, rejected	132
Final R_1, R_2	0.0694, 0.0613
Final shift/error maximum (average)	0.081 (0.017)
Number of variables	179
Final difference map	
Highest peak (e $\AA^{-3}$); location	0.55; 0.05; 0.09; 0.22
Lowest valley (e $\AA^{-3}$); location	-0.40; 0.49, 0.40, 0.72
Weighting scheme	$w = [\sigma^2 + (0.0249\ F_o)^2]^{-1}$
Error in an observation of unit weight	1.0589
F(0,0,0)	1202.0

* The density was measured at room temperature. Unit cell parameters used to calculate the density were measured at 22°C and were a = 10.423(2), b = 14.009(2), c = 20.897(3)Å, β = 101.86(2)°.

Table 10. Atomic coordinates for nonhydrogen atoms in $C_{28}H_{44}NO_5Tc$ ($\times 10^4$)

	x	y	z
Tc	0	939.4(3)	2500
O(1)	0	2131(3)	2500
O(2)	1741(2)	389(2)	2519(1)
C(1)	2378(4)	125(3)	3137(2)
C(2)	1641(4)	189(3)	3624(2)
O(3)	369(3)	469(2)	3414(1)
C(3)	2192(5)	-49(4)	4273(2)
C(4)	3488(5)	-355(4)	4416(3)
C(5)	4208(5)	-446(4)	3939(3)
C(6)	3656(4)	-205(3)	3286(2)
N	5000	2466(3)	2500
C(7)	4069(4)	1803(3)	2039(2)
C(8)	3007(4)	2284(3)	1521(2)
C(9)	2310(5)	1522(3)	1051(2)
C(10)	1162(5)	1916(5)	549(3)
C(11)	4262(4)	3115(3)	2887(3)
C(12)	3513(6)	2602(4)	3339(3)
C(13)*	3039(11)	3387(8)	3775(5)
C(14)*	2431(10)	2908(8)	4317(5)
C(13a)*	2470(9)	3227(9)	3574(7)
C(14a)*	3289(41)	3811(12)	4141(7)

Table 10. (continued)

Anisotropic temperature factors U_{ij} ($Å^2$)(x10^3)

Atom	U_{11}	U_{22}	U_{33}	U_{12}	U_{13}	U_{23}
Tc	41.6(3)	41.6(3)	73.1(4)	0	11.3(2)	0
O(1)	61(3)	50(3)	140(5)	0	8(3)	0
O(2)	44(2)	52(2)	62(2)	2(1)	15(1)	11(1)
C(1)	48(2)	41(2)	63(3)	-6(2)	7(2)	1(2)
C(2)	50(2)	53(2)	57(3)	-12(2)	8(2)	-10(2)
O(3)	50(2)	67(2)	57(2)	-4(1)	11(1)	-12(1)
C(3)	71(3)	89(4)	57(3)	-16(3)	5(2)	-10(2)
C(4)	70(3)	85(4)	65(3)	-12(3)	-17(3)	4(3)
C(5)	50(3)	77(3)	85(4)	-3(2)	-4(2)	7(3)
C(6)	49(2)	55(2)	75(3)	1(2)	7(2)	6(2)
N	45(2)	32(2)	79(4)	0	13(2)	0
C(7)	49(2)	39(2)	73(3)	-2(2)	15(2)	1(2)
C(8)	59(3)	53(3)	78(3)	1(2)	1(2)	4(2)
C(9)	67(3)	65(3)	67(3)	-3(2)	13(2)	-2(2)
C(10)	74(3)	103(4)	78(4)	-2(3)	-8(3)	-1(3)
C(11)	5(3)	43(2)	97(4)	8(2)	9(2)	-10(2)
C(12)	93(4)	59(3)	124(5)	10(3)	54(4)	-13(3)
C(13)*	43(6)	65(7)	106(10)	4(5)	-2(6)	-55(6)
C(14)*	58(6)	92(7)	102(9)	10(5)	15(6)	-43(7)
C(13a)*	73(9)	88(9)	112(11)	-22(8)	23(8)	-43(8)
C(14a)*	95(10)	122(12)	116(12)	4(8)	7(8)	-39(10)

Atomic coordinates** and isotropic temperature factors ($Å^2$) for hydrogen atoms (x10^3)

Atom	x	y	z	$U^{\#}$
H(3)	169	-1	458	86
H(4)	384	-57	480	88
H(5)	510	-68	404	85
H(6)	412	-31	294	73

Table 10 (continued)

Atom	x	y	z	U#
H(71)	457	144	184	64
H(72)	365	144	231	64
H(81)	237	261	175	76
H(82)	330	275	126	76
H(91)	209	104	130	78
H(92)	292	118	82	78
H(101)	58	219	81	99
H(102)	145	240	24	99
H(103)	74	142	30	99
H(111)	373	339	262	76
H(112)	496	362	319	76
H(121)*	267	221	304	96
H(122)*	413	206	364	96
H(131)*	228	378	349	88
H(132)*	384	377	402	88
H(141)*	215	344	460	92
H(142)*	290	256	454	92
H(143)*	174	252	414	92
H(1212a)*	299	197	307	96
H(122a)*	418	233	377	96
H(131a)*	210	372	329	121
H(132a)*	192	284	372	121
H(141a)*	407	330	446	142
H(142a)*	259	405	441	142
H(143a)*	358	456	403	142

* Disordered atoms with site occupation factors fixed at 0.5.

** Hydrogen atoms were fixed in calculated positions.

Temperature factors for hydrogen atoms were fixed at values 20% greater than the isotropic temperature factors of the atoms to which they were attached.

Table 11. Interatomic distances (Å) and angles (deg) for $C_{28}H_{44}NO_5Tc$

Tc-O(1)	1.648(5)	Tc-O(2)	1.956(3)	Tc-O(3)	1.958(3)
O(2)-C(1)	1.362(5)	O(3)-C(2)	1.361(5)	C(1)-C(2)	1.385(7)
C(2)-C(3)	1.384(6)	C(3)-C(4)	1.385(7)	C(5)-C(5)'	1.359(8)
C(5)-C(6)	1.394(7)	C(6)-C(1)	1.379(6)		
N-C(7)	1.519(5)	C(7)-C(8)	1.524(6)	C(8)-C(9)	1.514(6)
N-C(11)	1.511(6)	C(11)-C(12)	1.509(8)	C(12)-C(13)	1.554(13)
C(9)-C(10)	1.514(7)	C(12)-C(13a)	1.541(14)	C(13)-C(14)	1.543(17)
C(13a)-C(14a)	1.530(19)				
O(1)-Tc-O(2)	112.93(7)	O(1)-Tc-O(3)	109.40(9)	O(2)-Tc-O(3)'	81.5(1)
O(2)-Tc-O(3)'	83.6(1)	O(2)-Tc-O(2)'	134.1(1)	O(3)-Tc-O(3)'	141.2(1)
Tc-O(2)-C(1)	113.2(3)	O(2)-C(1)-C(2)	115.3(3)	O(2)-C(1)-C(6)	124.0(4)
Tc-O(3)-C(2)	112.9(3)	O(3)-C(2)-C(1)	115.5(4)	O(3)-C(2)-C(3)	124.0(4)
C(2)-C(1)-C(6)	120.6(4)	C(1)-C(6)-C(5)	118.9(5)	C(6)-C(5)-C(4)	120.0(4)
C(1)-C(2)-C(3)	120.4(4)	C(2)-C(3)-C(4)	118.2(5)	C(3)-C(4)-C(5)	121.9(5)
C(7)-N-C(7)'	105.7(3)	C(7)-N-C(11)	111.3(2)	C(11)-N-C(11)'	107.1(4)
C(7)-N-C(11)'	110.8(2)	N-C(7)-C(8)	117.0(3)	C(7)-C(8)-C(9)	109.3(4)
C(8)-C(9)-C(10)	113.4(4)	N-C(11)-C(12)	115.4(4)	C(11)-C(12)-C(13)	107.0(6)
C(11)-C(12)-C(13a)	114.5(6)	C(12)-C(13)-C(14)	110.1(8)	C(12)-C(13a)-C(14a)	102.7(8)

Table 12. Least squares planes and dihedral angles (deg)

Plane	Distance of atoms from plane (Å)
1. O(2)O(3)O(2')O(3')	Tc 0.7014(4), O(1) 2.348(5)
2. O(2)C(1)C(2)O(3)	O(2) -0.002(3), C(1) 0.011(4), C(2) -0.012(4), O(3) 0.003(3), Tc(1) -0.2732(4), C(3) -0.016(6), C(6) 0.076(4)
3. C(i) i= 1-6	C(1) -0.011(4), C(2) 0.007(4), C(3) 0.003(6), C(4) -0.013(6), C(5) 0.005(5), C(6) 0.007(4), O(2') -0.021(3), O(3) 0.066(3)
4. O(2)'C(1)'C(2)'O(3)'	
5. C(i)' i= 1-6	

Dihedral angles (deg):

Planes	Angle
1 - 2	162.4(3)
2 - 3	2.1(4)
3 - 5	141.1(5)
2 - 4	143.9(4)

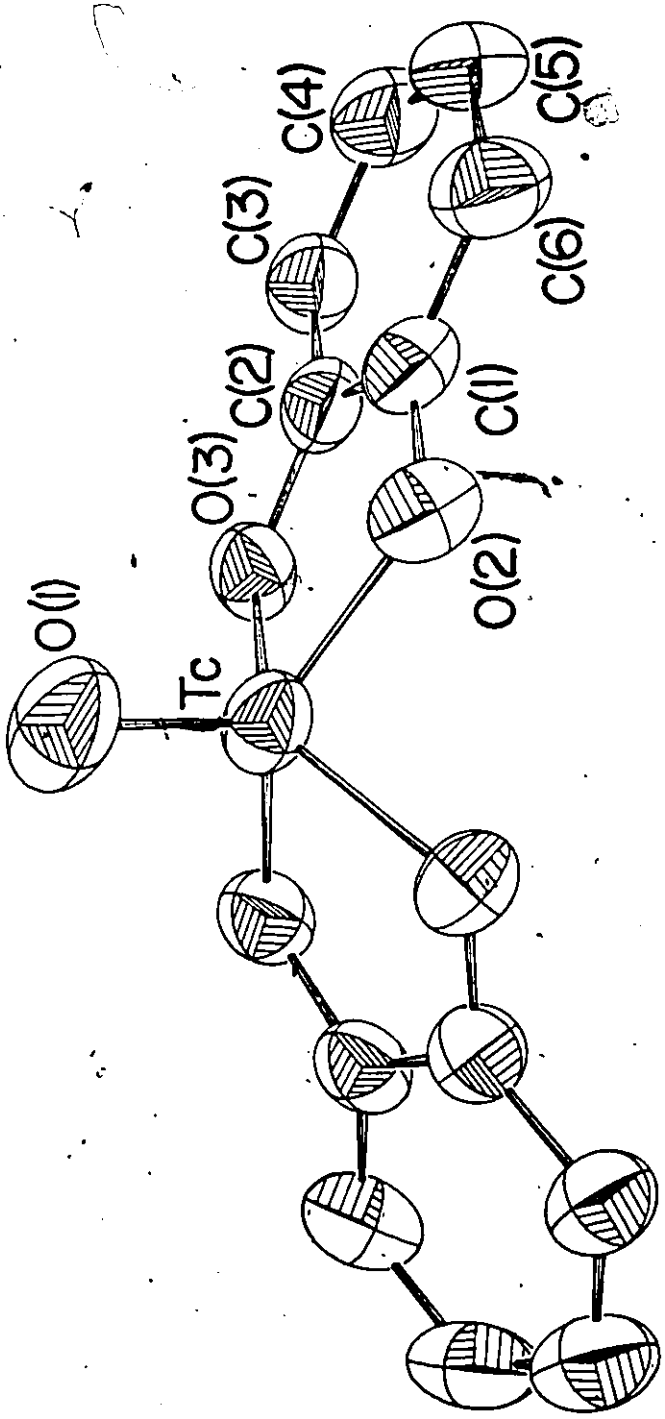

Figure 10. The anion $TcO(O_2C_6H_4)_2^-$

(1.3985(7)Å) and both C-O distances (1.362(5), 1.361(5)Å) correlate well with those found in $K_2VO(O_2C_6H_4)_2^-$ (104) and oxo-molybdenum complexes (105) (range 1.376(12)-1.397(6)Å, 1.352(6)-1.37(2)Å respectively). However, the C-O distances are longer than those normally found in complexes of many metals not containing oxo-groups (range 1.32(1)-1.355(6)Å) (104,105) and C(1)-C(2) is generally shorter than equivalent bonds in the same large group of metal complexes (1.402(7)-1.414(5)Å) although there are three exceptions (1.348(10)-1.366(11)Å) (105).

A structurally analogous low spin d^2 complex is found in the oxoosmium(VI) diester $OsO(O_2C_2H_4)_2$ (106). The Os-O (terminal) bond length is 1.66(1)Å; and the average O-(terminal)-Os-O(ester) bond angle is 110°. There is an Os=O stretch at 992 cm^{-1} in the infrared spectrum. All of these parameters agree well with those of $TcO(O_2C_6H_4)_2^-$.

The packing of the title compound within the unit cell is shown in Figure 11. The cation and anion form an ion pair with the crystallographic two-fold axis passing through O(1) and Tc in the anion and N in the cation. The cation, which has the n-butyl groups arranged in a flat cross, lies below the anion (the oxo group is defined as up) with the cross parallel to the base of the square pyramid. Bond lengths and angles within the cation are unremarkable. One pair of n-butyl groups eclipses the two catechol rings and the alternate pair of n-butyl groups lies between the catechol rings. The former pair is thus restricted in its geometry; the latter pair is not and shows the disorder mentioned above. The separation between a C(14) atom at (x,y,z) and another at (1/2-x, 1/2-y, -z) is 2.996(8)Å

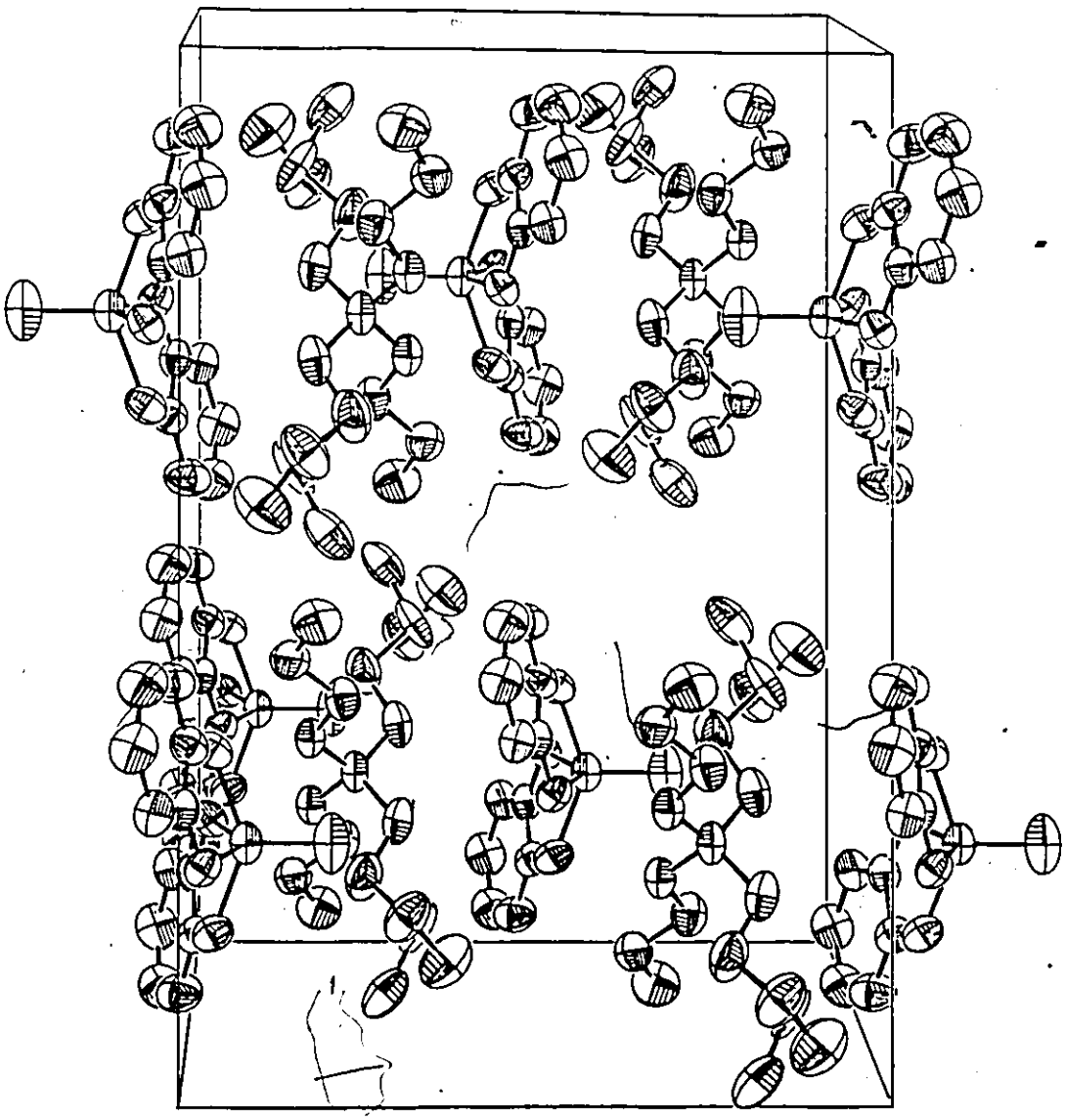

Figure 11. The unit cell contents of $C_{28}H_{44}NO_5Tc$. The b and c axes are parallel to the bottom and side of the page, respectively, and the view is down c^*

This is much less than the distance expected between two methyl groups which may be taken as the 4.154(8)Å between C(14) and a C(14P) atom related by the above transformation. This indicates that the maximum occupancy at the C(14) site is 0.5 rather than the 0.6 value obtained when the occupancy factors were refined. For this reason, the occupancy factors for the disordered atoms were fixed at 0.5.

The ion pairs are packed in layers parallel to the ab plane at roughly Z = 1/4, 3/4. Each layer is composed of rows of ion pairs along the a direction with the oxo-groups of one layer lying between cation pairs in the next row. Layers at Z = 1/4 and 3/4 have the oxo-groups pointing in opposite directions along b. Forces between layers are van der Waals.

There is a strong band in the infrared spectrum of this catecholato complex at 970 cm^{-1} which can be assigned to the Tc-oxo (apical) stretch. It is instructive at this point to compare the relevant structural parameters and ν(Tc=O) of representative members of the class of complexes with the $TcOS_xO_{4-x}$ core (Table 13). The average Tc-S bond length seems to be the same in the $TcOS_4$ and $TcOS_2O_2$ and the average Tc-O (ligand) distance also seems to be independent of core type, be it $TcOS_2O_2$ or $TcOO_4$. The distance of the metal from the basal plane varies a substantial amount from core to core but not in a systematic manner. There is, however, a slight but significant systematic variation in the Tc-oxo bond length across the series which is correlated with changes in the Tc=O stretching frequency. As sulfur atoms are replaced by oxygen atoms, the band shifts to higher

Table 13. Comparison of bond distances(Å) and ν(Tc=0)(cm^{-1}) for some $TcOX_4$ cores

Complex	Tc-oxo	Tc-S(av)	Tc-O(av)	Tc to basal plane	νTc=0	ref.
$TcO(O_2C_6H_4)_2^-$	1.648(5)		1.957(3)	0.701(1)	970	
$TcO(S(CH_2)_2O)_2^-$	1.662(5)	2.290(3)	1.950(6)	0.720(1)	948	(98)
$TcO(SCH_2COS)_2^-$	1.672(8)	2.320(4)		0.791	950	(73)
$TcO(S(CH_2)_2S)_2^-$	1.64(1)	2.300(13)		0.761(2)	940	(97,103)
$TcO\ Cl_4^-$	1.610(4)			0.66	1016	(25)
$TcO(SCH_2CONCH_2-)_2$	1.679(5)	2.287(3)		0.771(5)	945	(101,102)
$TcO(pyrazolyl)Cl_2$	1.656(3)				970	(26)
TcO(D-penicllamine)	1.657(4)	2.289(2)			958	(72)

energy, at least for the ethaneditholato - 2-mercaptoethanolato - catecholato series. Thus, as the average ligating atom becomes "harder", the Tc=O bond gets stronger. The result is expected since an inverse bond length - ν(M=O) relationship has already been demonstrated by Cotton and Wing (107) for molybdenum and Howard-Lock, Lock and Turner (108) for rhenium.

Recently, de Kieviet investigated (109) the structure of ^{99m}Tc-glucoheptonate (a renal agent) by studying the properties of a ^{99}Tc complex formed by Sn(II) reduction of a solution of $^{99}TcO_4^-$ and excess glucoheptonate. The product (which was not isolated) showed bands in the infrared spectrum at 930 and 970 cm^{-1}, suggesting the presence of the Tc=O moiety. It was further deduced from the infrared spectrum that the carboxylate-oxygen of the ligand was involved in the binding. The final identification (109) of this unisolated species as bis(glucoheptanato)oxotechnetium(V) is consistent with the complex whose structure is presented here and with the properties of the bis(1,2-ethanediolato)oxotechnetium(V) anion which has recently been characterized (100).

These results establish that stable bis(1,2-diolato)-oxotechnetium(V) complexes can be prepared and are resistant to hydrolysis in the presence of excess diol. They clearly suggest that the same type of core structure can exist in ^{99m}Tc-radiopharmaceuticals with oxygen-donor ligands.

4.3 The Crystal Structure of Methyltriphenylarsonium Oxo(N,N'-ethylenebis(2-mercaptoacetamido))technetate(V)

Crystals of the title compound were obtained from A. Davison. The synthesis, method of crystallization and elemental analysis of the salt have been reported elsewhere (101). The density was obtained by flotation in an aqueous zinc bromide solution. Precession photographs showed the crystals were monoclinic with systematic absences that were consistent with the space group $P2_1/c$. The Patterson map was analyzed by assuming two heavy atoms in the unit cell. Each of the eight possible solutions was tested and one selected for further refinement. The apparent inconsistency between weighted and unweighted residual indices (R_1 = 0.1167, R_2 = 0.0824) results from a large number of weak reflections in the data.

Crystal data and other numbers related to data collection and structure refinement are summarized in Table 14. The atom parameters from the final refinement are listed in Table 15, and interatomic distances and angles are listed in Table 16. Least squares planes and torsion angles are listed in Table 17.

The anion is shown in Figure 12. As predicted (102), the structure is dominated by the oxotechnetium(V) core with two sulfur and two nitrogen atoms of the N,N'-ethylenebis(2-mercaptoacetamide) ligand bent away from the oxo-group to form the base of a distorted square pyramid. The Tc-O bond distance (1.679(5)Å) is equivalent within experimental error to that in cis-$(TcO(SCH_2COS)_2)^-$ (1.672(8)Å) (73). The displacement of the technetium atom above the square plane is also similar (0.772(1)Å vs. 0.791(8)Å, respectively).

Table 14

Compound	$C_{25}H_{26}N_2O_3S_2AsTc$
Formula weight	640.54
Crystal size (mm)	plate, 0.28x0.26x0.14
Systematic absences	hoℓ; ℓ = 2n+1
	oko; k = 2n+1
Space group	$P2_1/c$
Unit cell parameters (Å and deg)	a = 10.203(2), β = 110.37(1)
	b = 13.449(2)
	c = 20.092(2)
Cell determination	15 reflections; $25.0^\circ < 2\theta < 30.1^\circ$
Volume ($Å^3$)	2584.7(7)
Z	4
ρ calc, ρobs (g cm^{-3})	1.65, 1.65(1)
Linear abs. coefficient (cm^{-1})	20.7
Maximum error on F_o(%)	< 1.5%
Maximum 2θ	55°, h, k, $\pm$ ℓ
Standard reflections (e.s.d. %)	131 (1.36) 1 -1 4 (1.62)

Table 14 (continued)

Temperature (^{o}C)	22
Number of independent reflections	2013
Number with $I > 0$	4928
Number with $I < 0$, rejected	1065
Final R_1, R_2	0.1167, 0.0524
Final shift/error, maximum (average)	
non-hydrogen atoms	0.443 (0.054)
all parameters	1.013 (0.073)
Number of variables	255
Final difference map	
Highest peak ($e\text{Å}^{-3}$), location	1.68; 0.70, -0.14, 0.14
Lowest valley ($e\text{Å}^{-3}$), location	-1.48; 0.40, 0.42, 0.34
Weighting scheme	$w = [\sigma^2 + (0.007\ F_o)^2]^{-1}$
Error in an observation of unit weight	0.7305
F(0,0,0)	1282.8

Table 15. Atomic coordinates ($x10^4$) and isotropic temperature factors ($Å^2$)($x10^3$) for non-hydrogen atoms in $C_{25}H_{26}N_2O_3S_2AsTc$

Atom	x	y	z	U_{iso}/U_{eq} **
Tc	3623.5(7)	3200.2(5)	556.1(3)	34.9(4)**
O(1)	4443(6)	3767(3)	1335(2)	48(4)**
S(1)	3020(2)	1611(1)	725(1)	49(2)**
C(1)	4533(9)	966(6)	666(4)	52(2)
C(2)	5402(8)	1543(6)	345(4)	46(2)
O(2)	6387(6)	1175(4)	224(3)	59(4)**
N(1)	4975(6)	2514(4)	214(3)	39(2)
C(3)	5644(9)	3155(7)	-171(4)	54(2)
C(4)	4546(8)	3834(6)	-638(4)	43(2)
N(2)	3528(6)	4007(4)	-291(3)	34(1)
C(5)	2420(8)	4602(6)	-654(4)	43(2)
O(3)	2309(6)	5047(4)	-1203(3)	57(4)**
C(6)	1343(10)	4692(7)	-306(5)	57(2)
S(2)	1288(2)	3584(2)	187(1)	54(2)**
As	-129.9(7)	1739.4(6)	1938.1(4)	34.6(4)**
C(7)	-919(10)	2552(7)	1121(5)	53(6)**
C(8)	-1510(7)	1422(5)	2340(4)	38(2)
C(9)	-2710(9)	1965(6)	2171(4)	51(2)
C(10)	-3720(9)	1716(7)	2476(5)	68(3)
C(11)	-3470(10)	953(7)	2948(5)	66(3)
C(12)	-2270(10)	417(7)	3128(5)	69(3)
C(13)	-1277(9)	636(6)	2821(5)	57(2)
C(14)	1335(7)	2486(5)	2601(4)	37(2)
C(15)	2460(9)	2759(6)	2415(4)	49(2)
C(16)	3517(9)	3345(7)	2884(4)	61(2)
C(17)	3421(9)	3617(6)	3512(4)	54(2)
C(18)	2340(9)	3345(7)	3703(3)	55(2)
C(19)	1257(9)	2752(6)	3251(4)	51(2)
C(20)	628(8)	679(5)	1686(4)	40(2)

Table 15. (continued)

Atom	x	y	z	U_{iso}
C(21)	1888(8)	196(6)	2140(4)	50(2)
C(22)	2466(10)	-641(8)	1942(6)	75(3)
C(23)	1789(11)	-1072(7)	1286(6)	74(3)
C(24)	481(10)	-695(7)	848(5)	66(3)
C(25)	-39(9)	113(6)	1034(4)	57(2)

Anisotropic temperature factors U_{ij} ($\AA^2$)($x10^3$)

Atom	U_{11}	U_{22}	U_{33}	U_{23}	U_{13}	U_{12}
Tc	51.7(4)	31.7(3)	33.3(3)	-0.5(3)	16.9(3)	31.1(4)
O(1)	84(4)	35(3)	38(3)	-8(2)	18(3)	2(3)
S(1)	72(2)	40(1)	54(1)	4(1)	28(1)	-2(1)
O(2)	44(4)	49(3)	92(4)	-17(3)	9(3)	13(3)
O(3)	77(4)	66(4)	42(3)	23(3)	21(3)	19(3)
S(2)	54(1)	62(1)	72(2)	9(1)	36(1)	10(1)
As	33.5(4)	41.2(4)	36.5(4)	2.4(4)	10.7(4)	-3.3(4)
C(7)	51(6)	61(6)	48(6)	24(5)	3(5)	-5(5)

Atomic coordinates and temperature factors ($\AA^2$) for hydrogen atoms ($x10^3$)

Atom	x	y	z	U*
H(1A)	415(7)	33(5)	41(3)	57
H(1B)	503(7)	79(5)	104(4)	57
H(3A)	640(7)	353(5)	15(4)	63
H(3B)	601(7)	277(5)	-39(4)	63
H(4A)	413(7)	366(5)	-104(3)	51

Table 15 (continued)

Atom	x	y	z	U*
H(4B)	499(6)	450(5)	-66(3)	51
H(6A)	159(7)	526(5)	0(4)	64
H(6B)	45(8)	477(5)	-66(4)	64
H(7A)	-137(8)	317(5)	121(4)	65
H(7B)	-20(8)	280(5)	87(4)	65
H(7C)	-164(8)	232(6)	86(4)	65
H(9)	-286(7)	247(5)	191(4)	57
H(10)	-431(8)	208(6)	234(4)	76
H(11)	-418(8)	66(5)	318(4)	78
H(12)	-202(8)	-19(6)	343(4)	85
H(13)	-46(8)	28(5)	290(4)	66
H(15)	262(7)	246(5)	200(4)	61
H(16)	411(7)	352(6)	269(4)	70
H(17)	413(7)	413(5)	380(4)	67
H(18)	218(7)	355(5)	411(4)	66
H(19)	61(7)	258(5)	343(4)	61
H(21)	231(7)	47(5)	263(4)	59
H(22)	308(9)	-66(6)	218(4)	80
H(23)	243(8)	-143(6)	119(4)	84
H(24)	-7(8)	-104(5)	44(4)	77
H(25)	-80(8)	42(5)	77(4)	67

* Temperature factors were fixed at values 20% greater than the isotropic temperature factors of the atoms to which they were attached.

** $U_{eq} = \frac{1}{3}(U_{11} + U_{22} + U_{33} + 2U_{13}\cos\beta)$

Table 16. Interatomic distances (Å) and angles (deg) for $C_{25}H_{26}N_2O_3S_2AsTc$

Tc-S(1)	2.282(2)	Tc-N(1)	1.971(7)	Tc-O(1)	1.679(4)
Tc-S(2)	2.295(2)	Tc-N(2)	1.991(6)	C(3)-C(4)	1.50(1)
S(1)-C(1)	1.81(1)	C(1)-C(2)	1.48(1)	C(2)-O(2)	1.22(1)
S(2)-C(6)	1.80(1)	C(5)-C(6)	1.50(1)	C(5)-O(3)	1.22(1)
C(2)-N(1)	1.373(9)	N(1)-C(3)	1.47(1)	As-C(7)	1.903(9)
C(5)-N(2)	1.371(9)	N(2)-C(4)	1.46(1)	As-C(8)	1.893(8)
As-C(14)	1.905(6)	As-C(20)	1.887(8)	C(8)-C(9)	1.37(1)
C(9)-C(10)	1.41(2)	C(10)-C(11)	1.36(1)	C(11)-C(12)	1.36(1)
C(12)-C(13)	1.39(2)	C(13)-C(8)	1.40(1)	C(14)-C(15)	1.37(1)
C(15)-C(16)	1.40(1)	C(16)-C(17)	1.35(1)	C(17)-C(18)	1.34(1)
C(18)-C(19)	1.41(1)	C(19)-C(14)	1.38(1)	C(20)-C(21)	1.39(1)
C(21)-C(22)	1.39(2)	C(22)-C(23)	1.38(1)	C(23)-C(24)	1.34(1)
C(24)-C(25)	1.37(1)	C(25)-C(20)	1.40(1)		
O(1)-Tc-S(1)	111.0(2)	O(1)-Tc-N(1)	110.8(2)	S(1)-Tc-N(1)	82.6(2)
O(1)-Tc-S(2)	108.9(2)	O(1)-Tc-N(2)	114.2(2)	S(2)-Tc-N(2)	82.2(2)
S(1)-Tc-S(2)	87.41(8)	S(1)-Tc-N(2)	134.6(2)	Tc-S(1)-C(1)	99.1(3)
N(1)-Tc-N(2)	77.8(2)	S(2)-Tc-N(1)	140.0(2)	Tc-S(2)-C(6)	97.8(3)
S(1)-C(1)-C(2)	115.5(6)	C(1)-C(2)-N(1)	112.6(8)	C(1)-C(2)-O(2)	122.2(7)
S(2)-C(6)-C(5)	111.0(6)	C(6)-C(5)-N(2)	113.7(7)	C(6)-C(5)-O(3)	121.9(7)
O(2)-C(2)-N(1)	125.2(8)	C(2)-N(1)-Tc	126.3(6)	C(2)-N(1)-C(3)	118.9(7)
O(3)-O(5)-N(2)	124.4(8)	C(5)-N(2)-Tc	124.0(6)	C(5)-N(2)-C(4)	115.5(6)
Tc-N(1)-C(3)	114.6(5)	N(1)-C(3)-C(4)	107.8(7)	C(7)-As-O(8)	110.1(4)
Tc-N(2)-C(4)	119.4(4)	N(2)-C(4)-C(3)	107.4(7)	C(7)-As-C(14)	107.1(3)
C(7)-As-C(20)	109.5(4)	C(8)-As-C(14)	109.7(3)	C(8)-As-C(20)	111.2(3)
C(14)-As-C(20)	109.2(3)	As-C(8)-C(9)	120.7(6)	As-C(8)-C(13)	120.0(6)
C(9)-C(8)-C(13)	119.4(8)	C(8)-C(9)-C(10)	119.8(8)	C(9)-C(10)-C(11)	119.6(9)
C(10)-C(11)-C(12)	121(1)	C(11)-C(12)-C(13)	120.0(9)	C(12)-C(13)-C(8)	120.0(8)
As-C(14)-C(15)	118.5(6)	As-C(14)-C(19)	120.5(6)	C(15)-C(14)-C(19)	121.0(7)
C(14)-C(15)-C(16)	119.3(8)	C(15)-C(16)-C(17)	119.4(9)	C(16)-C(17)-C(18)	122.0(8)
C(17)-C(18)-C(19)	120.6(9)	C(18)-C(19)-C(14)	117.8(9)	As-C(20)-C(21)	120.1(5)
As-C(20)-C(25)	120.8(5)	C(21)-C(20)-C(25)	119.2(7)	C(20)-C(21)-C(22)	119.8(7)
C(21)-C(22)-C(23)	119.4(8)	C(22)-C(23)-C(24)	120(1)	C(23)-C(24)-C(25)	121.8(8)
C(24)-C(25)-C(20)	119.3(7)				

Table 17. Least squares planes and torsion angles in $C_{25}H_{26}N_2O_3S_2AsTc$

Plane	Distance of atoms from plane(Å)
1. S(1)N(1)N(2)S(2)	Tc 0.772(1), N(1) 0.086(6), N(2)-0.074(6)
2. C(1)C(2)O(2)N(1)	S(1) -0.167(2), Tc 0.822(1), C(3) -0.142
3. C(6)C(5)-)3)n(2)	S(2) -0.807(2), Tc 0.168(1), C(4) 0.117(8)
4. C(8)C(9)C(10)C(11)C(12)C(13)	As 0.019(1)
5. C(14)C(15)C(16)C(17)C(18)C(19)	As -0.079(1)
6. C(20)C(21)C(22)C(23)C(24)C(25)	As -0.082(1)

Torsion angles (deg)

S(1)C(1)C(2)N(1)	6.2(7)
N(1)C(3)C(4)N(2)	30.2(7)
N(2)C(5)C(6)S(2)	-29.7(7)
C(7)AsC(8)C(9)	-17.7(9)
C(7)AsC(14)C(15)	-62.7(9)
C(7)AsC(20)C(25)	-37.4(9)

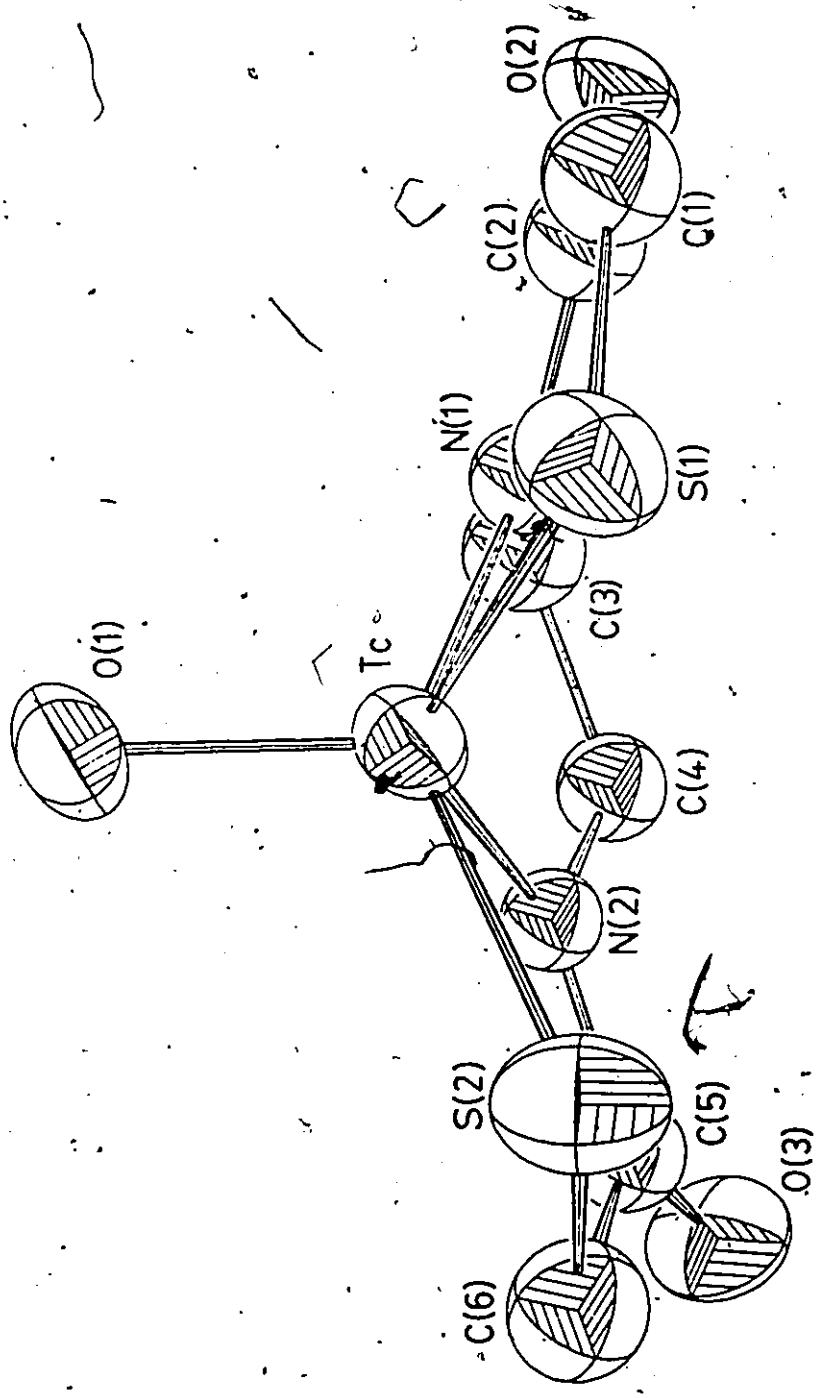

Figure 12. The anion $TcO(SCH_2CONCH_2)_2^-$

Although the remaining bond lengths are unremarkable, there are significant differences between angles that should be equivalent, particularly those involving the nitrogen atoms (e.g. Tc-N(1)-C(3) 114.6(5)^{o} and Tc-N(2)-C(4) 119.4(4)^{o}. These differences are apparently caused by buckling in the five-membered chelate rings surrounding the metal centre. The S(1)C(1)C(2)N(1), N(1)C(3)C(4)N(2) and N(2)C(5)C(6)S(2) torsion angles have values of 6.2(7), 30.2(7) and -29.7(7)^{o} respectively, demonstrating clearly the difference between the two SCCN rings. The distortion is further illustrated by the fact that N(1) is 0.086(6)Å above and N(2) is 0.074(6)Å below the least squares plane through the sulfur and nitrogen atoms. The conformation of the chelate rings is designated as δδλ or λλδ (for C(1)C(2), C(3)C(4), C(5)C(6)). The asymmetry in the anion is caused by the conformational requirements of the chelate rings.

The cation is shown in Figure 13. The As-C distances in the cation are virtually identical (average 1.897(7)Å) despite the differences between methyl and phenyl groups. The equivalence of these distances has been observed in other crystal structures containing this cation (110,111). As expected, the methyl protons are staggered with respect to the three phenyl rings. The latter exhibit normal bond lengths and angles and are planar to within 0.01Å. However, the arsenic lies slightly out of the plane of each of the rings (range 0.019(1) to 0.079(1)Å). Such displacements have been attributed to van der Waals repulsions between the phenyl rings (110).

The conformation of the cation can be defined in terms of the

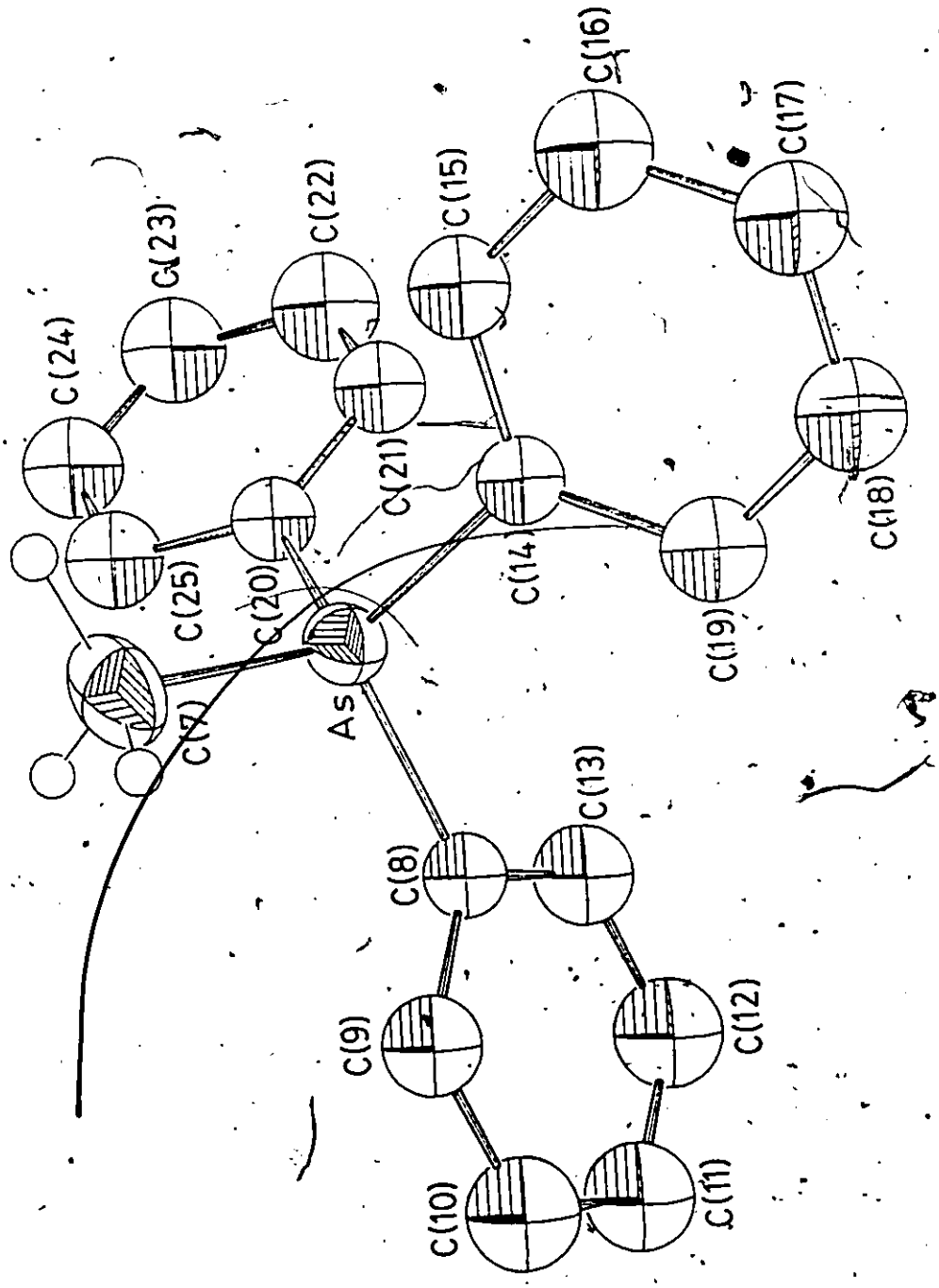

Figure 13. The cation $As(CH_3)(C_6H_5)_3^+$

torsion angles (C(7)AsC(α)C(β)) where C(β) is the carbon atom in the phenyl ring that is closest to the methyl group. A conformational analysis of triphenylphosphine in free and solid states, based on an ideal C_3 symmetry, gave a single, broad potential energy minimum at a torsion angle of $39 \pm 2^{\circ}$, the low energy limits being 30° and 55° (112). Experimentally, there is a bias to values at the higher end of this range (113). It is interesting to note that the cation in this compound does not have C_3 symmetry and that the torsion angles of -17.72°, -62.71° and -37.35° (for C(α)C(β) = C(8),C(9),C(14)C(15) and C(20)C(25), respectively) cover such a wide range. Such distortions are not unknown; they have been observed previously in triphenylphosphine complexes of transition metals and give rise to chiral centres (114). By analogy, the cation in Figure 13 has an S configuration.

The packing of the title compound within the unit cell is shown in Figure 14. The cations are arranged in convoluted layers parallel to the ab plane (at z = 1/4, 3/4). The layers are composed of undulating columns of cations centred on the two-fold screw axes and are separated by layers of anions at z = 1/2 The intricacy of the packing arrangement results from the asymmetry of the constituent ions which would also account for the absence of graphitic stacking (115). There are no interionic contacts either within or between the layers that are less than the sum of van der Waals radii.

The crystallographic information presented here provides an accurate assessment of the stereochemistry and dimensions of a technetium anion which may be the prototype for a new class of useful

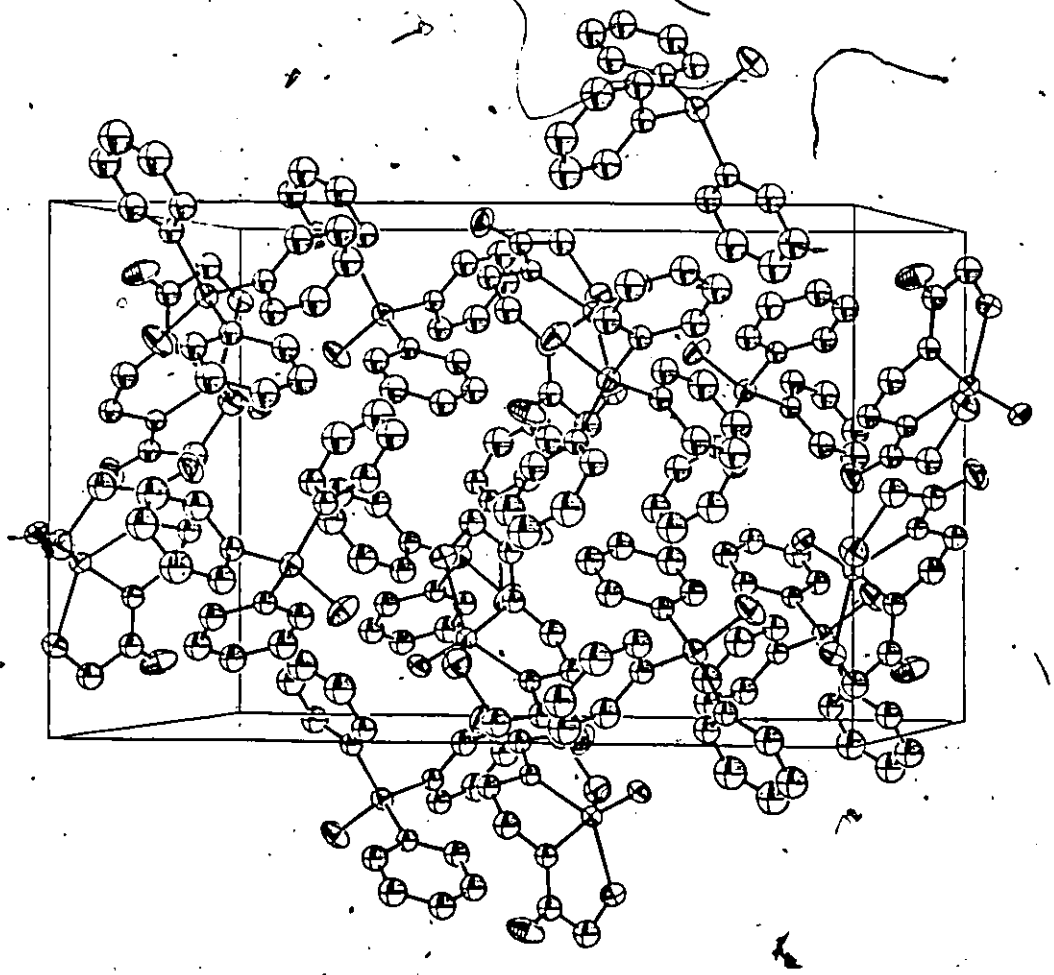

Figure 14. The unit cell contents of $C_{25}H_{26}N_2O_3S_2AsTc$. The c and b axes are parallel to the bottom and side of the page, respectively, and the view is down a*.

diagnostic agents. Detailed knowledge of this molecular geometry will be a useful baseline for assessing the effect of modifications or substitutions made on the template molecule and may possibly aid in a clearer understanding of structure-activity relationships within this class of complexes.

It is interesting to note that animal studies have shown that the above anion is excreted unchanged into both urine and bile (101, 115). Clinical evaluation of this anion in a limited number of renal-transplant patients demonstrated high kidney-to-background ratios and thus high extraction efficiencies in patients with good renal function but poor ratios in patients with moderate to severe decreases in renal function (116). Fritzberg has recently synthesized a derivative of the above anion in which a carboxylate group has been added to one of the carbon atoms in the ethylenediamine backbone (117). The new complex has an improved specificity for evaluation of renal function relative to that of the parent material but is difficult to separate from a second component produced in the reaction (117). Based on the above structure, the impurity is presumably a chelate-ring isomer. Further work to characterize these products using complexes of ^{99}Tc is in progress (117). Such studies represent one of very few examples of the rational development of new radiopharmaceuticals.

CHAPTER 5

SIMPLE TECHNETIUM COMPLEXES

5.1 Introduction

As mentioned in Chapter 1, technetium has been available for chemical studies on the macroscopic scale for only the last thirty years. Thus, much of technetium chemistry has remained unexplored. Some of the more recent work has involved the study of simple complexes which have exact counterparts in rhenium chemistry. Such studies serve to confirm trends observed elsewhere in the periodic table.

In the following section, the crystal structure determination of $K_3TcO_2(CN)_4$ is reported. This compound was found to be isostructural with its rhenium analog (118,119) which provides a basis for comparing the vibrational spectra of the two anions. In another section, the vibrational spectra of $Tc(CN)_7^{4-}$ are compared to those of heptacyano complexes of other metal ions. Finally, the results of a crystallographic examination of $(C_4H_9)_4NTc(NO)Br_4$ are presented.

5.2 The Crystal Structure and Vibrational Spectroscopy of $K_3TcO_2(CN)_4$

Crystals of the title compound were obtained from A. Davison. The synthesis, method of crystallization and elemental analysis of this material are reported elsewhere (120). The density of the crystals was obtained by flotation in a chloroform-bromoform mixture. Precession photographs showed the crystals to be triclinic with cell parameters very close to the values found for the rhenium analog. Crystal data

and other numbers relating to data collection and structure refinement are listed in Table 18. The atom parameters from the final refinement are listed in Table 19 and the interatomic distances and angles are listed in Table 20.

The unit cell contains discrete ions of K^+ and $TcO_2(CN)_4^{3-}$. The anion, shown in Figure 15, sits on a centre of symmetry which forces the O=Tc=O group to be linear. The coordination geometry around technetium is nearly a regular octahedron with the largest deviation from right angles being 2.03° (C(1)-Tc-C(2)). The bond angles in the two independent Tc-C-N groups differ significantly from linearity and from each other (173.0(2)°, Tc-C(1)-N(1); 178.3(2)°, Tc-C(2)-N(2)). Both effects may be caused by interactions with potassium ions which are not equivalent for N(1) and N(2) (Table 20). The Tc=O bond length (1.766(2)) is slightly longer than that found in other structures containing the TcO_2^+ unit (range 1.741(1)-1.752(1)Å)(28,121) but somewhat less than the M=O bond length found in the rhenium analog (1.781(3)Å)(118,119). As expected, the Tc=O distance is much longer in the trans-dioxo anion than in the mono-oxo species presented in Table 13. This difference is caused by mutual competition between the two oxygen atoms for the same metal orbitals (24).

One of the potassium ions, K(1), is located on an inversion centre with six (2O,4N) nearest neighbours at about 2.86Å resulting in a distorted octahedral geometry. The coordination about K(2) is much less regular with four nearest neighbours at about 2.8Å and two at about 3.2Å. Each nitrogen and oxygen atom of the anion is in close contact with three potassium ions. The contents of the unit cell are shown in Figure 16

Table 18

Compound	$C_4N_4O_2K_3Tc$
Formula weight	352.38
Crystal size (mm)	plate, 0.26 x 0.14 x 0.07
Systematic absences	none
Space group	$P\bar{1}$
Unit cell parameters (Å and deg)	a = 7.637(1); α = 109.96(1)
	b = 7.477(1) β = 105.44(1)
	c = 6.298(1) γ = 114.81(1)
Cell determination	15 reflections, $29.2^o < 2\theta < 31.9^o$
Volume ($Å^3$)	269.13(9)
Z	1
ρ_{calc}, ρ_{obs} ($g\ cm^{-3}$)	2.17, 2.16(1)
Linear abs. coefficient (cm^{-1})	24.23
Maximum error on F_o (%)	< 1.6
Maximum 2θ, reflections measured	55^o ± h, ± k, ± ℓ
Standard reflections (e.s.d. %)	2 -3 2 (1.90) -2 3 2 (1.90)

Table 18 (continued)

Temperature (^{o}C)	22
Number of independent reflections	1236
Number with $I > 0$	1225
Number with $I < 0$, rejected	11
Final R_1, R_2	0.0174, 0.0208
Final shift/error maximum (average)	0.058 (0.010)
Number of variables	188
Final difference map	
Highest peak (e $\AA^{-3}$); location	0.43; 0.16, 0.15, 0.11
Lowest valley (e $\AA^{-3}$); location	-0.82; 0.96, 0.10, 0.00
Weighting scheme	$w = [\sigma^2 + (0.0071\ F_o)^2]^{-1}$
Secondary extinction (g)	$2.5(1) \times 10^{-6}$
Error in an observation of unit weight	1.4167
F (0,0,0)	166.98

Table 19. Atomic coordinates for $C_4N_4O_2K_3Tc$ ($\times 10^4$)

Atom	x	y	z
Tc	0	0	0
K(1)	5000	0	5000
K(2)	1643.7(7)	3656.0(7)	-2914.1(8)
O	1359(2)	272(2)	2955(2)
C(1)	2940(3)	1208(3)	-348(3)
N(1)	4439(3)	1968(3)	-633(4)
C(2)	1013(3)	3506(3)	2005(3)
N(2)	1605(3)	5393(3)	3109(4)

Anisotropic temperature factors U_{ij} ($\AA^2$) ($\times 10^4$)

Atom	U_{11}	U_{22}	U_{33}	U_{23}	U_{13}	U_{12}
Tc	210(1)	175(1)	200(1)	108(1)	108(1)	117(1)
K(1)	281(3)	248(3)	440(3)	118(3)	193(3)	139(2)
K(2)	372(2)	311(2)	322(2)	190(2)	189(2)	206(2)
O	301(7)	262(6)	246(6)	144(5)	126(5)	170(6)

Table 19 (continued)

Atom	U_{11}	U_{22}	U_{33}	U_{23}	U_{13}	U_{12}
C(1)	275(9)	236(8)	285(8)	137(7)	141(7)	159(7)
N(1)	330(9)	397(10)	455(10)	219(8)	240(8)	191(8)
C(2)	293(9)	236(8)	258(8)	150(7)	155(7)	160(7)
N(2)	419(10)	251(8)	433(10)	157(8)	196(8)	187(8)

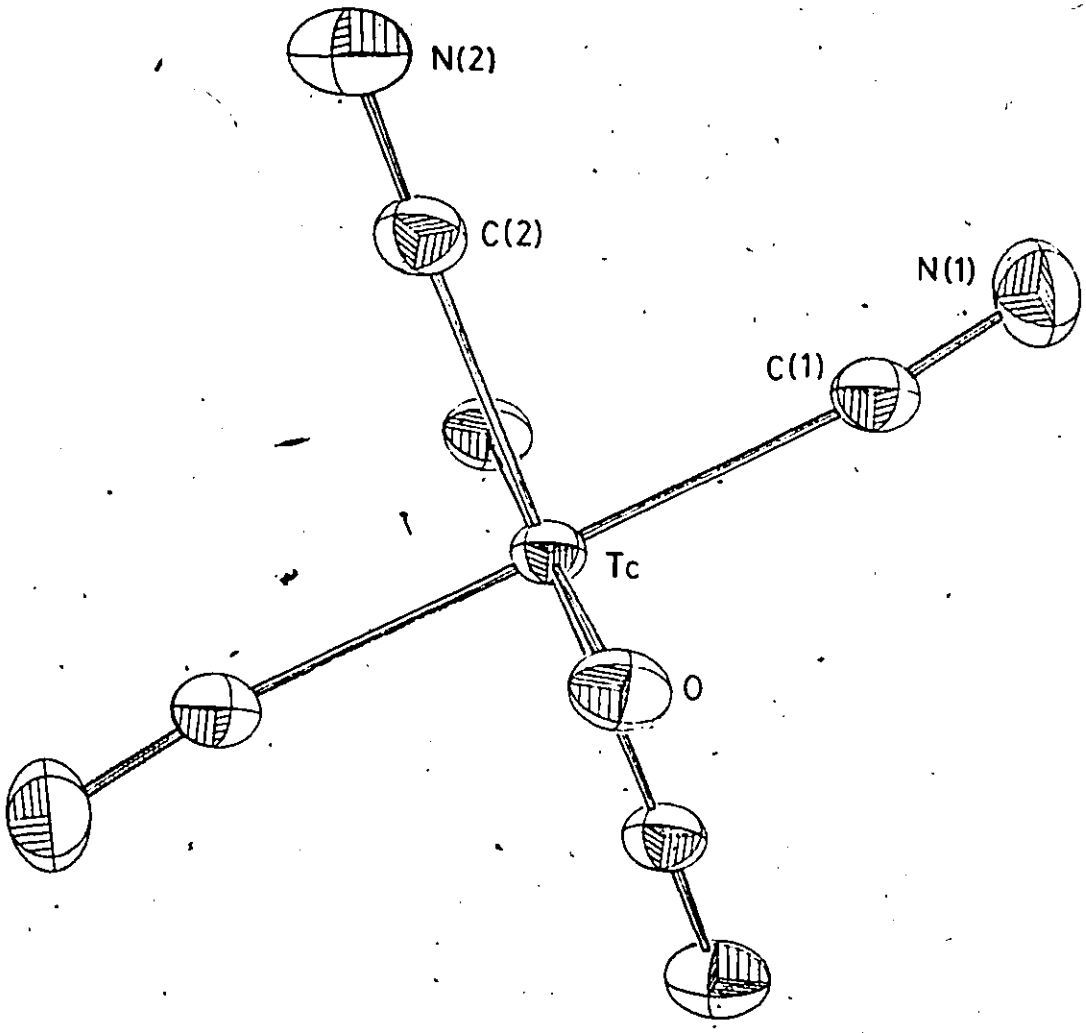

Figure 15. The anion $TcO_2(CN)_4^{3-}$

Table 20. Interatomic distances(Å) and angles(deg) for $C_4N_4O_2K_3Tc$

Tc-O	1.766(2)	K(1)...N(1)	2.882(2)	K(2)...N(1)	2.808(1)
Tc-C(1)	2.145(2)	K(1)...N(2)	2.840(2)	K(2)...N(1)'	3.175(1)
Tc-C(2)	2.141(2)	K(1)...O	2.860(2)	K(2)...N(2)	2.838(3)
C(1)-N(1)	1.140(3)	K(2)...O	2.822(2)	K(2)...N(2)'	3.190(3)
C(2)-N(2)	1.143(3)	K(2)...O'	2.855(2)		

O-Tc-C(1)	91.36(8)	O-K(2)-O'	82.34(5)	O'-K(2)-N(2)'	135.53(4)
O-Tc-C(2)	90.11(8)	O-K(2)-N(1)	122.27(6)	N(1)-K(2)-N(1)'	83.15(6)
C(1)-Tc-C(2)	87.97(9)	O-K(2)-N(1)'	71.62(5)	N(1)-K(2)-N(2)	102.23(7)
Tc-C(1)-N(1)	173.0(2)	O-K(2)-N(2)	126.03(5)	N(1)-K(2)-N(2)'	84.90(6)
Tc-C(2)-N(2)	178.3(2)	O-K(2)-N(2)'	76.19(6)	N(1)'-K(2)-N(2)	148.76(7)
O-K(1)-N(1)	75.63(6)	O'-K(2)-N(1)	138.90(6)	N(1)'-K(2)-N(2)'	131.88(7)
O-K(1)-N(2)	82.63(6)	O'-K(2)-N(1)'	73.91(5)	N(2)-K(2)-N(2)'	79.36(7)
N(1)-K(1)-N(2)	85.40(6)	O'-K(2)-N(2)	82.75(6)		

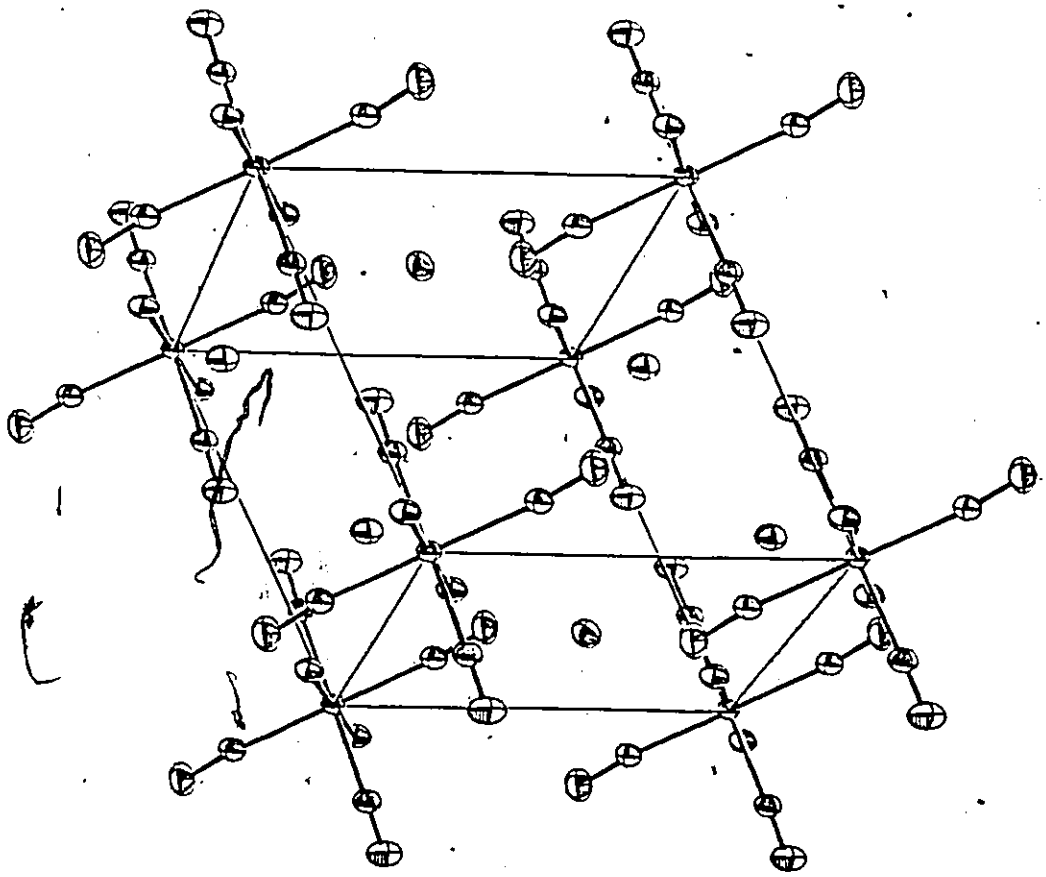

Figure 16. The unit cell contents of $C_4N_4O_2K_3Tc$. The a and b axes are approximately parallel to the bottom and side of the page, respectively, and the view is along c*.

The infrared and Raman spectra for $K_3TcO_2(CN)_4$ are listed in Table 21. Assignment of the bands was made by a direct comparison to the spectra of the rhenium analog (included in Table 21) which has been fully analyzed by a detailed force constant calculation (108). As expected, the largest frequency differences between the two compounds occur for modes involving metal-oxygen bonds. "Symmetry factored" force constants for metal-oxygen bonds can be obtained by considering only the M-O stretching vibrations of a molecule but allowing for the symmetry of the whole molecule (122). For a molecule with D_{4h} symmetry, the relationships between the internal force constants (f) and symmetry force constants F are as follows (122):

$$F(A_{1g}) = \frac{0.588851}{\mu_0}\left(\frac{\nu_s}{1000}\right)^2 = f_r + f_{rr}$$

and

$$F(A_{2u}) = \frac{0.588851}{(\mu_0 + 2\mu_{Tc})}\left(\frac{\nu_a}{1000}\right)^2 = f_r - f_{rr}$$

where ν_s, ν_a are the symmetric and antisymmetric stretching frequencies,

μ_0/μ_{Tc} are the reciprocal masses of the elements shown,

f_r is the stretching force constant, and

f_{rr} is the stretch-stretch interaction force constant.

By using these equations and values from Table 21, we obtain f_r = 5.381 mdyne Å^{-1} and f_{rr} = 1.016 mdyne Å^{-1} for the technetium complex. As expected, these values are both smaller than those found for the rhenium

Table 21. Vibrational Spectra(cm^{-1}) for $C_4N_4O_2K_3Tc$ and $C_4N_4O_2K_3Re$

$C_4N_4O_2K_3Tc$		$C_4N_4O_2K_3Re$		
Infrared*	Raman**	Infrared*	Raman**	Assignment
	2140(100,0.2)		2140(80,0.2)	$\nu(C\equiv N)$,sym
	2131(40,0.5)		2130(55,0.7)	$\nu(C\equiv N)$,asym
2120(100)		2121(55.)		$\nu(^{12}C\equiv^{14}N)$,asym
2095(0.2)				$\nu(^{12}C\equiv^{15}N)$,asym
2080(0.9)		2079(2.0)		$\nu(^{13}C\equiv^{14}N)$,asym
1610(15,br)				combination(824+783)
1382(55)				cyanato impurity
	824(95,0.2)		879(100,0.1)	ν(O=Re=O),sym
783(97)				ν(O=Tc=O),sym
		775(100)		ν(O=Tc=O),asym
	750(15,0.5)			ν(O=Re-O),asym
		474(20)		
		467(23) }470+		δ(Re-C$\equiv$N)
463(0.2)				δ(Tc-C$\equiv$N)
424(0.9)		433(15)		
		413(8) }424+		ν(M-C),asym
			395(10,0.7)	ν(M-C),asym
337(65,br)		337(37)		$\nu(\pi$C-M-C), in phase wag
	263(0.2,0.5)			
		252(20		ν(O=M=O), bend
	194(18,0.7)		202(15,0.8)	ν(O=M-C), bend

Table 21 (continued)

---

* Relative intensity of infrared peak (based on 100 for strongest peak) is given in parentheses.

** Relative intensity of Raman peak shown in parentheses, followed by polarization ratio.

\+ doublets.

compound (6.056 and 1.224 mdyne Å^{-1} respectively)(108) where the more diffuse 5d orbitals allow for greater overlap with ligand orbitals, thus forming a stronger bond.

The spectra presented in Table 21 are in good agreement with a recently published list of stretching frequencies above 750 cm^{-1} for this complex (120). A major exception involves the cyanide bands in the Raman spectrum of the solid. Since the values reported here correspond exactly to those of the rhenium analog, it is assumed that the published data is incorrect.

The comparison between technetium and rhenium can be extended to include the ethylenediamine (en) complexes (121,123). The values of interest are presented in Table 22. For both metals, the M=O bond length decreases by about 0.02Å and the stretching frequency increases by about 50 cm^{-1} in going from $MO_2(CN)_4^{3-}$ to $MO_2(en)_2^+$. These changes result primarily from the overall charges on the complexes (124). The cyanide ion has π-acceptor properties that act to reduce the electronic charge on the metal centre, making the latter more electronegative. Thus, in the cyanide complex, with its triple negative charge, the σ bonds to the oxygen atoms, and consequently the π bonds as well, will be weaker.

The cyclam complex of technetium, also listed in Table 21, appears to be anomalous in that the Tc=O bond length (1.751(4)Å) is virtually the same as that found in $TcO_2(en)_2^+$ (1.746(3)Å) but the asymmetric stretching frequency is 43 cm^{-1} lower. Without the corresponding symmetric stretching frequencies from Raman spectra of both complexes, it is not possible to compare force constants as shown

Table 22. Comparison of Bond Distances(Å) and ν_a(M=O)(cm^{-1}) for Some MO_2L_4 Complexes (M=Tc,Re)

Complex	M=O	ν_a(M=O)	M-L	ref.
$TcO_2(CN)_4^{3-}$	1.766(2)	783	2.143(3)	this work
$ReO_2(CN)_4^{3-}$	1.781(3)	775	2.135(5)*	(118)
$TcO_2(en)_2^+$	1.746(3)*	833	2.158(4)*	(121)
$ReO_2(en)_2^+$	1.765(7)*	819	2.162(16)	(124)
$TcO_2(cyclam)^+$	1.751(4)*	790	2.125(11)*	(28)

* average value

above for $TcO_2(CN)_4^{3-}$ and $ReO_2(CN)_4^{3-}$. Nevertheless, a shift of 43 cm^{-1} is a substantial change and implies a difference in force constant despite the equivalence of the Tc=O bond lengths. The reason for this behaviour is not clear but may be related to steric strain in the cyclam complex. Theoretical calculations have shown that in metal complexes of cyclam, a metal-nitrogen separation of 2.07Å produces a minimal amount of strain in the macrocyclic ligand (125). The M-N bond length in the technetium complex (2.125(11)Å) is considerably longer than this optimum value and the strain in the ligand is apparent in the observed bond and torsion angles which are larger than those found in the Ni(III) complex (28). That is, the Tc-N bond is long considering the constrictive effects of the cyclam ligand although it is short compared to $TcO_2(en)_2^+$ (Table 21). Whether these differences in Tc-N bond lengths and ligand strain would account for a change in force constant without affecting the Tc=O bond lengths, is not known. Further spectroscopic studies on these and related complexes would help resolve this dilemma.

5.3 The Vibrational Spectroscopy of $K_4Tc(CN)_7$

Samples of the title compound were synthesized using $K^{12}CN$ and $K^{13}CN$ according to published procedures (120). The infrared and Raman spectra obtained from these samples are presented in Table 23. Some of the bands are assigned to known hydrolysis products (120) which are present as impurities but an examination of all the data allows the assignments of the $Tc(CN)_7^{4-}$ frequencies as shown.

In the cyanide stretching region (2000-2150 cm^{-1}), the pattern

Table 23. Vibrational Spectra(cm^{-1}) for $K_4Tc(CN)_7$

Infrared		Raman		Species
^{12}C	^{13}C	^{12}C	^{13}C	
		2122(30,0.1)	2088(64,0.20)	$Tc(CN)_7^{4-}$
		2111(77,0.2)	2076(100,0.11)	$Tc(CN)_7^{4-}$
		2100(22,0.5)		$TcO(CN)_5^{2-}$
	2078(100)		2065(60,0.44)	$TcO_2(CN)_4^{3-}$
2103sh	2059sh			
2094(100)	2050(52)			$Tc(CN)_7^{4-}$
2080(60)				$TcO(CN)_5^{2-}$
		2070(27,0.7)	2022(60,0.71)	$Tc(CN)_7^{4-}$
		2065(11,0.7)		
2051(80)	2010(38)			$Tc(CN)_7^{4-}$
1385(35)	1385(52)			cyanato impurity
910(35),br				$TcO(CN)_5^{2-}$
	788(66)		825(60,0.15)	$TcO_2(CN)_4^{3-}$
540(35),br	530(22)			
450(9),br		564(100,0.36)	455(86,0.38)	$Tc(CN)_7^{4-}$
360(20),br		362(24,0.42)	363(29,0.33)	$Tc(CN)_7^{4-}$
337(65),br				$TcO_2(CN)_4^{3-}$
322(12)				
298(15)				
270(10)br		240(65,0.35)	238(46,0.33)	$Tc(CN)_7^{4-}$

of one depolarized and two polarized Raman bands and two noncoincident infrared bands parallels that found for the rhenium analog (126) and is consistent with D_{5h} symmetry (Raman, $2A_1' + E_2'$; infrared, $A_2'' + E_1'$).

For metal ligand modes (below 500 cm^{-1}), the Raman spectra of aqueous solutions exhibit three strong bands at 465, 362 and 240 cm^{-1}. The latter two bands may include two frequencies each but the band profile does not change upon polarization. All three bands are polarized to the same extent (polarization ratio is approximately 0.38) and a detailed assignment was not attempted. The high relative intensities of these bands would suggest that they should be characteristic of MX_7 systems. However, none of the published spectra of the isoelectronic complexes of Re (126), W or Mo (127) repeat the above pattern of relative intensities or polarization ratios in the low frequency region. The cause of this difference is not clear.

5.4 A Crystallographic Examination of $(C_4H_9)_4NTc(NO)Br_4$

Crystals of the title compound were obtained from A. Davison who is studying the anion as a potential starting material for low valent technetium complexes of chemical and radiopharmaceutical interest. Precession photographs indicated the crystals were tetragonal. A data set was collected using the cell parameters a=b=12.04, c=22.40Å. Systematic absences in this data were consistent with the space group P4/nnc. Refinement of atomic positions for technetium and four bromine atoms in this space group resulted in large isotropic temperature factors (up to 0.1$Å^2$) for all atoms and confusing electron difference maps. Both these observations indicated the possibility of

disorder in the unit cell or the incorrect choice of space group. Numerous efforts were made to resolve the ambiguities including the collection of data sets in space groups of lower symmetry and various crystals; the application of direct methods for structure solution; and refinement of (partial) occupancy factors. Throughout these attempts, calculated densities based on the title formula were unreasonably low; technetium and four bromine atoms were consistently found to be coplanar; ligands in axial positions could not be refined; isotropic temperature factors were larger than expected and the cation was not well defined. These difficulties were not overcome during the course of this work. Furthermore, Dr. Davison has reported that there are some ambiguities associated with the chemistry of the anion (96) which may mean that the above formulation is incorrect.

Crystallographic studies of low-valent technetium complexes containing the nitrosyl ligand will lead to a better understanding of these systems. In future, at least some of the difficulties experienced here could be minimized by working with the chlorine analog in order to reduce the disparity between the electron densities of anion and cation. This would serve to equalize the contributions of cation and anion to the intensities of observed reflections and lead to a more balanced refinement. In addition, the probability of disorder could be reduced by using a cation of lower symmetry.

CHAPTER 6

TECHNETIUM-99 NUCLEAR MAGNETIC RESONANCE SPECTROSCOPY

6.1 Introduction

Technetium-99 is the only n.m.r.-active technetium isotope ($I = 9/2$) possessing a significantly long half-life. It is obtained in 100% abundance and has a detection receptivity relative to ^{1}H of 0.275 which makes ^{99}Tc one of the most receptive nuclei known (128). Although ^{99}Tc possesses an appreciable quadrupole moment ($Q = -0.19(5) \times 10^{-28} m^2$) (129), the effect of quadrupole line broadening is attenuated by the large size of the spin, I, according to the relaxation equation 1 (49):

$$\pi\Delta\nu = \frac{1}{T_2} \approx \frac{1}{T_1} = \frac{3\pi^2}{10}\left(\frac{2I+3}{I^2(2I-1)}\right)\left(1+\frac{\eta^2}{3}\right)\left(\frac{e^2qQ}{h}\right)\tau_c \qquad (1)$$

where $\Delta\nu$ is the observed line width

T_2 is the spin-spin relaxation time

T_1 is the spin-lattice relaxation time

eq is the electric field gradient at the ^{99}Tc nucleus

η is an asymmetry parameter, $0 < \eta < 1$

and τ_c is the isotropic tumbling correlation time. That is, relatively narrow line widths are expected for species in which ^{99}Tc is found in a symmetric environment. Despite such favourable characteristics, this nuclide has been all but ignored as a n.m.r. nucleus, primarily because of its former scarcity and partly because of its radioactivity.

At the start of this work, very few references to technetium existed in the n.m.r. literature. The nuclear magnetic moment of ^{99}Tc was determined to be 5.6805(4) in 1952 (130). Kidd briefly mentioned that the line width for ^{99}Tc in aqueous solutions of pertechnetate, TcO_4^-, was 29 Hz. Figgis and coworkers (132) reported a single ^{17}O n.m.r. signal from ^{17}O-enriched TcO_4^- with $\delta(H_2O)$ 749 ppm and $\Delta\nu$ ca. 1150 Hz. Four additional reports, each dealing with TcO_4^- appeared during the course of this work (133,134,135,136). Some of these reports are discussed in the following section in which the n.m.r. characteristics of the pertechnetate anion are described in detail. These results, together with those presented in later sections for other compounds, constitute the most comprehensive study of this nucleus to date (137) and serve to establish the ranges of a number of ^{99}Tc n.m.r. parameters as a basis for further research. A list of all chemical shifts, line widths and coupling constants observed in this study are presented in Table 24 to be found at the end of this chapter.

6.2 Studies of the Pertechnetate Anion, TcO_4^-

Several characteristics of TcO_4^- support its selection as a standard for ^{99}Tc n.m.r. spectroscopy. Salts of the anion are easily purified by recrystallization from solutions of hydrogen peroxide. Because of the high sensitivity of ^{99}Tc and narrow line width ($\Delta\nu$ = 2.7 Hz) resulting from a cubic electric field at ^{99}Tc, an acceptable spectrum of TcO_4^- can be obtained from a single transient (signal/noise $\approx$ 210, pulse width 35 μs at 2.114 T on a 9.1 mm column of 0.210 M NH_4TcO_4 in D_2O). The position of the n.m.r. signal from TcO_4^- is independent of the choice

of cation (NH_4^+, Na^+, K^+, Cs^+) and of concentration of TcO_4^- between 0.210 and 4.90×10^{-7} M. Consequently, all chemical shift data for ^{99}Tc n.m.r. signals are quoted relative to TcO_4^-. The exact resonance frequency of ^{99}Tc was determined to be Ξ = 22508311 ± 10 Hz at 25°C which is in good agreement with an independent measurement (133).

The sensitivity of ^{99}Tc n.m.r. was demonstrated by allowing samples of $^{99m}TcO_4^-$ obtained from a ^{99}Mo generator to decay to $^{99}TcO_4^-$. The concentration of TcO_4^- in one of these samples was calculated to be approximately 8×10^{-7} M based on the known elution history of the generator. After 189,297 scans (using the Bruker WM 250 instrument), a spectrum of this sample in a 10 mm tube was obtained giving a line width of 11 Hz and a signal/noise ratio of about 10. A second sample, with a calculated concentration of 5.86×10^{-7} M was placed in a 10 mm tube and a solution of NH_4TcO_4 (2.00×10^{-5} M) in deuterated dimethyl sulfoxide was placed in an insert. After 85,893 scans, the ^{99}Tc n.m.r. spectrum showed two signals separated by 9.6 ppm. Taking into account the relative cross-sectional areas for the insert and 10 mm tube, the ratio of signal intensities was found to be equal to the ratio of the calculated concentrations. The separation of the two pertechnetate signals results from differences in the bulk diamagnetic susceptibilities of the solvents used. This technique could prove to be a very useful, quantitative method of measuring technetium species at the low concentrations used in nuclear medicine. These results also establish that a concentration of approximately 5×10^{-8} M for $^{99}TcO_4^-$ in a 10 mm tube is the lower limit of detectability for the Bruker WM 250 instrument.

The ^{17}O n.m.r. spectrum of $KTcO_4$ enriched in ^{17}O (21.9%) and ^{18}O (42.7%) is shown in Figure 17. Details of the enrichment procedure have appeared elsewhere (137). The spectrum consists of an equi-intensity decet arising from spin-spin coupling of ^{17}O to ^{99}Tc (J = 131.4 Hz). The chemical shift with respect to H_2O is 748.6 ppm and the observed line width is 23 Hz. These values are in good agreement with those obtained from a solution of NH_4TcO_4 containing a natural abundance of ^{17}O (133). The saddle shape of the decet is characteristic of partial quadrupole-collapse (138).

The ^{99}Tc n.m.r. spectrum of this sample is shown in Figure 18. The spectrum consists of a strong central line (TcO_4^-), an equiitensity sextet ($Tc^{17}OO_3^-$) and an eleven-line multiplet ($Tc^{17}O_2O_2^-$). In addition, a set of smaller splittings (8.8 Hz at 2.114 T) are observed on each of the main lines. These splittings are caused by primary isotopic shielding effects arising from a statistical distribution of $^{16}O/^{17}O/^{18}O$ isotopic isomers. The relative intensities of these isotopic isomers can be calculated using the expression $(x + y + z)^4$ where x, y and z are the concentrations of ^{16}O, ^{17}O, and ^{18}O, respectively. As shown in Figure 19, the agreement between observed and calculated intensities is very good and confirms the cause of these splittings. The more massive isotopic isomers occur at lower frequencies. The isotopic shift per oxygen mass unit is 0.22 ppm. This value has been obtained independently by Tarasov and coworkers (136).

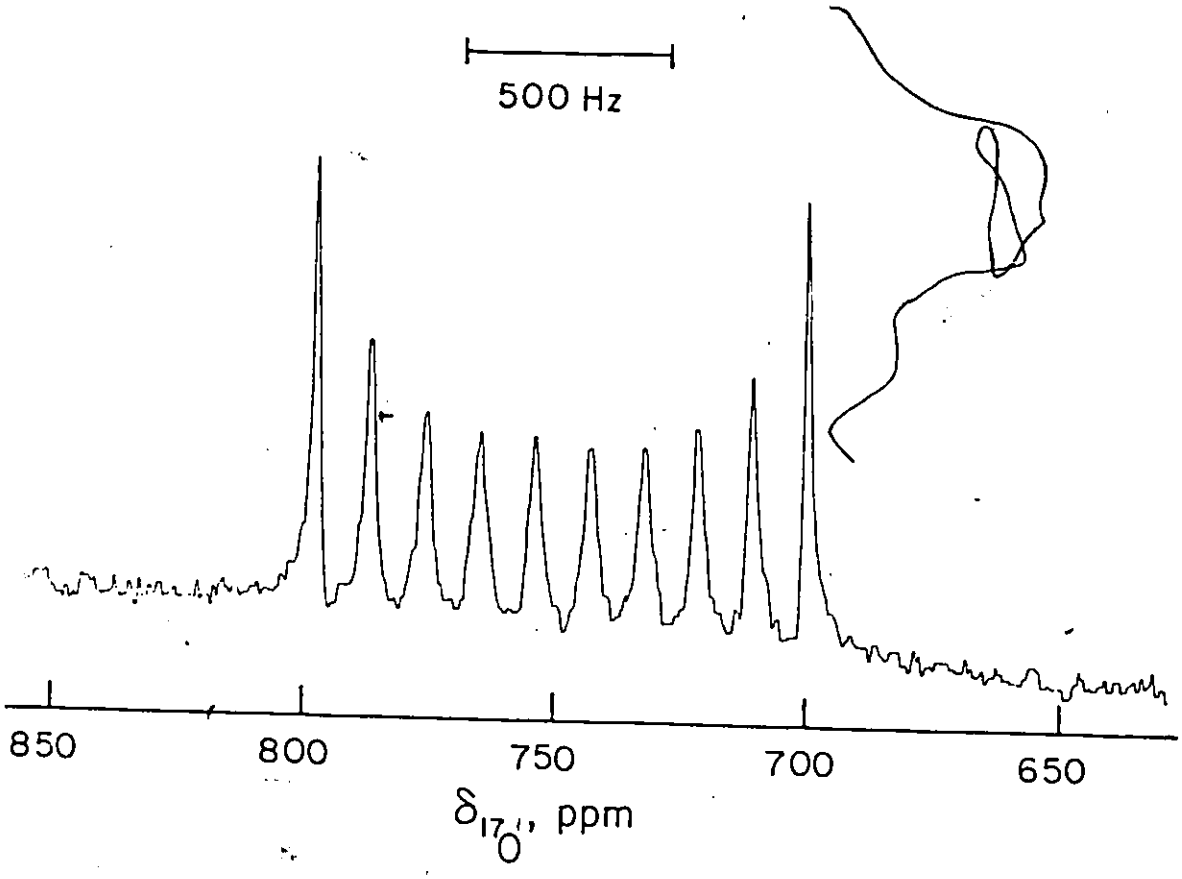

Figure 17. The ^{17}O n.m.r. spectrum of ^{17}O-enriched $KTcO_4$ in H_2O at 25°C.

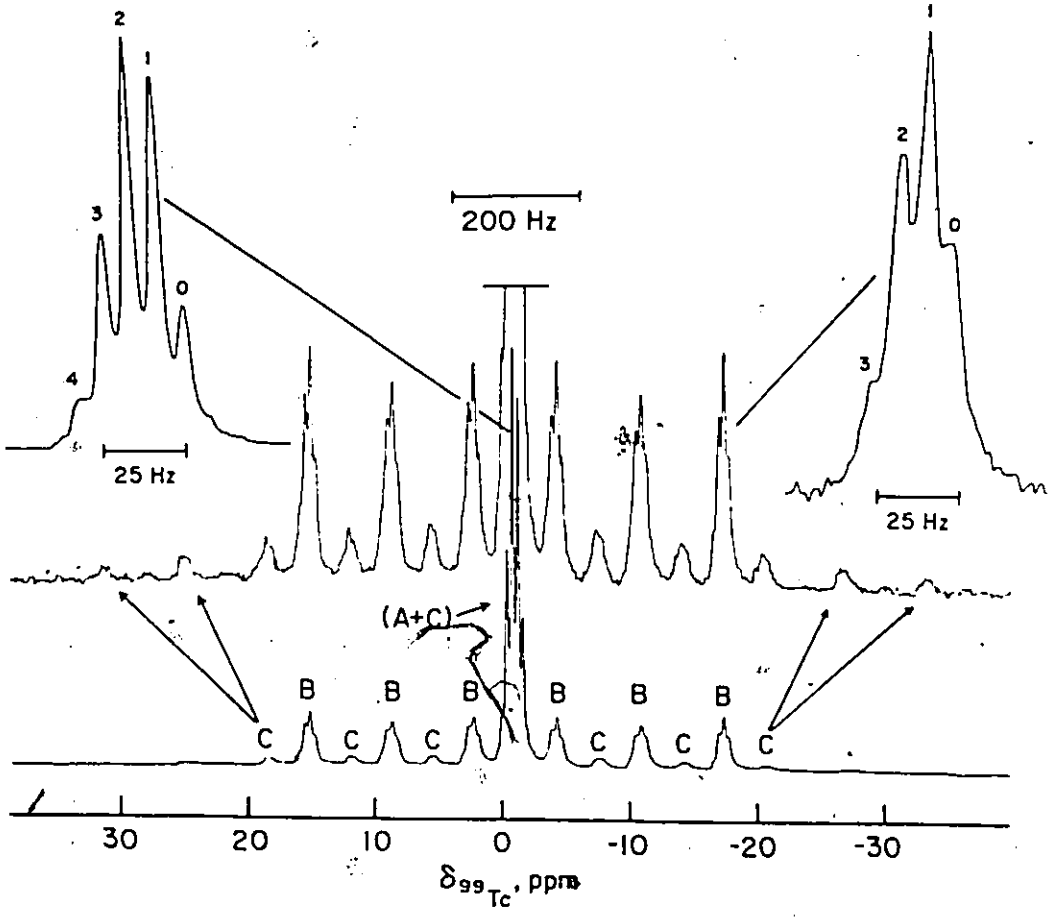

Figure 18. The ^{99}Tc n.m.r. spectrum of ^{17}O (21.9%) and ^{18}O (42.7%) enriched $KTcO_4$ in H_2O at 25°C. Isotopic isomers are denoted by (A) TcO_4^-, (B) Tc $^{17}OO_3^-$ and (C) Tc $^{17}O_2O_2^-$, where a non-superscripted O represents ^{16}O and/or ^{18}O. Assignments for the insets corresponding to A and B are Tc $^{16}O_x{}^{18}O_{4-x}^-$ (A) and Tc $^{17}O^{16}O_x{}^{18}O_{3-x}^-$ (B), where x, the number of ^{16}O atoms is indicated.

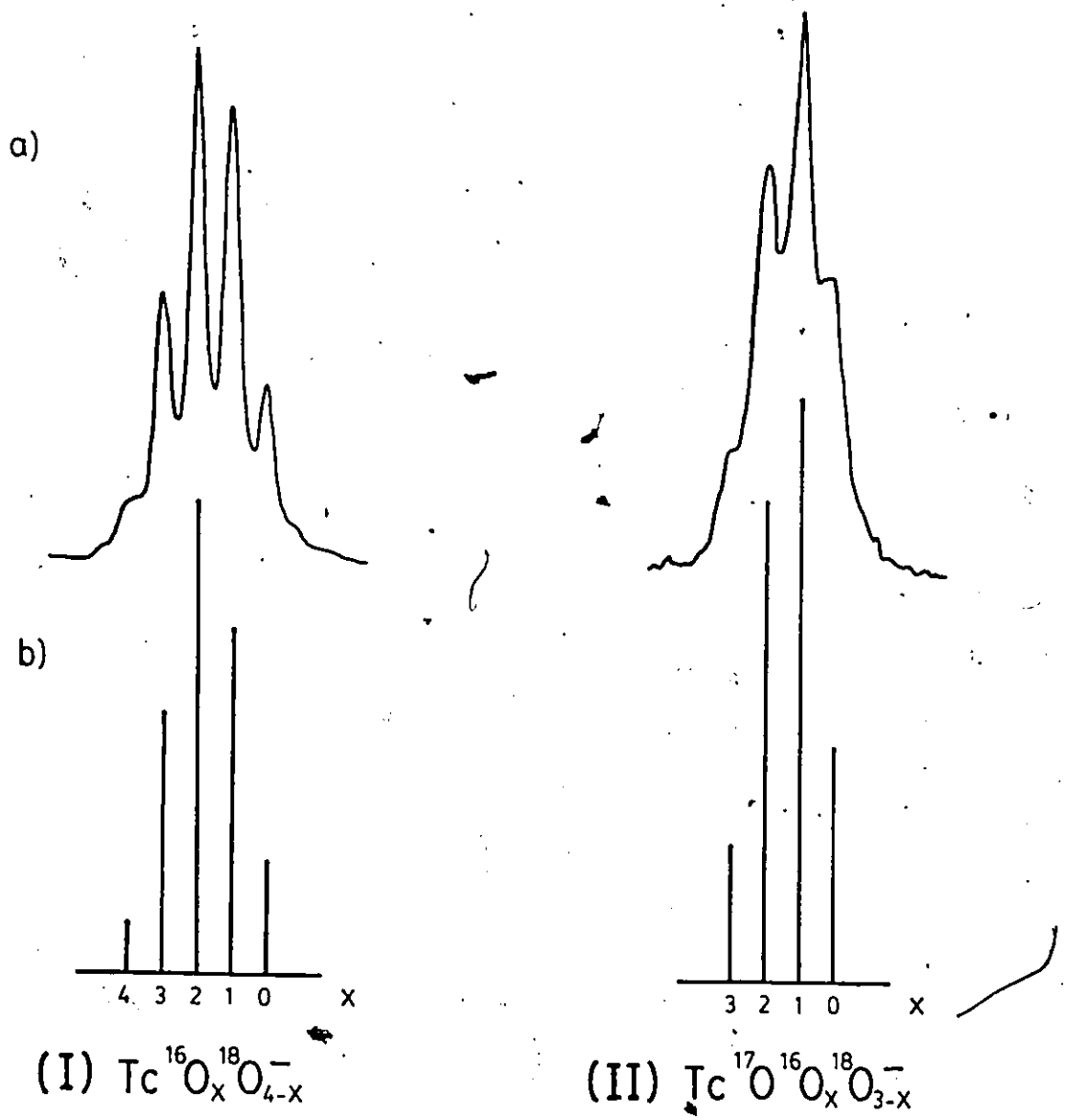

Figure 19. Observed (a) and calculated (b) intensity ratios for $^{16}O/^{17}O/^{18}O$ isotopic isomers of $KTcO_4$. In decreasing values of x, the calculated percentages are 1.57, 7.56, 13.67, 11.00 and 3.32 for I(b) and 3.89, 14.07, 16.97 and 6.82 for II(b).

The line width for aqueous TcO_4^- was found to be 2.7 Hz which is an order of magnitude smaller than that reported by Kidd (131). From equation 1, the line width corresponds to a value of 0.118 s for T_1 and is in good agreement with the T_1 value of 0.139 s determined by the inversion-recovery method in the present study. As discussed in section 6.1, the line widths of ^{99}Tc resonance are mainly due to the direct quadrupolar relaxation. Even though ^{99}Tc should possess an electric field gradient of zero in TcO_4^-, the efficient relaxation of ^{99}Tc is presumably brought about by quadrupolar relaxation since the electric field gradient can be modulated by mixing the asymmetric molecular vibrations. This theory, first originated by Valiev (139), has more recently been extended to the case of a quadrupolar nucleus at the centre of a molecule belonging to a cubic point group (140). The effective electric field gradient at ^{99}Tc in aqueous TcO_4^- estimated from equation 1 with T_1 = 0.139 s and $\tau_c = 8.1 \times 10^{-12}$ s is eq = -0.15×10^{15} esu based on a T_1 value estimated from an inaccurate line width (29 Hz) and quadrupole moment (0.3×10^{-28} m^2). The quadrupole moment used in the present calculations ($-0.19(5) \times 10^{-28}$ m^2) (129) agrees with the predictions of the single-particle nuclear shell model. Both calculations assume $\tau_c = 8.1 \times 10^{-12}$ s.

6.3 Dipotassium Enneahydridotechnetate(VII), K_2TcH_9

The synthesis of the title compound was first reported by Ginsberg (141) who identified the material by infrared spectroscopy and X-ray powder patterns which were very similar to those observed for the rhenium analog. Ginsberg (141) also reported a ^1H n.m.r.

spectrum that was compatible with the TcH_9^{2-} anion, consisting of a broad, partially quadrupole collapsed line ($\Delta\nu$ = 189 Hz) to low frequency of tetramethylsilane. The ^{99}Tc and ^1H n.m.r. spectra of TcH_9^{2-} which are shown in Figure 20, were obtained by repeating the preparation of the hydride according to the published procedure (141). K_2TcH_9 was dissolved in 40% KOH in H_2O solvent at -19°C and the spectra were recorded at -12°C. The ^{99}Tc resonance was shifted 3672 ppm to low frequency of TcO_4^- and displayed partially resolved binomial decet fine structure with a ^{99}Tc-^1H coupling of 24 Hz. A ^{99}Tc line width of 22 Hz was measured from the ^1H-decoupled spectrum. The coupling is also in agreement with the observed ^1H spectrum which consisted of a partially quadrupole-collapsed decet having a line width of 224 Hz. The spectra are consistent with a hydride structure that is fluxional on the n.m.r. time scale and provide definitive proof for the existence of TcH_9^{2-}. A significant low-frequency shift relative to TcO_4^- is anticipated for Tc(VII) bonded to electropositive centres such as hydridic protons. The observed ^{99}Tc chemical shift typifies hydride chemical shifts and represents the most shielded ^{99}Tc nucleus observed thus far. The low frequency position of the ^1H resonance is also characteristic of protons of a hydridic nature bonded to technetium.

6.4 Oxyfluorides of Technetium(VII)

Pertechnetyl fluoride, TcO_3F was first synthesized by Selig and coworkers (142) by fluorination of pertechnetate in anhydrous HF. Hydrogen fluoride solutions of TcO_3F were prepared here by condensing anhydrous HF onto ^{17}O-enriched $KTcO_4$ in FEP reaction tubes at -196°C.

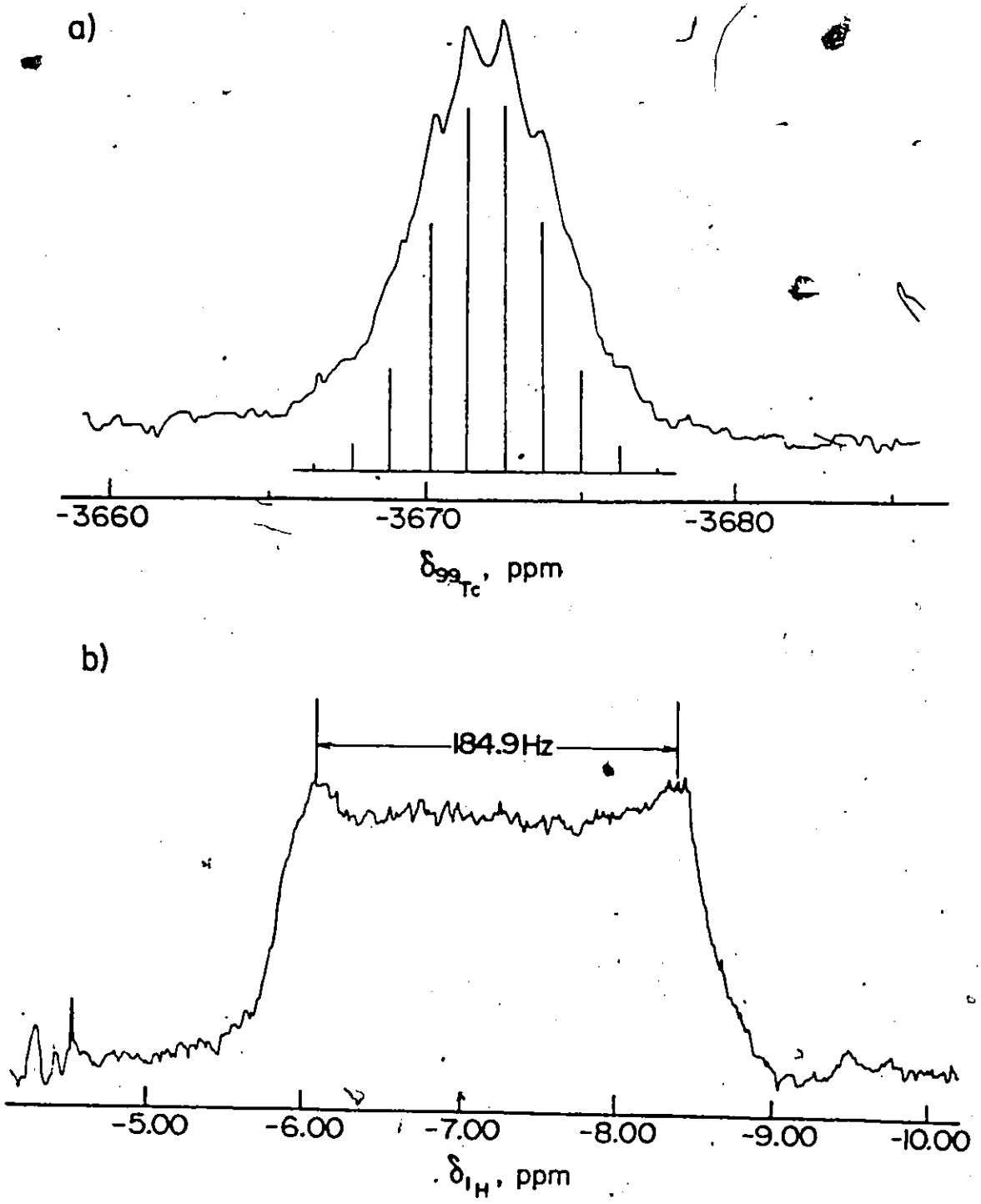

Figure 20. The ^{99}Tc (a) and ^{1}H (b) n.m.r. spectra of TcH_9^{2-} (K_2TcH_9 dissolved in 40% KOH) recorded at -12°C.

$KTcO_4$ rapidly dissolves in HF upon warming to room temperature, yielding colourless to pale yellow solutions. The high frequency shifts of both the ^{99}Tc (43.7 ppm, $\Delta\nu$ = 23 Hz) and ^{17}O (1048 ppm, $\Delta\nu$ = 108 Hz) resonances relative to TcO_4^- are indicative of fluorination. The ^{99}Tc-^{17}O coupling (J = 139.8 Hz) is, however, similar to that of TcO_4^- (J = 131.4 Hz), suggesting that there is little distortion from the tetrahedral O-Tc-O bond angle. Interestingly, no ^{19}F-^{99}Tc coupling or ^{19}F resonance could be observed, although a Raman spectrum of the sample showed that only TcO_3F was formed. It was concluded that TcO_3F behaves as a weak fluoride ion base and undergoes exchange with HF according to the reaction:

$$TcO_3F + HF \rightleftharpoons TcO_3^+ + HF_2^-$$

This was confirmed by condensing a fivefold excess of AsF_5 into the sample at -196°C. The resulting solution yielded new ^{99}Tc (160.7 ppm) and ^{17}O (1214 ppm) resonances to high frequency of TcO_3F. The line width of the ^{99}Tc signal was quite broad ($\Delta\nu$ = 670 Hz) and the ^{17}O resonance ($\Delta\nu$ = 720 Hz) was a partially quadrupole-collapsed decet with a "square top" such that no multiplet lines are resolved. These chemical shifts and line widths are consistent with the hitherto unreported TcO_3^+ cation which would have D_{3h} symmetry in solution. Removal of HF and excess AsF_5 from the above solution followed by redissolution in HF produced the same chemical shifts and indicated that the salt, $TcO_3^+AsF_6^-$, was stable to pumping at room temperature.

It was of interest to synthesize other members of the series TcO_xF_{7-2x}. Noble gas fluorides have been used previously to synthesize

examples of high-oxidation-state species of the elements that were inaccessible by other means (143,144) and these methods were applied here. A twofold excess of XeF_6 was added to a HF solution of TcO_3F which also contained H_2O from the solvolysis of TcO_4^-. The resulting solution yielded a new ^{99}Tc resonance (245.9 ppm, $\Delta\nu$ = 135 Hz) to high frequency of both TcO_3F and TcO_3^+. The signal was split into a 1:2:1 triplet (J = 259 Hz) arising from ^{99}Tc-^{19}F spin-spin coupling involving two equivalent fluorine atoms directly bonded to ^{99}Tc. The ^{17}O and ^{19}F n.m.r. spectra consisted of partially quadrupole-collapsed decets arising from spin coupling to ^{99}Tc (Table 24). Fluorination of TcO_3F with KrF_2 in HF also yielded the above product, which reacted further with this potent fluorinating agent to give a second new oxyfluoride in HF solution. The latter species, which has been studied by ^{99}Tc, ^{17}O and ^{19}F n.m.r. (Table 24), yielded singlets in each instance.

The ^{99}Tc n.m.r. spectrum in Figure 21 shows the resonances of the two products obtained from the reaction of KrF_2 with TcO_3F. The low frequency triplet is tentatively assigned to $Tc_2O_5F_4$ and the broad ^{99}Tc singlet to TcO_2F_3 where the structures of the compounds are as follows:

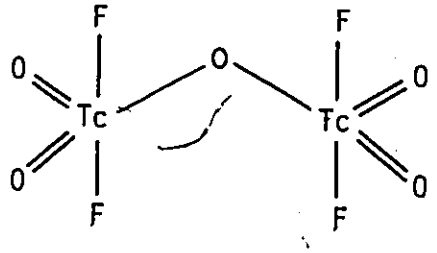

$Tc_2O_5F_4$

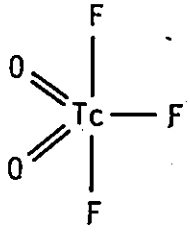

TcO_2F_3

Table 24. Chemical shifts*, line widths(Hz)# and coupling constants(J) for various technetium species

Species	δ,ppm				J(^{99}Tc-X),Hz		
	^{99}Tc	^{17}O	^{19}F	^{1}H	^{17}O	^{19}F	^{1}H
TcH_9^{2-}	-3672(22)			-7.22(224)			24
**$Tc(CNCR_3)_6^{+}$	-1908(74)						
$Tc(CN)_7^{4-}$	-1329(5000)						
TcO_4^{-}	0(2.7)	748.6(23)			131.4		
TcO_3F	43.7(23)	1048(108)			139.8		
TcO_3^{+}	160.7(670)	1214(720)					
$Tc_2O_5F_4$	245.9(135)	1234(780)	22.6(2280)≠		87(±5)	259	
TcO_2F_3	396.3(375)	1211(700)	-6.5(370)/				
$TcO_2(CN)_4^{3-}$	806(0(642)						

* Chemical shifts are expressed relative to TcO_4^{-}(^{99}Tc), H_2O(^{17}O),$CFCl_3$(^{19}F) or $(CH_3)_4Si$(^{1}H).
\# Line widths are the values given in parentheses
** R = H,CH_3
≠ Values of 29.3(720) were observed at -80°C
/ Spectrum measured at -47°C

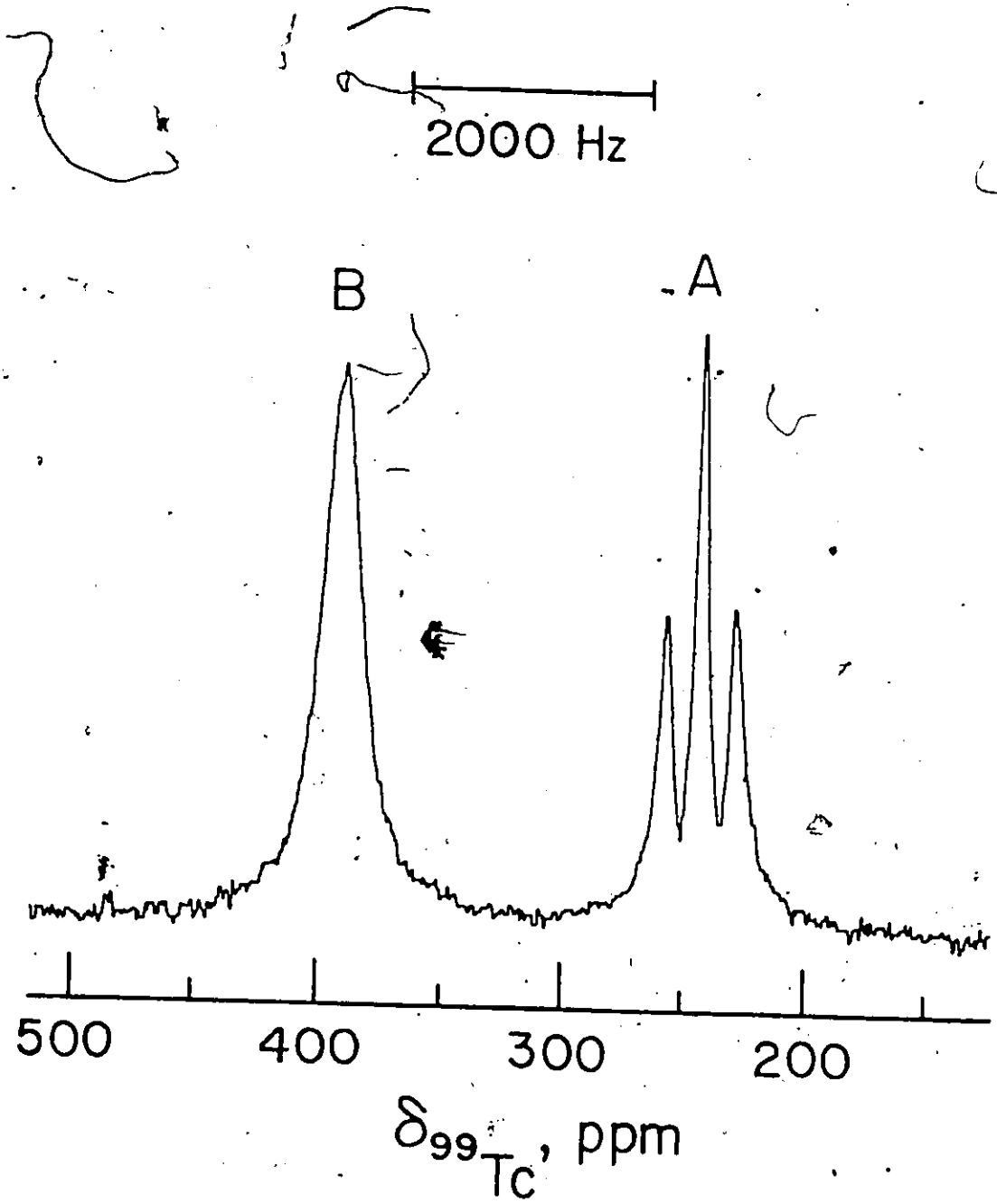

Figure 21. The ^{99}Tc n.m.r. spectrum of $Tc_2O_5F_4$ (A) and TcO_2F_3 (B) resulting from the incomplete reaction of KrF_2 with $KTcO_4$ in HF.

In reactions of TcO_3F with XeF_6, both xenon tetrafluoride and O_2 gas were observed as expected from the balanced equation:

$$2TcO_3F + XeF_6 \rightarrow Tc_2O_5F_4 + XeF_4 + 0.5\ O_2$$

Small amounts of xenon oxide tetrafluoride, resulting from the reaction of XeF_6 with H_2O formed by HF solvolysis of TcO_4^-, was also detected. Oxygen and krypton gases are liberated in reactions of TcO_3F with KrF_2 according to the reactions given by:

$$2TcO_3F + KrF_2 \rightarrow Tc_2O_5F_4 + Kr + 0.5\ O_2$$

$$Tc_2O_5F_4 + KrF_2 \rightarrow TcO_2F_3 + Kr + 0.5\ O_2$$

In the case of KrF_2 reactions, water generated in the solvolysis of TcO_4^- is quantitatively oxidized to yield O_2 and HF.

Chemical exchange of fluorine atoms among solvent and TcO_2F_3 accounts for the failure to observe ^{99}Tc-^{19}F coupling in this case as well as the observation of only a single broad ^{19}F environment at low temperature (Table 24). The broad ^{17}O resonance for TcO_2F_3 is attributable to partial collapse of the ^{99}Tc-^{17}O coupling brought about by quadrupole relaxation of ^{99}Tc in the asymmetric electric field of a trigonal bipyramid and by fluctuating electric field gradients arising from chemical exchange of fluorine ligands. The possibility that $TcOF_5$ rather than TcO_2F_3 is formed in the reaction of $Tc_2O_5F_4$ with excess KrF_2 can be ruled out. $TcOF_5$ should behave like the related pseudo-octahedral $ReOF_5$ (145) and IOF_5 (146) molecules and would not be expected to exhibit chemical exchange among its axial and equatorial fluorine

environments and HF solvent. The absence of two nonlabile fluorine environments as well as the observed exchange behaviour attributed to TcO_2F_3 is consistent with the formulation of the latter oxyfluoride and inconsistent with $TcOF_5$ formation.

The observation of ^{99}Tc-^{19}F coupling for $Tc_2O_5F_4$ indicates the rate of fluorine exchange is slow. Only one oxygen environment could, however, be observed for the oxygen-bridged structure proposed for $Tc_2O_5F_4$. The partially resolved ^{99}Tc-^{17}O coupling is consistent with the lower symmetry around ^{99}Tc. Failure to observe a unique bridging ^{17}O environment is caused by the effects of two ^{99}Tc nuclei spin-spin coupled to one ^{17}O. This would give rise to a broad, partially quadrupole-collapsed 19-line multiplet having one-fourth the intensity of the terminal oxygen environment. The line width and low intensity of the line presumably precludes observation of the bridging environment of $Tc_2O_5F_4$ with the present instrumentation and level of ^{17}O enrichment.

6.5 Species in Lower Oxidation States

The ^{99}Tc resonance for $TcO_2(CN)_4^{3-}$ (section 5.2) was found to be 806.0 ppm to high frequency of TcO_4^-. This represents the most deshielded ^{99}Tc environment observed thus far and is contrary to the trend anticipated on the basis of oxidation state alone. The effect can be traced to the paramagnetic contribution to ^{99}Tc shielding which is small in technetium(VII)(d^0) compounds compared to that for species in lower oxidation states.

The chemical shifts observed for ^{99}Tc in $Tc(CNCR_3)_6^+$, (R = H,

CH_3) and $Tc(CN)_7^{4-}$ (Table 24) are within the established range and the respective line widths of 74 and 5000 Hz parallel the relative symmetries of the two complexes (approximately O_h and D_{5h}). The broadening of the ^{99}Tc resonances as the symmetry is lowered is to be expected from equation 1 above and may prove to be a limiting factor in ^{99}Tc n.m.r. spectroscopy. Indeed, none of the oxotechnetium(V) complexes described in earlier chapters yielded an observable ^{99}Tc resonance. Further research is necessary to establish the limitations of ^{99}Tc n.m.r. spectroscopy.

CHAPTER 7

CONCLUSIONS

In the preceding chapters, results were presented that pertain to various aspects of technetium chemistry including the relative stabilities of different oxidation states in aqueous media, similarities to known rhenium chemistry and the development of ^{99}Tc nuclear magnetic resonance spectroscopy. These studies were prompted by two major considerations, the desire to explore the properties of a relatively new and unstudied element and to gain a better understanding of the structural features and chemical properties of radiopharmaceuticals based on technetium-99m. Both of these objectives were realized, at least in part, during the course of this work.

With respect to the basic chemistry of technetium, the cyano complexes, $TcO_2(CN)_4^{3-}$ and $Tc(CN)_7^{4-}$, described in Chapter 5 are directly analogous to those found previously for rhenium. These results provide further evidence that technetium is not an anomaly in the periodic table. The parallel between technetium and rhenium also exists for the structures and stabilities of the complexes containing the oxotechnetium(V) core which were discussed in Chapters 3 and 4. Several new technetium(VII) species including TcO_3^+, $Tc_2O_5F_4$ and TcO_2F_3 were described in Chapter 6. These compounds were used to establish ranges for chemical shifts, line widths and coupling constants in ^{99}Tc nuclear magnetic resonance spectroscopy. Throughout these studies, the utility of numerous instrumental techniques, particularly X-ray crystallography, vibrational spectroscopy and multinuclear magnetic

resonance spectroscopy, in the characterization of new compounds of technetium was demonstrated.

The crystal structures of three complexes related to radiopharmaceuticals were described in Chapters 3 and 4. In the case of the Tc-penicillamine complex, a tracer study indicates that the formulation of a known hepatobiliary agent as an oxotechnetium(IV) species is incorrect. Support for the extension of this correction to other radiopharmaceuticals was found in the structure of the Tc-catechol complex where four oxygen ligands are bound to an oxotechnetium(V) core. The crystal structure of the oxo(N,N'-ethylenebis(2-mercaptoacetamido) technetate(V) anion forms an integral part of a larger effort to systematically design an improved scanning agent.

There are many opportunities for further research. The instability of penicillamine complexes of technetium in lower oxidation states invites further experimentation to characterize fully the transient species and to study the stabilizing effects of ligand modification. There are many radiopharmaceuticals based on ^{99m}Tc which have not yet been characterized. The potential of ^{99m}Tc as a flag in the study of biological processes such as nutrient metabolism and drug action has not been extensively explored. Finally, the nuclear magnetic resonance spectroscopy of ^{99}Tc requires further study to allow radiopharmacists and chemists to take full advantage of this very sensitive nucleus. Progress in each of these areas will involve cooperation among workers in several fields of science.

REFERENCES

1. M. E. Weeks, "Discovery of the Elements, 6th Edition", Journal of Chemical Education, Easton, Pa., (1956), p. 653.
2. K. V. Kotegov, O. N. Pavlov and V. P. Shvedov, Adv. Inorg. Chem. Radiochem., 11, 2 (1968).
3. C. Perrier and E. Segré, J. Chem. Phys., 5, 712 (1937).
4. C. Perrier and E. Segré, Nature, 159, 24 (1947).
5. K. Schwochau in "Inorganic Chemistry: Topics in Current Chemistry, Vol. 96", F. L. Boschke, Ed., Springer-Verlag, New York (1981), pp. 109-147.
6. A. M. Weinberg and E. Wigner, "The Physical Theory of Neutron Chain Reactors", University of Chicago Press, Chicago (1959), p. 110.
7. G. Bandoli, U. Mazzi, E. Roncari and E. Deutsch, Coord. Chem. Rev. 44, 191 (1982).
8. R. Colton in "The Chemistry of Rhenium and Technetium", F. A. Cotton and G. Wilkinson, Eds., Interscience, London (1965).
9. R. D. Peacock in "The Chemistry of Technetium and Rhenium", P. L. Robinson, Ed., Elsevier, Amsterdam (1966).
10. F. A. Cotton and G. Wilkinson, "Advanced Inorganic Chemistry, 3rd Edition, Interscience, New York (1972).
11. D. K. Huggins and H. D. Kaesz, J. Amer. Chem. Soc., 83, 4474 (1961).
12. G. Wilkinson and J. M. Birmingham, J. Amer. Chem. Soc., 77, 3421 (1955); M. L. H. Green, L. Pratt and G. Wilkinson, J. Chem. Soc. London, 3916 (1958).

13. E. O. Fischer and M. W. Schmidt, Angew. Chem. Int. Ed. Eng., 6, 93 (1967).

14. R. Colton, Nature, 193, 872 (1962).

15. R. Colton, Nature, 194, 374 (1962).

16. A. Guest and C. J. L. Lock, Can. J. Chem., 49, 603 (1971).

17. A. Guest and C. J. L. Lock, Can. J. Chem., 50, 1807 (1972).

18. J. H. Canterford and A. B. Waugh, Inorg. Nucl. Chem. Lett., 7, 395 (1971).

19. J. Burgess, C. J. W. Fraser, I. Haigh and R. D. Peacock, J. Chem. Soc. Dalton Trans., 501 (1973).

20. P. W. Frais, Ph.D. Thesis, McMaster University, Hamilton (1972).

21. V. I. Spitsyn, A. F. Kuzina and A. A. Oblova, Russ. Chem. Rev. (Engl., Transl.) 46, 1030 (1977); Usp. Khim., 46, 1947 (1977).

22. K. R. Seddon, Coord. Chem. Rev., 37, 199 (1981).

23. J. E. Turp, Coord. Chem. Rev., 45, 281 (1982).

24. M. J. Clarke and P. H. Fackler in "Structure and Bonding, Vol. 50", Springer-Verlag, New York (1982), pp. 55-78.

25. F. A. Cotton, A. Davison, V. W. Day, L. D. Gage and H. S. Trop, Inorg. Chem., 18, 3024 (1979).

26. R. W. Thomas, G. W. Estes, R. C. Elder and E. A. Deutsch, J. Amer. Chem. Soc., 101, 4581 (1979).

27. E. A. Deutsch, R. C. Elder and A. Packard, unpublished results cited in ref. 7.

28. S. A. Zuckman, G. M. Freeman, D. E. Troutner, W. A. Volkert, R. A. Holmes, D. G. Van Derveer and E. K. Barefield, Inorg. Chem., 20, 2386(1981).

29. H. S. Trop, Ph.D. Thesis, Massachusetts Institute of Technology, Cambridge (1979), Cited in ref. 5.

30. H. S. Trop, A. Davison, G. H. Carey, B. V. DePamphilis, A. G. Jones and M. A. Davis, J. Inorg. Nucl. Chem., 41, 271 (1979).

31. A. G. Jones, A. Davison, M. J. Abrams, J. W. Brodack, A. I. Kassis, S. Z. Goldhaber, B. L. Holman, L. Stemp, T. Manning and H. B. Hechtman, J. Nucl. Med., 23, P16 (1982). Abstract.

32. G. Hevesy, Biochem. J., 17, 29 (1923).

33. H. D. Burns in "The Chemistry of Radiopharmaceuticals", N. D. Heindel, H. D. Burns, T. Honda and L. W. Brady, Eds., Masson et Cie, Paris (1978), p. 35.

34. H. N. Wagner, in ref. 33, p. 1.

35. P. Richards, Comitato Nazionale Ricerche Nucleari, 2, 223 (1960) cited in ref. 33.

36. R. L. Hayes in ref. 33, p. 155.

37. V. I. Levin, L. S. Kozyrevaalexandrova, T. N. Sokolova and V. G. Zalessky, Radiochem. Radioanal. Lett., 39, 141 (1979).

38. B. Nabardi, R. Najafi and R. S. Mani, Int. J. Appl. Radiat. Isot. 33, 473 (1982).

39. R. E. Boyd, Radiochim. Acta, 30, 123 (1982).

40. H. D. Burns, P. Worley, H. N. Wagner, L. Marzilli and V. Risch, in ref. 33, p. 269.

41. L. G. Marzilli, R. F. Dannals and H. D. Burns in "Inorganic Chemistry in Biology and Medicine", A. E. Martell, Ed., ACS Symposium Series No. 140, American Chemical Society, Washington (1980) p. 91.

42. W. C. Eckelman and S. M. Levenson, Int. J. Appl. Radiat. Isot., 28, 67 (1977).

43. N. D. Heindel in ref. 33, p. 11.

44. E. A. Deutsch and B. L. Barnett in ref. 40, p. 103.

45. A. Davison, C. Orvig, H. S. Trop, M. Sohn, B. V. DePamphilis and A. G. Jones, Inorg. Chem., 19, 1988 (1980).

46. F. A. Bovey, "Nuclear Magnetic Resonance Spectroscopy", Academic Press, New York (1969).

47. J. W. Emsley, J. Feeney and L. H. Sutcliffe, "High Resolution Nuclear Magnetic Resonance Spectroscopy", 2 vols. Pergamon Press, London (1965).

48. E. D. Becker, "High Resolution NMR: Theory and Chemical Applications", 2nd Ed., Academic Press, New York (1980).

49. R. K. Harris in "NMR and the Periodic Table", R. K. Harris and B. E. Mann, Eds., Academic Press, London (1978) p. 1.

50. T. J. Venanzi, J. Chem. Ed., 59, 144 (1982).

51. For a more detailed description see "Syntex P2, Operation Manual", Syntex Analytical Instruments, Stanford Industrial Park, Palo Alto, California.

52. For a more detailed discussion, see:

(a) G. H. Stout and L. H. Jensen, "X-ray Structure Determination", MacMillan, New York (1968).

(b) M. M. Woolfson, "An Introduction to X-ray Crystallography", Cambridge University Press, Cambridge (1970).

(c) P. Luger, "Modern X-ray Analysis on Single Crystals", Walter de Gruyter, New York (1980).

53. A. C. Larson, Acta Crystallogr. 23, 664 (1967).

54. J. M. Stewart, XRAY 76, Technical Report TR-446, Computer Science Centre, University of Maryland, College Park, Maryland (1976).

55. G. M. Sheldrick, SHELX 76, Cambridge University, England (1976).

56. M. E. Pippy and F. R. Ahmed, "Mean plane and Torsión Angles", Report NRC-22, National Research Council Canada, Ottawa (1978).

57. C. K. Johnson, ORTEP II, Report ORNL-5138, Oak Ridge National Laboratories, Tennessee (1976).

58. D. T. Cromer and J. T. Waber in "International Tables for X-ray Crystallography", J. A. Ibers and W. C. Hamilton, Eds., Kynoch Press, Birmingham, England, Vol. IV, Table 2.2B, p. 99 ff.

59. D. T. Cromer in ref. 58, Table 2.3.1, pp. 149-150.

60. W. C. Hamilton, Acta Crystallogr., 18, 502 (1965).

61. K. J. Franklin, McMaster University Thesis Tables #1, December 1982, Available from Thode Library, McMaster University.

62. M. Tubis, G. T. Krishnamurthy, J. S. Endow and W. H. Blahd, in "Radiopharmaceuticals". G. Subramanian, B. A. Rhodes, J. F. Cooper and V. J. Sodd, Eds., The Society of Nuclear Medicine, New York (1975). p. 55.

63. M. Tubis, G. T. Krishnamurthy, J. S. Endow and W. H. Blahd, J. Nucl. Med., 13, 652 (1972).

64. G. T. Krishnamurthy, M. Tubis, W. H. Blahd and J. S. Endow, Radiology, 115, 201 (1975).

65. R. G. Robinson, D. Bradshaw, B. A. Rhodes, J. A. Spicer, R. J.

65. Visentin and A. H. Gobuty, Int. J. Appl. Radiat. Isot. 28, 105 (1977).

66. R. G. Robinson, D. Bradshaw, B. A. Rhodes, J. A. Spicer and A. H. Gobuty, Int. J. Appl. Radiat. Isot. 28, 919 (1977).

67. A. Yokoyama, H. Saji, H. Tanaka, T. Odori, R. Morita, T. Mori and K. Torizuka, J. Nucl. Med., 17, 810 (1976).

68. A. Yokoyama, H. Saji, K. Horiuchi and Y. Terauchi, J. Labelled Compd. Radiopharm., 13, 263 (1977).

69. A. Yokoyama, H. Saji, K. Horiuchi, H. Tanaka, T. Odori, R. Morita, T. Mori and K. Torizuka, Int. J. Nucl. Med. Biol., 5, 45 (1978).

70. A. Yokoyama, K. Horiuchi, N. Hata, H. Saji, H. Tanaka and W. C. Eckelman, J. Labelled Compd. Radiopharm., 16, 80 (1979).

71. K. Horiuchi, A. Yokoyama, K. Tsuiko, H. Tanaka and H. Saji, Int. J. Appl. Radiat. Isot., 32, 545 (1981).

72. K. J. Franklin, H. E. Howard-Lock and C. J. L. Lock, Inorg. Chem. 21, 1941 (1982).

73. B. V. De Pamphilis, A. G. Jones, M. A. Davis and A. Davison, J. Amer. Chem. Soc., 100, 5570 (1978).

74. C. J. L. Lock and C. Wan, Can. J. Chem., 53, 1548 (1975).

75. F. A. Cotton and S. J. Lippard, Inorg. Chem., 4, 1621 (1965).

76. L. Pauling, "Nature of the Chemical Bond", 3rd Ed., Cornell University Press, Ithaca, New York (1960), p. 260.

77. C. J. L. Lock and G. Turner, Can. J. Chem., 55, 333 (1977).

78. L. G. Warner, T. Ottersen and K. Seff, Acta Crystallogr., Sect. B., 30, 1077 (1974).

79. S. N. Rao, R. Parthasarathy and F. E. Cole, Acta Crystallogr., Sect. B, 29, 2373 (1973).

80. P. DeMeester and D. J. Hodgson, J. Amer. Chem. Soc., 99, 101, (1977).

81. H. M. Helis, P. DeMeester and D. J. Hodgson, J. Amer. Chem. Soc., 99, 3309 (1977).

82. E. Deutsch; R. C. Elder, B. A. Lange, M. J. Vaal and D. G. Lay, Proc. Natl. Acad. Sci., U.S.A., 73, 4287 (1976).

83. M. Tsutsui, C. P. Hrung, D. Ostfeld, T. A. Srivastava, D. L. Cullen and E. F. Meyer, J. Amer. Chem. Soc. 97, 3952 (1975).

84. G. Firnau, Eur. J. Nucl. Med., 1, 137 (1976).

85. A. Kramer, private communication, Johns Hopkins Medical School, Sept. 1980.

86. "Sadtler Standard Spectra", Sadtler Research Laboratories, Philadelphia (1967). Vol. 5, Spectrum No. 2305.

87. L. Flohe, E. Breitmaier, W. A. Gunzler, W. Voelter and G. Jung, Hoppe-Seyler's Z. Physiol. Chem., 353, 1159 (1972).

88. H. C. Freeman, C. J. Moore, W. G. Jackson and A. M. Sargeson, Inorg. Chem., 17, 3513 (1978).

89. K. Nakamoto, "Infrared and Raman Spectra of Inorganic and Coordination Compounds", 3rd Ed., Wiley-Interscience, New York (1978).

90. F. R. Dollish, W. G. Fateley and F. F. Bentley, "Characteristic Raman Frequencies of Organic Compounds, Wiley-Interscience, New York (1974).

91. W. B. Colthup, L. H. Daly and S. E. Wiberley, "Introduction to Infrared and Raman Spectroscopy", Academic Press, New York (1964).

92. H. E. Howard-Lock, C. J. L. Lock and P. S. Smalley, submitted to J. Crystallogr. Spectrosc. Res. (November, 1982).

93. R. B. Smith, J. Coupal, F. H. DeLand and J. W. Triplett, J. Nucl. Med., 20, 45 (1979).

94. D. F. Evans, J. Chem. Soc., 2003 (1959).

95. K. Nakamoto, Y. Morimoto and A. E. Martell, J. Amer. Chem. Soc. 83, 4528 (1961).

96. A. Davison, personal communication (October, 1982).

97. E. F. Byrne and J. E. Smith, Inorg. Chem., 18, 1832 (1979).

98. A. G. Jones, B. V. DePamphilis and A. Davison, Inorg. Chem. 20, 1617 (1981).

99. P. Richards and J. Steigman in ref. 62, p. 23.

100. A. Davison, B. V. DePamphilis, K. J. Franklin, A. G. Jones and C. J. L. Lock, accepted by Inorg. Chem., (October 1982).

101. (a) A. G. Jones, A. Davison, M. R. LaTegola, J. W. Brodack, C. Orvig, M. Sohn, A. K. Toothaker, C. J. L. Lock, K. J. Franklin, C. E. Costello, S. A. Carr, K. Biemann and M. L. Kaplan, J. Nucl. Med., 23, 810 (1982).

(b) A. Davison, K. J. Franklin, C. Orvig and C. J. L. Lock, submitted to Acta Crystallogr. Sect. C., (November 1982).

102. A. Davison, A. G. Jones, C. Orvig and M. Sohn, Inorg. Chem. 20, 1629 (1981).

103. J. E. Smith, E. F. Byrne, F. A. Cotton and J. C. Sekutowski, J. Amer. Chem. Soc., 100, 5571 (1978).

104. S. R. Cooper, Y. B. Koh and K. N. Raymond, J. Amer. Chem. Soc., 104, 5092 (1982).

105. C. G. Pierpont and R. M. Buchanan, Coord. Chem. Rev., 38, 45 (1981).

106. F. L. Phillips and A. C. Skapski, Acta Crystallogr. Sect. B, 31, 1814 (1975).

107. F. A. Cotton and R. M. Wing, Inorg. Chem., 4, 867 (1965).

108. H. E. Howard-Lock, C. J. L. Lock and G. Turner, Spectrochim. Acta, in press (1982).

109. W. de Kieviet, J. Nucl. Med., 22, 703 (1981).

110. A. T. McPhail, G. M. Semeniuk and D. B. Chesnut, J. Chem. Soc., (A), 2174 (1971).

111. R. Eisenberg, Z. Dori, H. B. Gray and J. A. Ibers, Inorg. Chem. 7, 741 (1968).

112. C. P. Brock and J. A. Ibers, Acta Crystallogr. Sect. B, 29, 2626 (1973).

113. W. DeW. Horrocks and E. Greenberg, Inorg. Chem., 10, 2190 (1971).

114. V. G. Albano, P. Bellon and M. Sansoni, J. Chem. Soc. (A), 2420 (1971).

115. A. R. Fritzberg, W. C. Klingensmith, W. P. Whitney and C. C. Kuni, J. Nucl. Med., 22, 258 (1981).

116. W. C. Klingensmith, J. P. Gerhold, A. R. Fritzberg, V. M. Spitzer, C. C. Kuni, C. J. Singer and R. Weil, J. Nucl. Med., 23, 377 (1982).

117. A. R. Fritzberg, C. C. Kuni, W. C. Klingensmith, J. Stevens and W. P. Whitney, J. Nucl. Med., 23, 592 (1982).

118. R. K. Murmann and E. O. Schlemper, Inorg. Chem., 10, 2352 (1971).

119. R. H. Fenn, A. J. Graham and N. P. Johnson, J. Chem. Soc. (A), 2880 (1971).

120. H. S. Trop, A. G. Jones and A. Davison, Inorg. Chem., 19, 1993 (1980).

121. M. E. Kastner, M. J. Lindsay and M. J. Clarke, Inorg. Chem., 21, 2037 (1982).

122. B. Jezowska-Trzebiatowska, J. Hanuza and M. Baluka, Spectrochim. Acta, A27, 1753 (1971).

123. C. J. L. Lock and G. Turner, Acta Crystallogr. Sect. B, 34, 923 (1978).

124. G. Turner, Ph.D. Thesis, McMaster University, Hamilton (1976).

125. L. Y. Martin, L. J. DeHayes, L. J. Zompa and D. H. Busch, J. Amer. Chem. Soc., 96, 4046 (1974).

126. W. P. Griffith, P. M. Kiernan and J.-M. Brégeault, J. Chem. Soc. Dalton Trans., 1411 (1978)

127. A.-M. Soares and W. P. Griffith, J. Chem. Soc. Dalton Trans., 1886 (1981).

128. R. G. Kidd, Annu. Rep. NMR Spectrosc., 10A, 1 (1980).

129. D. Wendlandt, J. Bauche and P. Luc, J. Phys. B., 10, 1989 (1977).

130. H. Walchli, R. Livingston and W. J. Martin, Phys. Rev., 85, 479 (1952).

131. R. G. Kidd and R. J. Goodfellow, in ref. 49, p. 222.

132. B. N. Figgis, R. G. Kidd and R. S. Nyholm, Proc. Roy. Soc. A., A269, 469 (1962).

133. M. J. Buckingham, G. E. Hawkes and J. R. Thornback, Inorg. Chim. Acta, 56, L41 (1981).

134. R. G. Kidd, J. Magn. Reson., 45, 88 (1981).

135. V. P. Tarasov, V. I. Privalov and I. A. Buslaev, Dokl. Akad. Nauk SSSR, 262, 1433 (1982); Chem. Abstr. 96, 209615f (1982).

136. V. P. Tarasov, V. I. Privalov, G. A. Kirakosian, A. A. Gorbik and I. A. Buslaev, Dokl. Akad. Nauk SSSR, 263, 1416 (1982); Chem. Abstr., 97, 15949t (1982).

137. K. J. Franklin, C. J. L. Lock, B. G. Sayer and G. J. Schrobilgen, J. Amer. Chem. Soc., 104, 5303 (1982).

138. M. Suzuki and R. Kubo, Mol. Phys., 7, 201 (1963).

139. K. A. Valiev and M. M. Zaripov, Sov. Phys.-JETP (Engl. Transl.) 14, 545 (1962).

140. D. M. Doddrell, M. R. Bendall, P. C. Healy, G. Smith, C. H. L. Kennard, C. L. Ralston and A. H. White, Aust. J. Chem., 32, 1219 (1979).

141. A. P. Ginsberg, Inorg. Chem., 3, 567 (1964).

142. J. Binenboym, U. El-Gad and H. Selig, Inorg. Chem., 13, 319 (1974).

143. K. Leary, A. Zalkin and N. Bartlett, Inorg. Chem., 13, 775 (1974).

144. R. J. Gillespie and G. J. Schrobilgen, Inorg. Chem., 13, 1230 (1974).

145. N. Bartlett, S. Beaton, L. W. Reeves and E. J. Wells, Can. J. Chem., 42, 2531 (1964).

146. R. J. Gillespie and J. W. Quail, Proc. Chem. Soc., 278 (1963).